Recent Advances on Visible Light Triphenylamine-based Photoinitiators of Polymerization

Frédéric Dumur

Recent Advances on Visible Light Triphenylamine-based Photoinitiators of Polymerization

Frédéric Dumur[a]*

[a] Aix Marseille Univ, CNRS, ICR, UMR 7273, F-13397 Marseille, France

frederic.dumur@univ-amu.fr

Abstract

During the past decades, visible light photoinitiators have been extensively studied due to the development of cheap and energy-saving irradiation sources, namely light-emitting diodes (LEDs). With aim at developing chromophores with absorption perfectly fitting the emission of LEDs, triphenylamine has been identified as a versatile building block for designing Type I and Type II photoinitiators of polymerization. In this review, an overview of different photoinitiators comprising a triphenylamine unit is presented. To evidence the interest of these structures, comparisons with benchmark photoinitiators is presented.

Keywords

Photoinitiator; triphenylamine; photopolymerization; LED; low light intensity; 4D printing

Introduction

During the past decades, photoinitiators of polymerization activable under low light intensity and in the visible range have been the focus of intense research efforts.[1–8] Interest for molecules activable in the visible range and under low-light intensity is supported by the recent safety concerns raised by the use of UV light and the need to use energy efficient irradiation setups. As a consequence, photopolymerists are now enforced to investigate new and greener polymerization conditions. Efforts for elaborating new photoinitiating systems are also supported by the wide range of applications in which photopolymerization is involved, ranging from adhesives, dentistry, microelectronics and 3D/4D printing.[9–15] Interest for photopolymerization is also supported by the different advantages this polymerization technique offers compared to the traditional thermal polymerization. Notably, a spatial and a temporal control can be obtained during the polymerization process (See Figure 1).[16,17] Photopolymerization can also be carried out without solvents, avoiding the release of volatile organic compounds (VOCs).[2] Release of ozone can also be advantageously avoided by use of visible light, what also constitutes a characteristic of UV-induced polymerization processes.[18] Finally, one of the main advantages to replace the traditional UV light by visible light is directly related to the light penetration inside the photocurable

resin.[19,20] Indeed, as shown in the Figure 2, light penetration remains limited in the UV range, not exceeding 600 µm.

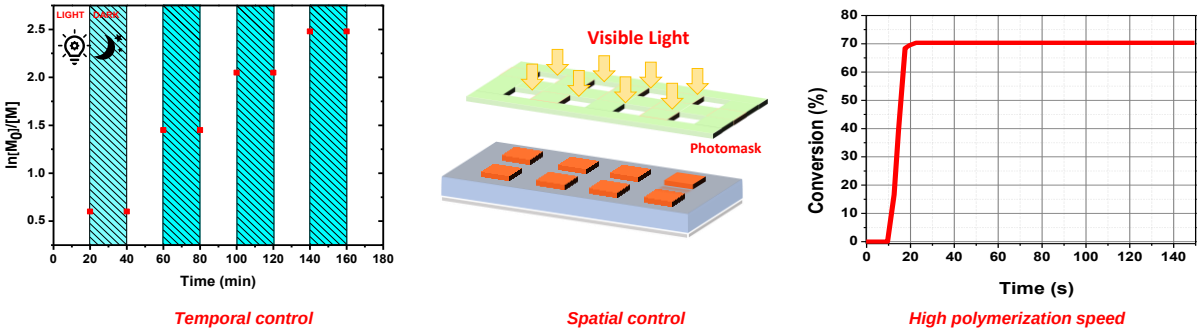

Figure 1. The different characteristics of photopolymerization.

This drawback can be overcome in the visible range. Indeed, if the light penetration is of a few millimeters at 405 nm, this latter can reach 5 cm at 800 nm, enabling the polymerization of thick and filled polymers. With aim at developing highly efficient photoinitiating systems, a wide range of structures have been examined over the years and porphyrins,[21,22] push-pull dyes,[23–36] iodonium salts,[37–43] carbazoles,[44–51] phenothiazines,[52,53] cyanines,[54–58] zinc complexes,[59] diketopyrrolopyrroles,[60–62] iridium complexes,[63–69] pyrenes,[70–76] 2,3-diphenylquinoxaline derivatives,[77,78] chromones and flavones,[79–81] squaraines,[82–85] coumarins,[86–97] helicenes,[98,99] polyoxometalates,[100,101] metal organic framework (MOFs),[102–104] dihydroanthraquinones,[105] benzophenones,[106–114] camphorquinones,[115,116] acridones,[117,118] thioxanthones,[119–128] naphthalimides,[37,129–143] perylenes,[144–147], iron complexes,[23,103,148–152] chalcones,[153–165] copper complexes,[166–179] acridine-1,8-diones,[180–182] Schiff Bases [183] and cyclohexanones[184–187] can be cited as the main families of dyes examined for photoinitiation during the last decade. Indeed, with aim at designing visible light photoinitiators, the search for new structures disconnected to the traditional photoinitiators such as benzophenone or thioxanthone that are historical photoinitiators has been the focus of intense research efforts during the last decade. Indeed, from a synthetic viewpoint, shift of the absorption spectra of traditional UV photoinitiator until the visible range is a hard work so that new structures disconnected from these historical structures and exhibiting a strong absorption in the visible range are mow commonly investigated.

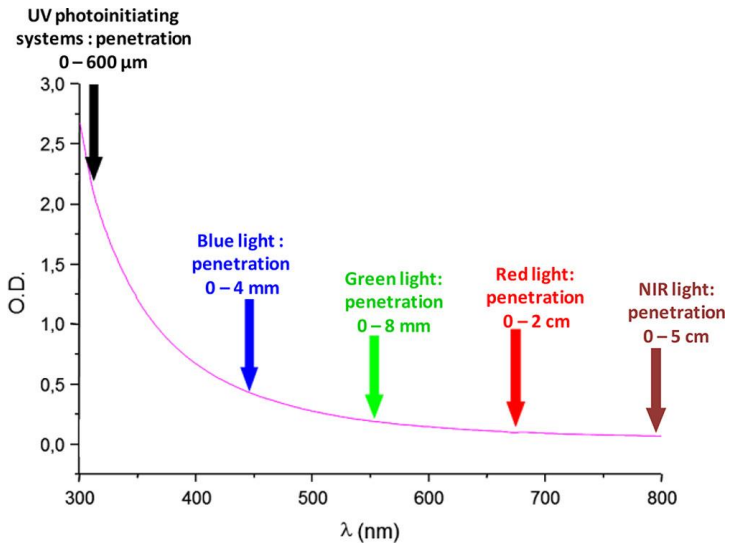

Figure 2. Light penetration in a polystyrene latex with an average diameter of 112 nm. Reprinted with permission from Bonardi et al.[19]

Among dyes that can be used for photoinitiation, triphenylamine is a promising scaffold for the design of visible dyes. Indeed, triphenylamine is a strong electron-donating group that can be used for the design of push-pull dyes when connected to an electron accepting group.[188–192] By its tridimensional structure, triphenylamine is also capable to drastically improve the solubility of the resulting dyes compared to those prepared with its parent structure, namely carbazole.[193,194] Indeed, contrarily to carbazole which is a planar structure favoring π-π staking interactions, tridimensionality of triphenylamine is a serious advantage addressing this issue. Aromatic rings of triphenylamine are also sites of choice for various chemical modifications.[188,195–197] Especially, most of the common chemical transformations constituting the basis of Organic Chemistry can be applied to triphenylamine.[198] Triphenylamine also exhibits a low oxidation potential so that triphenylamine-based dyes can easily fit the redox potentials of additives introduced into the photocurable resins.[199,200] Indeed, most of the photoinitiating systems comprise additives and interaction efficiency is the key element to produce efficient photoinitiating systems. Triphenylamine also exhibits biological activities that can be used for the design of bioactive photoinitiators.[201–203] Compared to the aforementioned dyes, triphenylamine-based photoinitiating systems exhibit advantages and disadvantages that are listed in the Table 1.

Table 1. Comparisons between ferrocene-based photoinitiating systems and other photoinitiating systems.

Parameters	Triphenylamine-based photoinitiating systems	Other organic dyes
Cost/synthesis	Triphenylamine is a cheap compound. Triphenylamine can also be easily chemically modified. As an interesting feature, triphenylamines are	Depending on the structures, starting compounds can be expensive. Parallel to this, solubility can be a major

	highly soluble in most of the common organic solvents	issue, especially when polyaromatic structures are targeted.
Environmental impact	Triphenylamine derivatives can be purified by column chromatography or recrystallization.	The same purification procedures can be developed than for ferrocene derivatives
Photochemical stability	Triphenylamine derivatives are photochemically stable.	Synthetic dyes are also photochemically stable.
Absorption range	Absorption spectra of triphenylamines can be easily tuned so that dyes absorbing over the whole visible range can be designed	The same holds true for synthetic dyes.
Photoinitiating ability	Triphenylamines can compete with benchmark photoinitiators. Besides, the reversibility of the redox process occurring on the ferrocene side can be a crucial advantage for the design of photocatalytic systems.	Synthetic dyes can compete with benchmark photoinitiators. Besides, reversibility of the redox process is not still ensured.
Availability	Triphenylamine is available from numerous suppliers.	Most of the chemical used to elaborate dyes are also accessible. The limitation can be the cost for some of the starting materials.

In this review, an overview of the different photoinitiators comprising a triphenylamine unit is presented. Over the years, numerous structures have been designed, ranging from Type I photoinitiators to Type II photoinitiators activable under visible light and under low light intensity. More precisely, triphenylamines were incorporated in push-pull dyes, benzophenone derivatives, dithienophospholes, polythiophenes, pyrene derivatives, curcuminoids, flavonols, chalcones, hexaarylbiimidazole derivatives and oxime esters. To evidence the interest of these structures, numerous comparisons with benchmark photoinitiators have been established, evidencing the pertinence of the approach.

1. Triphenylamine-based photoinitiators of polymerization

1.1. Push-pull dyes

As mentioned in the introduction section, triphenylamine constitutes a good electron donating group that can be used for the design of push-pull dyes when combined with the appropriate electron-withdrawing group. In 2020, a comparison was notably established between four dyes (2-5) comprising indane-1,3-dione or 1*H*-cyclopentanaphthalene-1,3-dione

as the electron-withdrawing groups (See Figure 3).[204] For comparison, two dyes i.e. 1 and 6 comprising 4-dimethylaminophenyl as the electron-donating groups were designed. Interestingly, all dyes showed a broad absorption over the visible range, extending between 400 and 600 nm. By elongating the aromaticity of the electron withdrawing group in 4, 5 and 6, a red-shift of the absorption maxima by ca. 30 nm could be determined for all dyes compared to their analogues 1-3, combined with a significant increase of the molar extinction coefficient (See Figure 4).[205] Indeed, by elongating the π-conjugation within the dyes, an improvement of the oscillation strength can be obtained, increasing the molar extinction coefficients.[206] Based on their absorption spectra, all dyes were suitable candidates for photoinitiation at 405 nm. When tested as photosensitizers for the free radical polymerization (FRP) of Ebecryl 40 in three-component dye/Iod/amine (0.1%/2%/2% w/w/w), low monomer conversions were obtained with dyes 1-3 comprising indane-1,3-dione as the electron acceptor. Conversely, high monomer conversions and short polymerization times could be determined with 4 and 5 bearing a different electron accepting group, peaking at 92 and 95% respectively after 400 s of irradiation at 405 nm. Notably, a polymerization ended after only 20 s could be determined for these two dyes. Besides, low monomer conversion was obtained with 6, despites the presence of 1*H*-cyclopentanaphthalene-1,3-dione as the electron-withdrawing group. It therefore clearly indicates the crucial importance of carefully selecting both the electron donor and the electron-acceptor for designing efficient photosensitizers. While getting a deeper insight into the polymerization mechanism, photolysis experiments done in acetonitrile solution with the three-component dye/Iod/amine combination revealed that almost no photolysis occurred with 4 whereas the formation of a photoproduct could be clearly evidenced with 5. Considering that an oxidative or a reductive process can concomitantly occur with the three-component systems, interaction of dyes with the iodonium salt and the amine were separately examined. When tested in dye/Iod and dye/EDB combinations, a faster photolysis rate was determined for the dye/Iod combination, indicating that the oxidative process was the main reaction pathway to generate radicals.

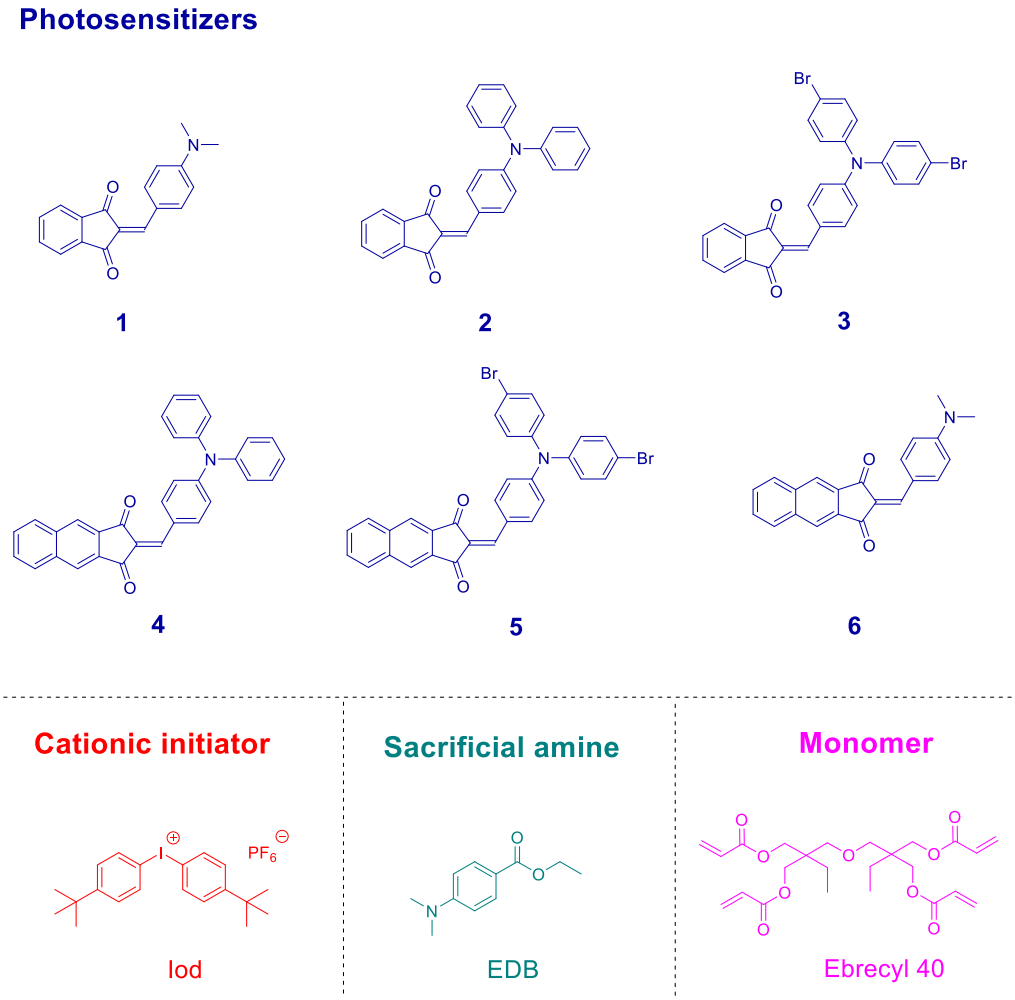

Figure 3. Chemical structures of dyes 1-6, monomer and additives.

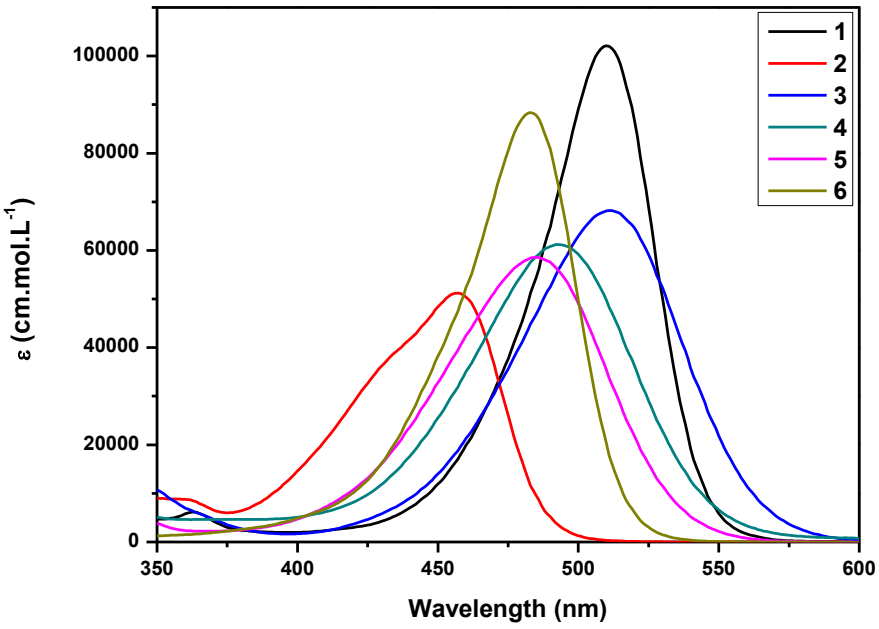

Figure 4. UV-visible absorption spectra of dyes 1-6 in chloroform. Adapted with permission from Sun et al. [204].

Overall, the following mechanism could be proposed with the three-component photoinitiating system, based on five equations (See Scheme 1). Notably, strength of the three-component systems relies in the coexistence of the oxidative and reductive processes (equations r2 and r3), optimizing the generation of initiating radicals.

(r1) $Dye \rightarrow {}^{*}Dye \quad (h\nu)$

(r2) $^{*}Dye + Ar_2I^{+} \rightarrow Dye^{\bullet+} + Ar_2I^{\bullet} \rightarrow Dye^{\bullet+} + Ar^{\bullet} + ArI$

(r3) $^{*}Dye + EDB \rightarrow Dye^{\bullet-} + EDB^{\bullet+} \rightarrow Dye\text{-}H^{\bullet} + EDB^{\bullet}_{(-H)}$

(r4) $Dye^{\bullet+} + EDB \rightarrow Dye + EDB^{\bullet+}$

(r5) $Dye\text{-}H^{\bullet} + Ar_2I^{+} \rightarrow Dye + Ar^{\bullet} + ArI + H^{+}$

Scheme 1. Proposed photoinitiation step mechanisms for the three-component dyes/iodonium salt/amine redox combination.

In 2020, two push-pull dyes (7 and 8) exhibiting a weaker electronic delocalization than dyes 2-5 were proposed as visible light photoinitiators of polymerization (See Figure 5).[207] Indeed, in this last case, electron-withdrawing groups were directly introduced onto the triphenylamine core. Notably, the phenyl rings of triphenylamine were substituted with nitro and cyano groups in dye 7 and 8 respectively. From the absorption viewpoint, surprisingly, dye 7 which exhibits the strongest electron-withdrawing groups showed a slightly blue-shifted absorption spectrum compared to that of dye 8 bearing cyano groups. Thus, absorption maxima located at 352 and 357 nm could be respectively determined for dye 7 and dye 8. If differences in their molar extinction coefficients could be determined at their absorption maxima (26610 $M^{-1}.cm^{-1}$ for dye 7 vs. 17700 $M^{-1}.cm^{-1}$ for dye 8), almost similar molar extinction coefficients could be determined at 405 nm for the two dyes.

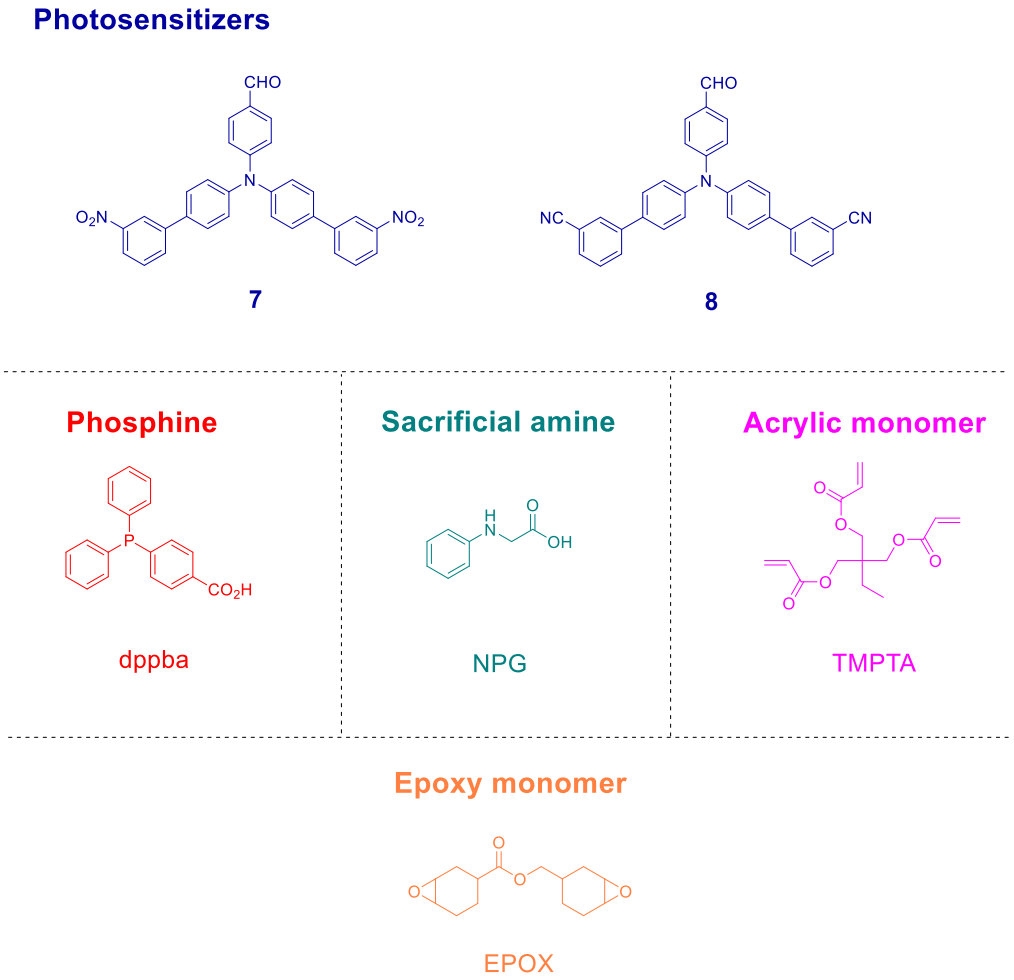

Figure 5. Chemical structures of dyes 7 and 8, monomers and additives.

Comparison of the efficiency trend during the cationic polymerization of (3,4-epoxycyclohexane)methyl 3,4-epoxycyclohexylcarboxylate (EPOX) upon irradiation at 405 nm with the two-component dye/Iod (0.5%/1% w/w) systems revealed dye 8 to exhibit a higher reactivity than dye 7. Indeed, a faster polymerization rate could be determined for dye 8 at the beginning of the polymerization. However, after 800 s of irradiation at 405 nm, a final monomer conversion of 66% could be however obtained with dye 7, higher than that obtained with the more reactive dye 8 (57%). This efficiency trend was confirmed during the FRP of trimethylolpropane triacrylate (TMPTA). Notably, four different combinations were used, namely dye/Iod, dye/NPG, dye/EDB or dye/Iod/NPG where NPG and EDB respectively stands for *N*-phenylglycine and ethyl 4-(dimethylamino)benzoate. Noticeably, the dye/NPG combination could outperform the dye/EDB two-component system and the lower performance of the second system was assigned to a back-electron transfer phenomenon adversely affecting the generation of initiating radicals. Upon introduction of the iodonium salt, almost similar final monomer conversions were observed with the three-component dye/Iod/NPG system compared to that obtained with the two-component dye/NPG combination (See Table 2). High efficiency of the two-component dye/NPG system was assigned to the decarboxylation reaction occurring on NPG, avoiding any back electron

transfer reaction and generating additional initiating radicals.[95,208] As a result of this, Ar•, $NPG_{(-H;-CO2)}$• were considered as the initiating species during the FRP of acrylate, and $dye^{•+}$ as the initiating species for the CP. Compared to the previous mechanism and considering that the sacrificial amine can decarboxylate, four additional equations (r6-r9, see Scheme 2) were proposed to support the polymerization efficiency.

(r6) $^*Dye + NPG \rightarrow (Dye\text{-}H)^• + NPG_{(-H)}^•$

(r7) $NPG_{(-H)}^• \rightarrow NPG_{(-H;-CO2)}^• + CO_2$

(r8) $NPG_{(-H;-CO2)}^• + Ar_2I^+ \rightarrow NPG_{(-H;-CO2)}^+ + Ar^• + ArI$

(r9) $(Dye\text{-}H)^• + Ar_2I^+ \rightarrow Dye + H^+ + Ar^• + ArI$

Scheme 2. Proposed photoinitiation step mechanisms of dyes/iodonium/amine redox combination.

Table 2. Final TMPTA conversion using different two (0.5%/1% w/w) and three-component (0.5%/1%/1% w/w) photoinitiating systems after 100 s of irradiation at 405 nm.

	Dye/Iod	**Dye/NPG**	**Dye/EDB**	**Dye/Iod/NPG**
Dye 7	25%	62%	55%	59%
Dye 8	48%	61%	52%	57%

1.2. Benzophenone derivatives

Benzophenone (BP) is an historical UV photoinitiator of polymerization.[109,209–211] To improve the photochemical reactivity of benzophenone and/or in order to provide additional properties to this well-known photoinitiator, an efficient strategy consisted in designing hybrid structures.[106,212] This strategy was notably applied by combining benzophenone to triphenylamine.[110] Indeed, by combining traditional UV sensitive photoinitiators to dyes absorbing in the visible range, chromophores onto which these UV sensitive photoinitiators can provide a sufficient absorption in the visible range in order the resulting hybrid structure to be capable to initiate a polymerization in the visible range, but also to increase the molar extinction coefficient of the UV sensitive photoinitiators by extension of aromaticity. As a result of this combination, benzophenone-based hybrid structures can absorb at wavelengths where benzophenone do not naturally absorbs.[74,107,135,213–215] This point was notably examined with 9 and 10 (See Figure 6).[110] Comparisons were notably established with benzophenone (BP) and thioxanthone (2-ITX) that are two benchmark photoinitiators.[216] As shown in the Figure 7 and the Table 3, benefits of the combination of benzophenone and triphenylamine could be clearly evidenced. Indeed, if 9 and 10 showed red-shifted absorption maxima compared to that of BP (361 and 375 nm vs. 340 nm for BP),

jointly, a significant enhancement of the molar extinction coefficient could be detected, benefiting from the contribution of triphenylamine.

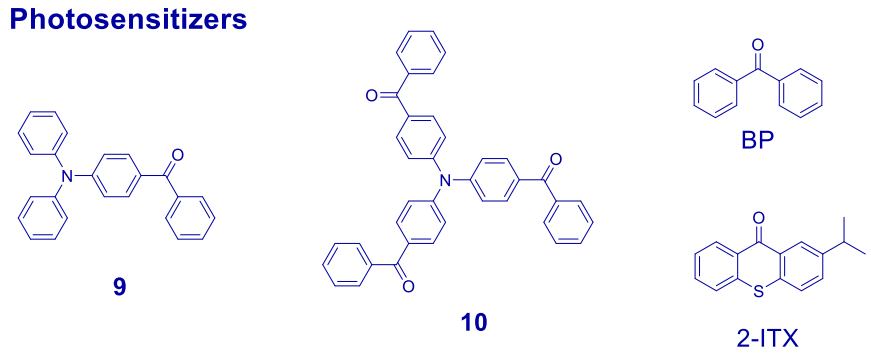

Figure 6. Chemical structures of benzophenone derivatives 9 and 10, BP and 2-ITX.

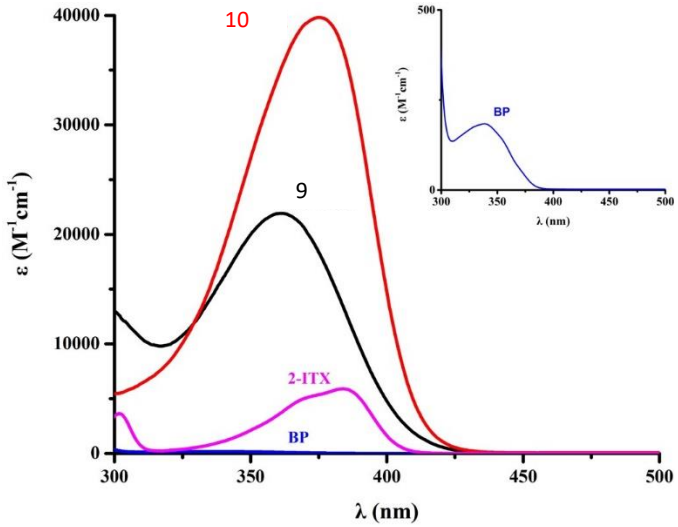

Figure 7. UV-visible absorption spectra of dyes 9 and 10, BP and 2-ITX in acetonitrile. inset: UV-Visible absorption spectrum of BP. Reprinted with permission from Liu et al. [110]

Thus, molar extinction coefficients of 21900 and 39800 $M^{-1}.cm^{-1}$ were respectively determined for 9 and 10 in acetonitrile, far from the value determined for BP (160 $M^{-1}.cm^{-1}$). Interest of these combinations was evidenced at 405 nm, BP not absorbing at this wavelength, contrarily to 9 and 10.

Table 3. Light absorption properties of different dyes in acetonitrile.

	λ_{max} (nm)	ε_{max} ($M^{-1}.cm^{-1}$)	ε at 405 nm ($M^{-1}.cm^{-1}$)
9	361	21900	3100
10	375	39800	8700
BP	340	160	0
2-ITX	383	5900	600

FRP experiments carried out to evaluate the photoinitiation ability of 9 and 10-based photoinitiating systems at 405 nm with a LED during the FRP of TMPTA revealed the two-component systems based on EDB to exhibit better photoinitiating abilities than those prepared with BP or 2-ITX as the dyes. As shown in the Figure 8, the two-component dye/Iod and dye/EDB (0.3%/1%, w/w) could both furnish high monomer conversions, higher than 57% in all cases. As anticipated, use of the three-component photoinitiating system could give higher final monomer conversions than that obtained with the two two-component systems, consistent with the presence of both the oxidative and the reductive pathways contributing to generating initiating species. Comparisons of the performance obtained with BP and 2-ITX revealed the two hybrid structures to furnish higher monomer conversions than the benchmark photoinitiators. However, if significant differences of conversion were found for BP, 9 and 10 could however outperform 2-ITX, but only with a slight improvement of the monomer conversions (See Table 4).

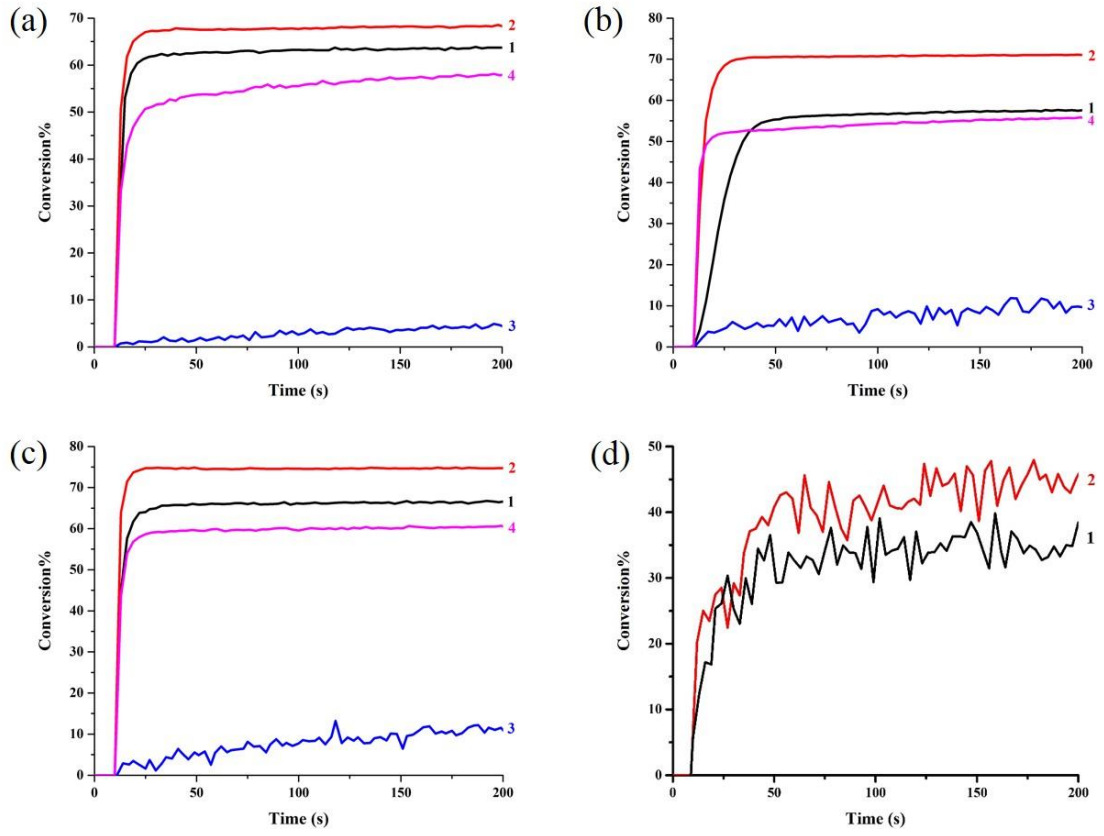

Figure 8. Photopolymerization profiles of TMPTA in laminate upon irradiation at 405 nm with a LED in the presence of (a) dye/Iod (0.3%/1%, mol/mol), (b) dye/EDB (0.3%/1%, mol/mol), (c) dye/Iod/EDB (0.3%/1%/1%, mol/mol/mol); Photopolymerization profiles of EPOX upon irradiation at 405 nm with a LED under air (~ 25 μm) in the presence of (d) dye/Iod (0.3%/1%, mol/mol): curve 1: 9; curve 2 : 10; curve 3 : BP; curve 4 : 2-ITX. Reprinted with permission from Liu et al. [110]

Table 4. Final monomer conversions determined for TMPTA and EPOX upon irradiation at 405 nm with a LED.

photoinitiating system	TMPTA /%				EPOX /%
	dye	dye/Iod	dye/EDB	dye/EDB/Iod	PI/Iod
9	53	64	57	66	38
10	54	69	71	75	45
BP		5	10	12	4
2-ITX		58	55	61	40

Interestingly, 9 and 10 could also be used as monocomponent systems, furnishing monomer conversions comparable to that obtained with 2-ITX, demonstrating that the two structures exhibit a high ability for H-abstraction from the monomer upon irradiation. Besides, with regards to the monomer conversions obtained with Iod and EDB, 9 and 10 nevertheless exhibit a better bimolecular reactivity than as mono-component systems. Examination of photoinitiating ability of the two dyes during the CP of EPOX revealed the two-component 10/Iod (0.3%/1%, mol/mol) system to furnish a higher EPOX conversion than the 2-ITX/Iod system (45 vs 40% monomer conversion after 200 s of irradiation at 405 nm under air). Even if a slightly lower EPOX conversion was obtained with 9 (38%), this conversion remains however of significance compared to that obtained with BP/Iod (4% conversion). Finally, considering the high reactivity of 10 in FRP and CP, direct laser write experiments were carried out. As shown in the Figure 9, a remarkable spatial resolution could be obtained during the FRP of TMPTA and the CP of EPOX.

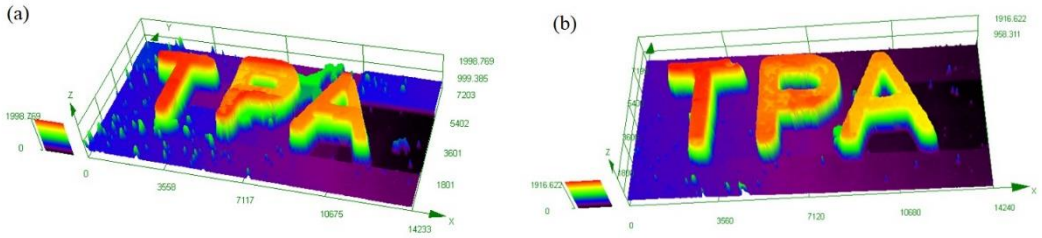

Figure 9. 3D printed structures obtained upon irradiation with a laser diode emitting at 405 nm characterized by numerical optical microscopy (a) TMPTA-based polymer prepared by using 10/Iod/EDB system; (b) EPOX-based polymer prepared by using 10/Iod system. Reprinted with permission from Liu et al. [110]

In 2021, the same authors examined a series of triphenylamine substituted with one, two and three 4-methoxybenzoyl groups (See Figure 10).[109] Compared to the previous series, no modification of the absorption maxima could be demonstrated, despites the presence of methoxy substituents onto 11-13. Among the most interesting finding, migratability of 13 was determined as being considerably reduced compared to 11 and 12, as a result of its tridimensional character. Thus, a 3-fold reduction of extracted photoinitiators could be determined for TMPTA resins prepared with three-component dyes/Iod/EDB (0.3%/1%/1%

w/w/w) systems. Ratios of 2%, 1.54% and 0.61% of extractability were determined for 11-13 respectively.

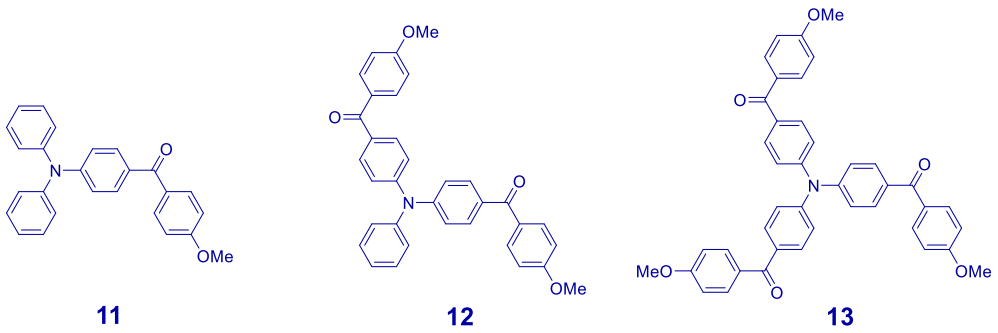

Figure 10. Chemical structures of 11-13.

Considering the remarkable photoinitiating ability of 9, comparisons were also established between 9 and different triphenylamine-based benzophenones differing by the substitution pattern of the triphenylamine moiety.[217] Influence of the distance between the triphenylamine moiety and benzophenone was notably examined as exemplified with the dye 17 (See Figure 11). Here again, benefits of the triphenylamine moiety on the absorption spectra of 14-17 were clearly evidenced. Thus, if the absorption of benzophenone was inexistent after 300 nm, an onset of absorption at 450 nm could be determined for 9, and 14-17. Notably, absorption maxima located at 341, 368, 369 and 374 nm could be found for 14-17 respectively in dichloromethane (See Figure 12). All dyes showed a remarkable thermal stability, decomposition temperatures ranging from 256 to 301°C being determined under nitrogen. The highest decomposition temperature was determined for 17 (301°C), followed by 16 (300°C), 15 (287°C), 14 (258°C) and 9 (256°C). These values are greatly higher than that determined for benzophenone (115°C). The higher decomposition temperature of 16 and 17 compared to the others was assigned to the higher polyaromaticity of these two dyes. Among the five dyes, the highest monomer conversion determined during the FRP of TMPTA under UV light irradiation were obtained with benzophenone and 9 while using the two-component dye/TEOA combination. Especially, a two-fold reduction of the monomer conversion was obtained with the two-component 17/TEOA system. Interestingly, the worse monomer conversion was obtained with 15, bearing electron donating methoxy groups. As a result of this substitution, 15 was more difficult to oxidize than 9 and 17, adversely affecting its photoinitiating ability. Efficiency of the electron transfer was also determined as being dependent of the steric hindrance of triphenylamines. Thus, compared to dye 9, a severe reduction of the monomer conversion was determined with 16 bearing a naphthalene substituent. These trends were confirmed upon irradiation with a white LED.

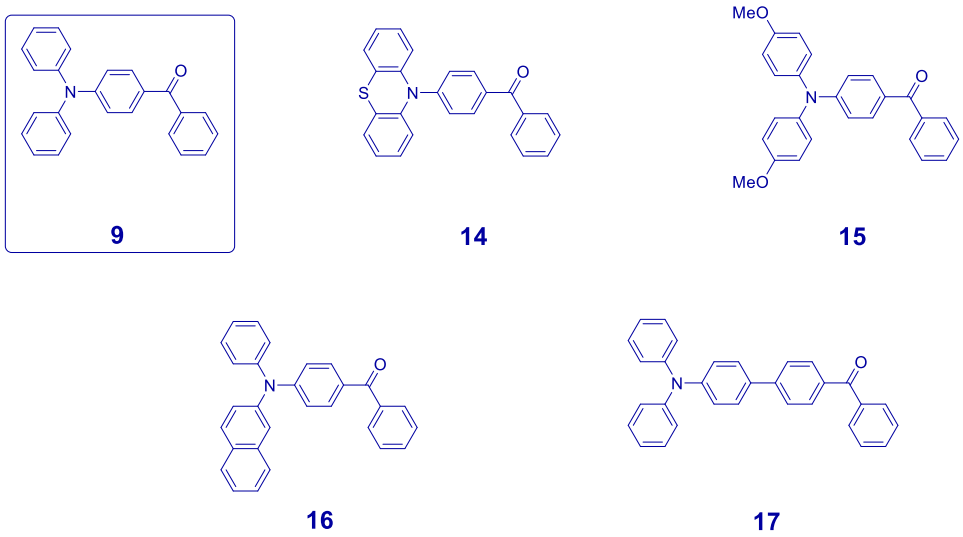

Figure 11. Chemical structures of 9, 14-17.

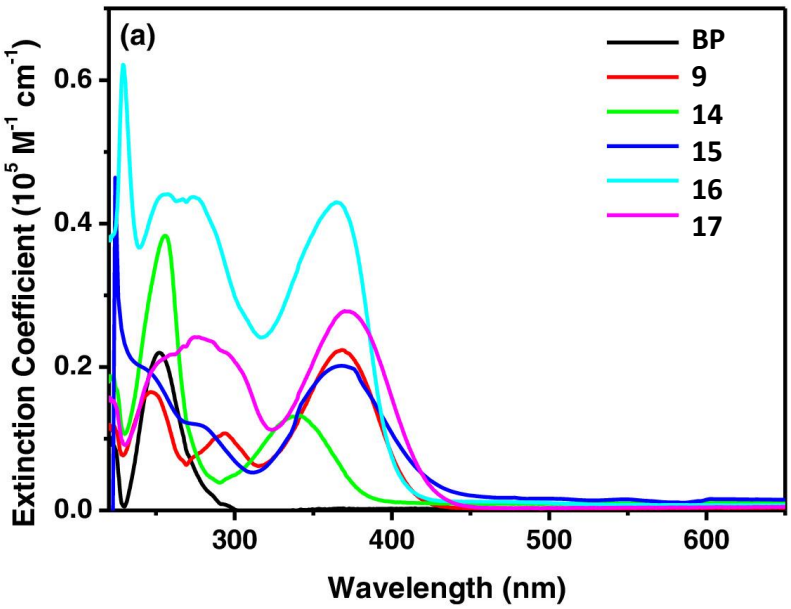

Figure 12. UV-visible absorption spectra of 9, 14-17 in dichloromethane. Reproduced with permission of Huang et al.[217]

Finally, the covalent linkage of benzophenone and triphenylamine by mean of an acetylene bridge was examined with 18 (See Figure 13).[218] By using an acetylene bridge as the spacer, an efficient electronic communication could be obtained between the two partners. Evaluation of the solvatochromic properties of 18 in solvents of different polarities revealed a positive solvatochromism, consistent with a significant electronic redistribution upon photoexcitation. As a result of this, the excited state of 18 showed clear intramolecular charge transfer features. Noticeably, 18 could not initiate FRP processes when combined with TEOA in two-component systems. Conversely, when combined with an iodonium salt, the resulting

two-component system was more competitive than the reference camphorquinone/TEOA combination.

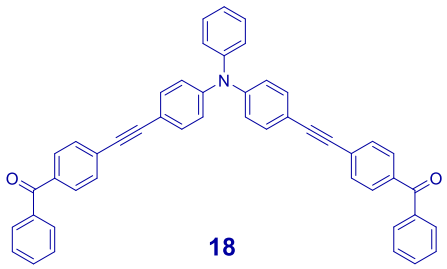

Figure 13. Chemical structure of 18.

1.3. Dithienophosphole derivatives

Organic Electronics is a source of inspiration for photopolymerists as the requirements for dyes usable in Molecular Electronics are similar to those needed for designing photoinitiators of polymerization. Notably, dyes should exhibit a broad absorption over the visible range. Dyes should also be capable to easily oxidize or reduce in order to exchange electrons with the adjacent layers in multilayered devices. In 2018, dithienophospholes previously used for the design of Organic Light-Emitting Diodes[219] were used as visible light photoinitiators of polymerization.[220] Two dyes i.e. 19 and 20 were examined, with and without triphenylamine moiety (See Figure 14).

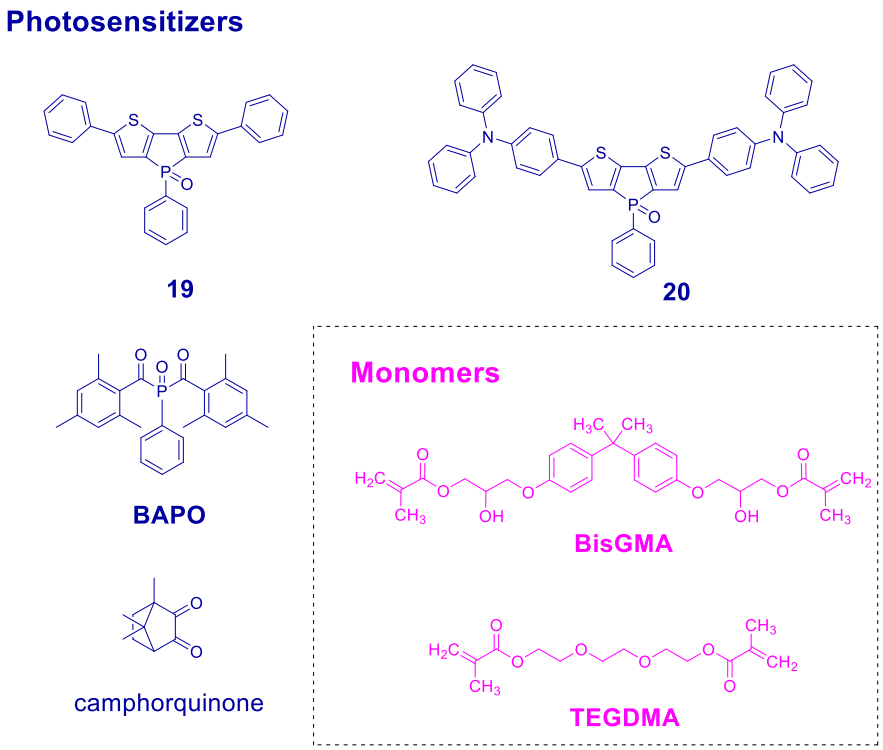

Figure 14. Chemical structures of dithienophosphole derivatives 19 and 20, and monomers.

As shown in the Figure 15, major differences could be found between 19 and 20 in acetonitrile. Notably, if an absorption maximum located at 420 nm was determined for 19, a redshift by ca 45 nm was found for 20, peaking at 465 nm. Jointly, a 3-fold enhancement of the molar extinction coefficient could be found for 20. Considering that the two dyes exhibit the same molar extinction coefficients at 405 nm, around 12 000 $M^{-1}.cm^{-1}$, polymerization tests were carried out at this wavelength (See Table 5). During the CP of EPOX at 405 nm with two-component dye/Iod combinations (0.5%/1% w/w), the efficiency trend was determined as being directly related to the molar extinction coefficient at 405 nm so that the following order of reactivity was determined : 20 >> 19 >> BAPO, going from 53% monomer conversion for 20 to 15% for BAPO.

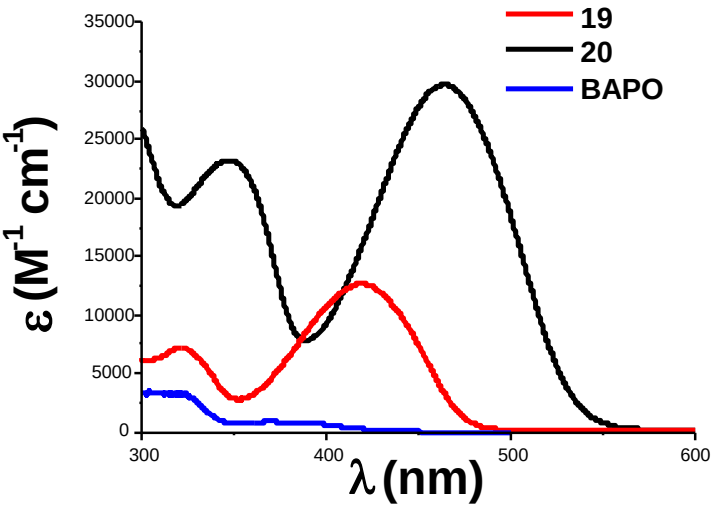

Figure 15. UV-visible absorption spectra of dithienophospholes 19 and 20 in acetonitrile, and BAPO in dichloromethane. Reprinted with permission from Al Mousawi et al.[220]

Table 5. Absorption properties for dithienophospholes 19 and 20, and BAPO.

Absorption properties	19	20	BAPO
λ_{max} (nm)/ε@λ_{max} ($M^{-1}cm^{-1}$)	420/~12600	465/~30000	-----
ε@λ = 405nm ($M^{-1}cm^{-1}$)	~12000	~12800	~500

n.a: No absorption of light.

This efficiency trend was confirmed during the FRP of TMPTA. As shown in the Figure 16, in two-component dye/Iod (0.5%/1% w/w) systems, higher performances were obtained with 20 (47% conversion after 100 s in laminate) vs. 41% for 19. Upon introduction of an amine (EDB), a significant enhancement of the final monomer conversion was obtained, reaching 80% for the three-component 20/Iod/EDB (0.01%/1%/1% w/w/w) vs. 30% for the two-component

20/Iod (0.01%/1% w/w). Conversely, only a low monomer conversion was obtained with the two-component 20/EDB (0.01%/1% w/w), around 2%. Therefore, the role of EDB as a sacrificial amine to regenerate the oxidized photosensitizer without participating in the production of radicals via a reductive pathway could be clearly evidenced. Considering the high reactivity of 20, a photosensitizer concentration as low as 0.01% could be used, without adversely affecting the monomer conversion.

The BisGMA/TEGDMA (70%/30% w/w) blend is widely used in dentistry [221–226] so that polymerization of this resin was examined under air upon irradiation at 405 nm with a LED. Remarkably, tack free polymers could be obtained, even for thick samples. Here again, addition of EDB as the electron donor contributed to increase of the final monomer conversion, up to 63% for the three-component 20/Iod/EDB (0.01%/1%/1%) system instead of 53% for the two-component 20/Iod (0.01%/1% w/w) system (See Figure 17).

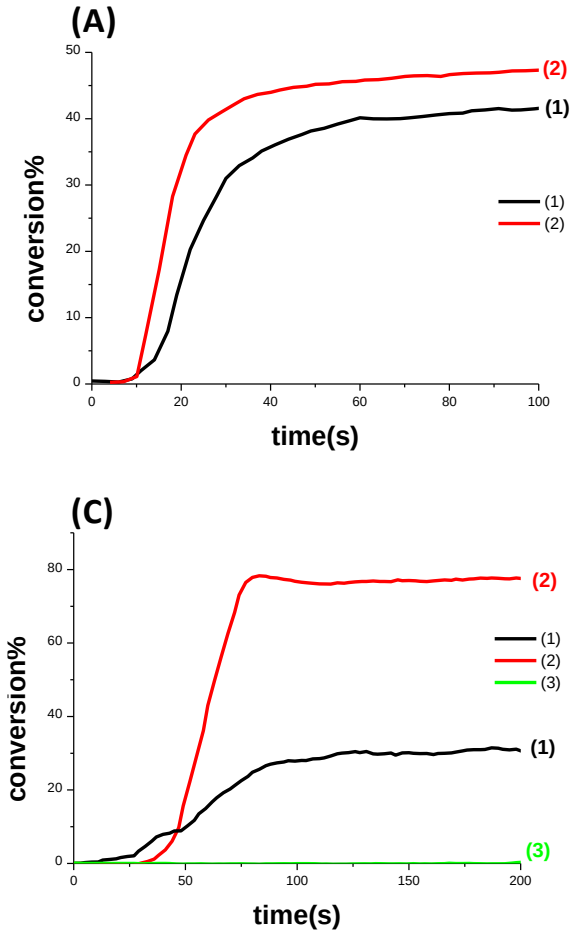

Figure 16. Polymerization profiles of TMPTA in laminate (thickness = 25 μm) upon exposure to LED@405 nm in the presence of (1) 19/Iod (0.5%/1% w/w) and (2) 20/Iod (0.5%/1% w/w). Reprinted with permission from Al Mousawi et al.[220]

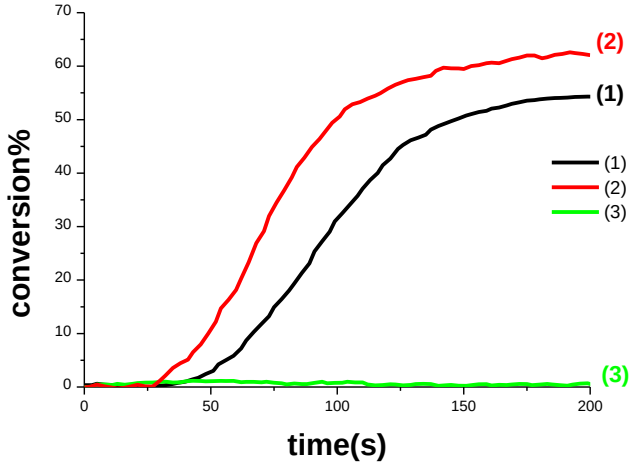

Figure 17. Polymerization profiles of BisGMA/TEGDMA under air (1.4 mm thick sample) in the presence of (1) 20/Iod (0.01%/1% w/w), (2) 20/Iod/EDB (0.01%/1%/1% w/w), and (3) 20/EDB (0.01%/1% w/w). Reprinted with permission from Al Mousawi et al.[220]

These values are greatly higher than what can be obtained with the reference four-component system based on camphorquinone (50% monomer conversion in the same irradiation conditions).[227]

1.4. Polythiophene derivatives

Thiophene is a structure widely used for the design of semiconductors used in Organic Electronics. Due to its remarkable electron-donating ability, numerous thiophene derivatives have also been used for the design of chromophores used in Organic Photovoltaics. In 2015, a series of star-shaped *tris*(4-(thiophen-2-yl)phenyl)amine derivatives was tested as photoinitiators at 405 and 455 nm (See Figure 18).[136] Due to their important π-electron delocalization, 21 and 22 exhibit a broad absorption band ranging between 300 and 500 nm, making these polythiophene structures suitable candidates for photoinitiation at different wavelengths (See Figure 19). Especially, the huge molar extinction coefficients (129 600 $M^{-1}.cm^{-1}$ and 141 700 $M^{-1}.cm^{-1}$ for 21 and 22 respectively) at the absorption maxima were notably assigned to the presence of the three branches contributing to enhance the molar extinction coefficients.[228]

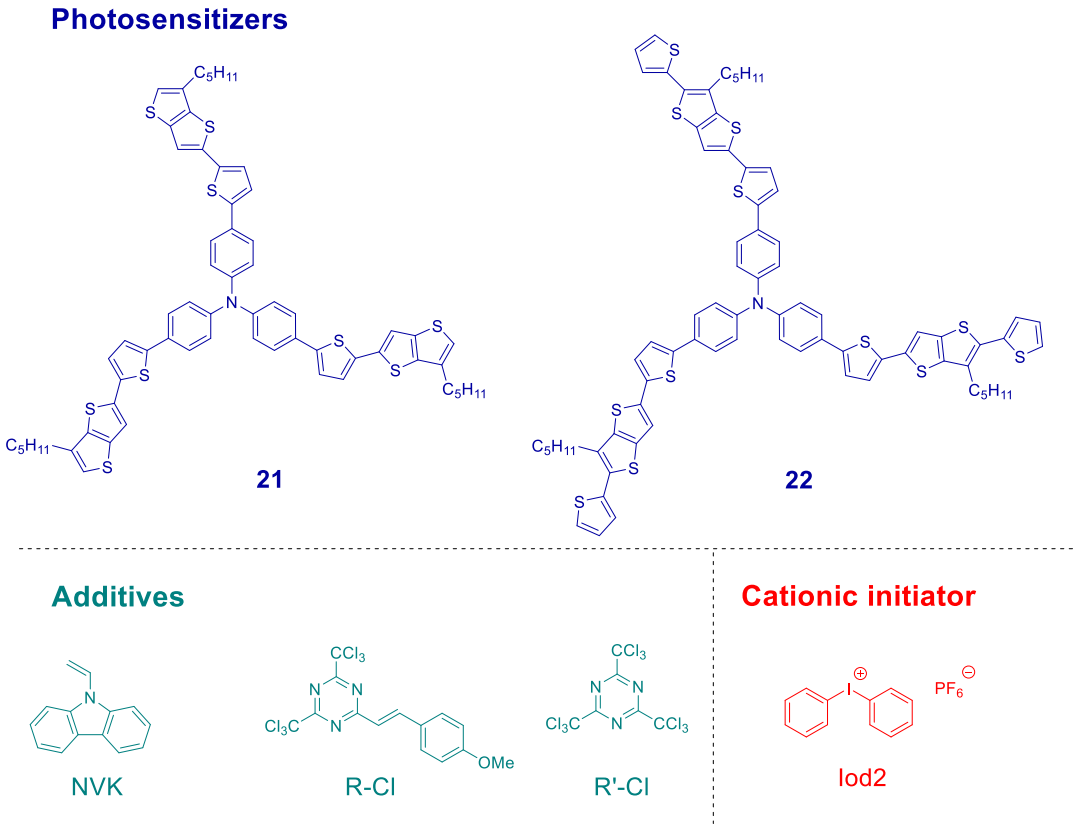

Figure 18. Chemical structures of polythiophene derivatives 21 and 22, and additives.

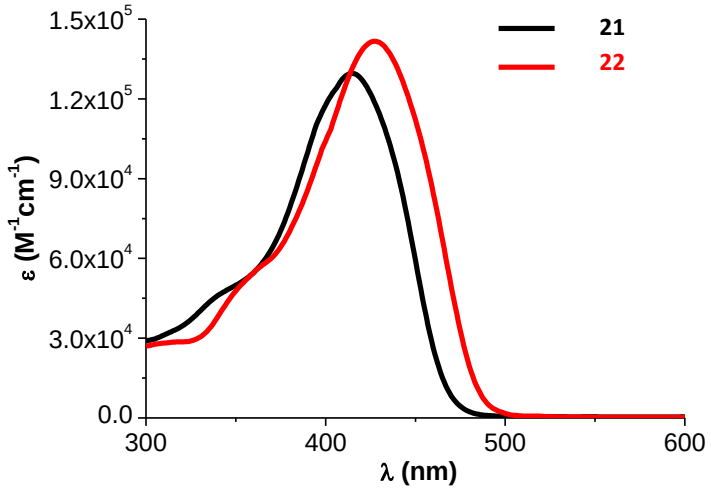

Figure 19. UV-visible absorption spectra of 21 in acetonitrile/toluene (50%/50%, V/V) and 22 in tetrahydrofuran. Reprinted with permission from Zhang et al. [136]

When tested as photoinitiators for the CP of EPOX, the 21/Iod2 (0.5%/2% w/w) combination furnished the best conversion at 455 nm (60% conversion vs 49% with a halogen lamp), this wavelength corresponding to the maximum absorption of the dye. A lower conversion was obtained upon irradiation at 455 nm with 22, due to the low solubility of this dye in EPOX. Additionally, a lower reactivity was also expected for this dye, due to the presence of additional thiophene units favouring the delocalization of the positive charge and

lowering the reactivity of $22^{\bullet+}$. While using the three-component dye/Iod2/NVK (0.5%/2%/3% w/w/w) systems (where NVK stands for *N*-vinylcarbazole), on a slight improvement of the final monomer conversions were obtained upon irradiation with a halogen lamp compared to the two-component dye/Iod2 (0.5%/2% w/w) system excited in the same conditions, evidencing the high reactivity of the $dye^{\bullet+}$ radical cation towards EPOX. Indeed, NVK is classically used in photocurable resins to generate the highly reactive Ph-$NVK^{\bullet+}$ radical cations.[2,65,173,229] Interestingly, upon irradiation at 405 nm, an improvement of the monomer conversion was obtained for the 22/Iod2/NVK system, peaking at 55% vs 41% with the halogen lamp. Noticeably, irrespective of the photoinitiating systems used, the two dyes clearly outperformed the camphorquinone-based photoinitiating system since no polymerization could be detected at 405, 455 nm or upon irradiation with a halogen lamp with this reference system. Lastly, stability of the photocurable resins prepared with 22 over time was also examined. Thus, after one month of storage, only a decrease of 4% of the monomer conversion was obtained for the EPOX resin comprising the 22/Iod2/NVK photoinitiating system (See Table 6). The high reactivity of 22 over 21 was confirmed during the FRP of BisGMA/TEGDMA under air. If the two-component 21/Iod2 system furnished a moderate conversion upon irradiation at 405 and 455 nm with a LED, an improvement of the monomer conversion was obtained while replacing the iodonium salt by 2-(4-methoxystyryl)-4,6-*bis*(trichloromethyl)-1,3,5-triazine (R–Cl) or 2,4,6-*tris*(trichloro-methyl)-1,3,5-triazine (R'–Cl). An enhancement of the monomer conversion by ca 20% could be determined. Remarkably, upon irradiation at 405 and 455 nm, 16-based photoinitiating systems can efficiently overcome the oxygen inhibition, contrarily to the camphorquinone-based photoinitiating systems and *bis*(2,4,6-trimethylbenzoyl)-phenylphosphineoxide) BAPO that can only furnish low monomer conversions. Here again, a good stability of the BisGMA/TEGDMA resins upon storage was demonstrated since only a minor variation of the monomer conversion was demonstrated after one month of storage (~ 3%) (See Table 7).

Table 6. EPOX conversions obtained under air upon exposure to different light sources for 800 s in the presence of 21/22-based PISs; CQ/Iod2 or CQ/Iod2/NVK as references; 21/22 or CQ: 0.5 wt%; Iod2: 2 wt%; NVK: 3 wt%.

PIS	LED (385 nm)	LED (405 nm)	LED (455 nm)	LED (470 nm)	Halogen lamp
21		np[a]			
21/Iod2		55%	60%	54%	49%[b]
21/Iod2/NVK	63%	57%			57% | 61%[c]
22/Iod2		43%	41%	30%	31%
22/Iod2/NVK		55%			41%
CQ/Iod2					np[a]
CQ/Iod2/NVK					np[a]

[a] no polymerization; [b] tack free coatings are obtained when conversions are ≥ 49%; [c] measured after storage at room temperature for one week.

Table 7. Photopolymerization conversions of BisGMA/TEGDMA blend (70%/30%, w/w) obtained **under air** upon exposure to LED at 385 nm, 405 nm or 455 nm, or halogen lamp for 300 s in the presence of 21/22-based PISs; BAPO or CQ based PISs as references. 21/22, BAPO, or CQ: 0.5 wt%; Iod2, EDB or MDEA: 2 wt%; NVK, R-Cl or R'-Cl: 3 wt%.

.

PISs	Halogen lamp	LED (385nm)	LED (405nm)	LED (455 nm)
21/Iod2			37%	26%
21/Iod2/NVK	18%	35%	50% ǀ 48%[a]	42%
22/Iod2/NVK			24%	
21/EDB			np[b]	
21/EDB/R-Cl	8%		55% ǀ 58%[a]	34%
21/EDB/R'-Cl			56%	
BAPO			44%	
CQ/Iod2/NVK				np[b]
CQ/MDEA				8%

[a] measured after storage at room temperature for one week.
[b] no polymerization.

Based on photolysis experiments, the following mechanism could be proposed for *tris*(4-(thiophen-2-yl)phenyl)amine (TPAD). Notably, in the context of the oxidative process, Ph• and Ph-NVK• are the two initiating radicals for the FRP of BisGMA/TEGDMA (See equations r10-r14 in scheme 3). Conversely, for the reductive pathway, $EDB_{(-H)}$• and R• are produced and constitute excellent initiating species (See equations r15-r18 in Scheme 3).

$$TPAD \rightarrow {}^{1}TPAD\ (h\nu) \quad \text{and} \quad {}^{1}TPAD \rightarrow {}^{3}TPAD \qquad (r10)$$

$$^{1,3}TPAD + Ph_2I^+ \rightarrow TPAD^{\bullet+} + Ph_2I^{\bullet} \qquad (r11)$$

$$Ph_2I^{\bullet} \rightarrow Ph^{\bullet} + Ph\text{-}I \qquad (r12)$$

$$Ph^{\bullet} + NVK \rightarrow Ph\text{-}NVK^{\bullet} \qquad (r13)$$

$$Ph\text{-}NVK^{\bullet} + Ph_2I^+ \rightarrow Ph\text{-}NVK^+ + Ph^{\bullet} + Ph\text{-}I \qquad (r14)$$

$$^{1,3}TPAD + EDB \rightarrow TPAD^{\bullet-} + EDB^{\bullet+} \rightarrow TPAD\text{-}H^{\bullet} + EDB_{(-H)}^{\bullet} \qquad (r15)$$

$$TPAD^{\bullet-} + R\text{-}Cl \rightarrow TPAD + (R\text{-}Cl)^{\bullet-} \qquad (r16)$$

$$TPAD\text{-}H^{\bullet} + R\text{-}Cl \rightarrow TPAD + H^+ + (R\text{-}Cl)^{\bullet-} \qquad (r17)$$

$$(R\text{-}Cl)^{\bullet-} \rightarrow R^{\bullet} + Cl^- \qquad (r18)$$

Scheme 3. Mechanism supporting the polymerization efficiency of thiophene-substituted triphenylamine.

1.5. Pyrene derivatives

One efficient strategy to significantly increase the molar extinction coefficient of well-known photoinitiators consists in obtaining a strong coupling of its molecular orbitals with that of a polyaromatic structure that will contribute to drastically increase the molar extinction coefficient.[214,230] In this field, pyrene is a promising photoinitiator of polymerization but suffers from a lack of absorption in the visible range.[75] This issue was addressed by generating a hybrid pyrene-triphenylamine structure (See Figure 20).[71] By connecting three pyrene units to triphenylamine, improved absorption properties in the visible range could be obtained. Thus, if pyrene does not absorb in the visible range (λ_{max} = 334 nm in acetonitrile), conversely, an absorption spectrum extending until 450 nm could be determined in toluene for 23 (λ_{max} = 365 nm in toluene). Especially, a redshift of the absorption maximum of 31 nm could be obtained for 18 compared to pyrene. When tested as photoinitiators for the CP of EPOX-Si, no major difference was found between pyrene and 18. Indeed, when tested in two-component 23/Iod (0.2%/2% w/w) system upon irradiation with a Xe-Hg lamp under air, a final monomer of 52% being obtained after 200 s of irradiation with 23, close to that obtained with pyrene (51% conversion). Noticeably, a thermal polymerization process could be evidenced with 23. Indeed, after 24 h, a final monomer conversion of 55% was determined for EPOX-Si with the two-component 23/Iod (0.2%/2% w/w) system. This ability to proceed smoothly was evidenced by EPR experiments, the presence of $23^{\bullet+}$ being detected even 24h after the polymerization test. Conversely, no polymerization was detected for the pyrene-based resin, even after several days.

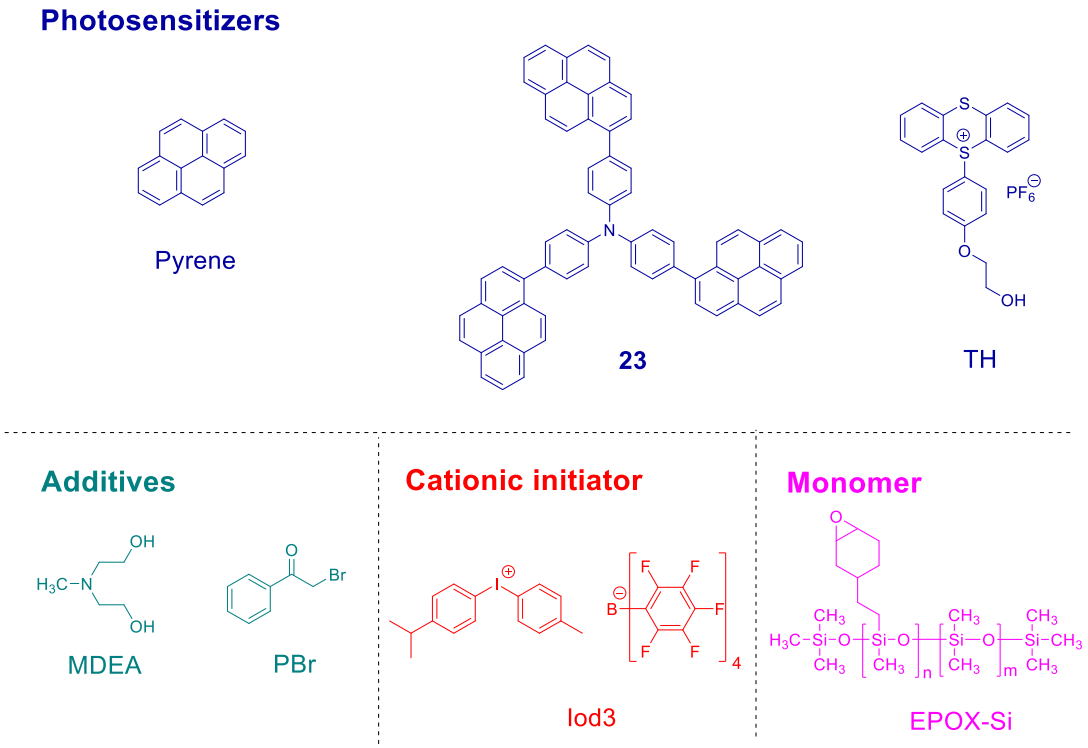

Figure 20. Chemical structures of pyrene-based triphenylamine 23, different additives and monomers.

1.6. Curcuminoid derivatives

Recently, biosourced or bioinspired photoinitiators of polymerization have been the focus of intense research efforts due to their low costs and easy availability.[208] In this field, curcumin is a yellow-orange pigment that can be found in Indian spice plant and this molecule exhibits promising anti-tumoral, anti-HIV, anti-inflammatory, and anti-oxidant properties.[231–233] Parallel to its pharmalogical properties, curcumin has been extensively used as photoinitiators of polymerization,[234–238] its absorption maximum ranging between 410 and 430 nm depending of the organic solvent used.[239] Curcumin is also soluble in most of the common monomer and this molecule is also none toxic, making this molecule an appealing scaffold for the design of various derivatives. Notably, curcumin was used as photoinitiator as soon as 2005 by Crivello and coworkers for the sensitization of iodonium salts.[240,241] In 2018, a curcuminoid comprising two triphenylamine units standing at both ends (24) was designed and compared with its dimethylamino analogue 25 (See Figure 21).[242] Interestingly, by elongating the π-conjugation in 24 and 25, dyes absorbing in the 350-600 nm range were obtained, with an absorption maximum located at 467 and 470 nm respectively for 24 and 25. While examining the solvatochromism of 24 and 25 in solvents of different polarities, a positive solvatochromism could be evidenced, the enol form being favored over the ketone form in polar solvents.

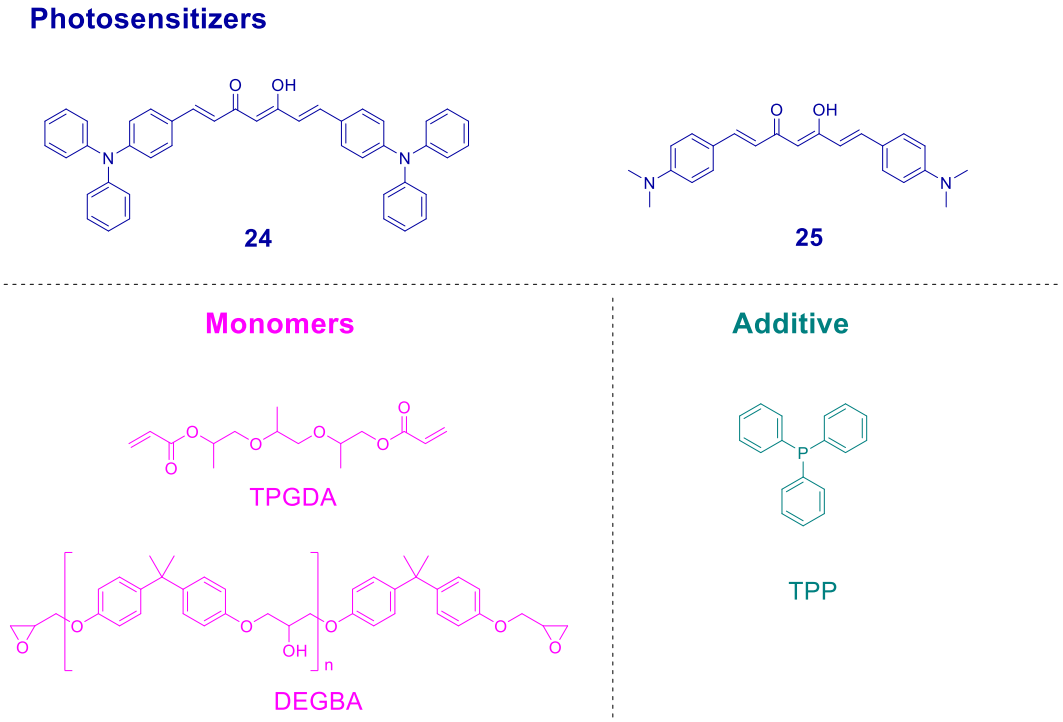

Figure 21. Chemical structures of curcuminoid derivatives 24 and 25, different monomers and additive.

Interestingly, 25 could not initiate the CP of diglycidyl ether of bisphenol A (DGEBA), the dimethylamino groups contributing to terminate the propagating cationic chains.[243] Conversely, using the two-component 24/Iod (0.2%/3% w/w) system, a final monomer

conversion of 56% could be obtained after 300 s upon irradiation with a blue LED. For comparison, a conversion of 42% was obtained with curcumin in the same condition. While irradiation with a green LED, a significant decrease of the conversion (46% for 24, 24% for curcumin) was detected, attributable to a reduction of the molar extinction coefficient of the different dyes at this wavelength. Upon addition of NVK, an improvement of the monomer conversion was obtained with the different three-component dye/Iod/NVK (0.2%/3%/2% w/w/w) systems (61% for 24, 47% with curcumin) and this enhancement was assigned to the formation of the highly reactive Ph-NVK$^+$ species. During the FRP of tripropylene glycol diacrylate (TPGDA), a different order or reactivity could be determined upon irradiation with a blue LED. Indeed, using the same two-component systems, a similar monomer conversion was obtained with 25 and curcumin (87%) outperforming that of 24 (83%). However, upon irradiation with a green LED and due to the lack of absorption of curcumin at this wavelength, no polymerization could be detected anymore. Conversely, due to the specific lateral substitution of 24 and 25, a final monomer conversion of 77 and 73% could be determined after 150 s of irradiation. Introduction of triphenylamine (TPP) (2% w) into the previous photoinitiating system increased markedly the monomer conversion, triphenylamine being capable to overcome the oxygen inhibition.[234,244] Thus, upon irradiation with a blue LED, a monomer conversion of 70% was obtained with the three-component 24/Iod/TPP (0.2%/3%/2% w/w/w) system after 20 s of irradiation contrarily to 21% with the two-component 24/Iod (0.2%/3% w/w) system. Interestingly, a good bleaching was observed during the polymerization process, enabling to get colorless coatings (See Figure 22).

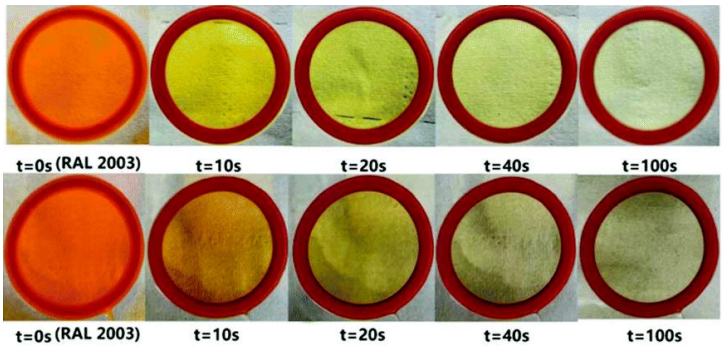

Figure 22. Modification of the sample colors during polymerization for TPGDA-based resins, using two-component dye/Iod (0.2%/3% w/w) systems. Top : 24, Bottom : 25. Reprinted with permission from Han et al. [242]

1.7. Benzylidene ketone derivatives

The search for photoinitiating systems exhibiting photobleaching properties is a long-standing issue.[245,246] Especially, this issue is of crucial importance for the photopolymerization of ceramic suspension. Indeed, to achieve the polymerization of thick sample, a decrease of the optical density should be obtained during the polymerization process so that a higher light penetration within the sample can be obtained.[247,248] In this field, the camphorquinone/amine system is a popular combination but requires long irradiation time to

get a reduction of the optical density by ca 50% (around 1000 s).[249–254] Therefore, the search for new dyes capable to bleach more rapidly and more efficiently than the camhorquinone/amine combination have been actively researched. In this field, a family of structures strongly related to curcumin was identified as being promising, namely benzylidene ketones.[215,255–269] In 2019, a benzylidene ketone comprising a triphenylamine unit was examined as photoinitiator for the polymerization of ceramic suspensions (See Figure 23).[270] Interestingly, 26 showed a broad absorption band extending between 350 and 500 nm, making this dye a suitable candidate for long-wavelength irradiation with LEDs emitting at 460 and 520 nm. As interesting feature, polymerization efficiency of TPGDA in the presence of two-component 26/TEA (where TEA stands for triethanolamine) could be improved by increasing the amine content from 0.75% to 6%, from 40 to 70% upon irradiation at 460 nm. Using the two-component 26/TEA (0.1%/3% w/w) system, an efficient photobleaching of the resin was observed, within 20 s upon irradiation at 460 nm. Considering that efficient photoinitiating system could be prepared with an amine, the mechanism depicted in the Scheme 4 was proposed. Notably, after promoting a photoinduced electron transfer from TEA to the dye, a proton transfer from the oxidized amine $TEA^{\bullet+}$ towards the radical anion $26^{\bullet-}$ can occur, producing a radical $26^{\bullet}$ in which the π-conjugation was interrupted, suppressing the color to the dye and enabling to get colorless coating.

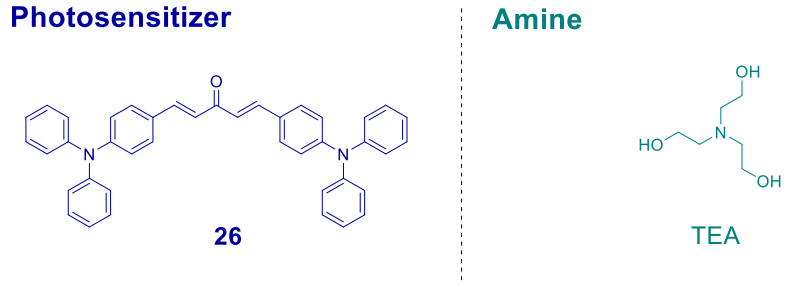

Figure 23. Chemical structure of 21 and TEA.

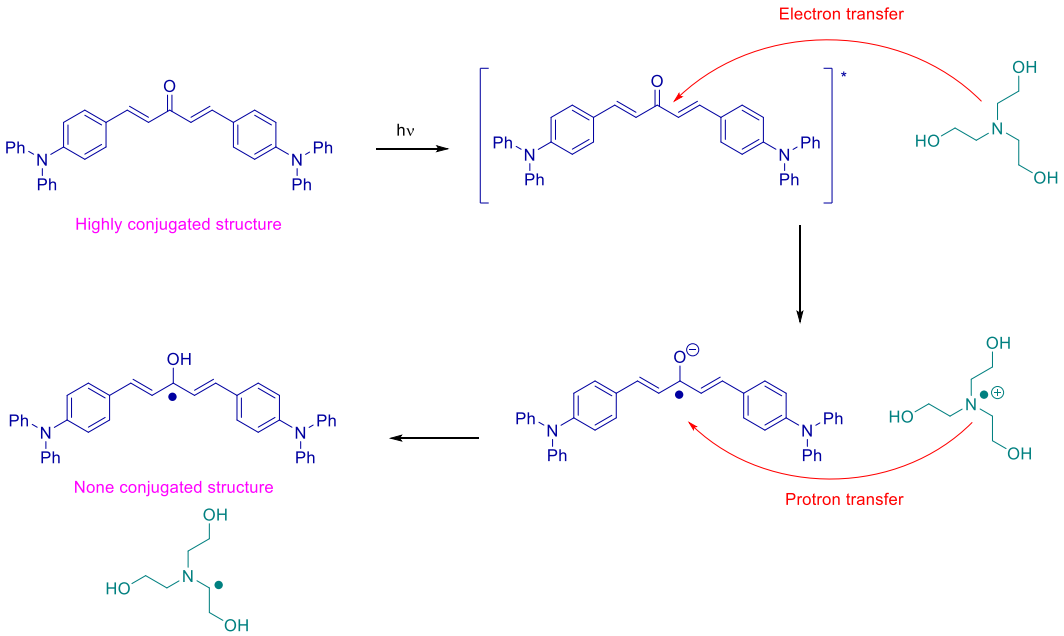

Scheme 4. Mechanism supported the photobleaching observed during photopolymerization.

Considering that the light penetration is the key element for the curing of thick sample, deep photopolymerization experiments were carried out with TPGDA using 26, and concentrations ranging between 1 wt% to 0.016 wt% were examined in two-component system, the amine content being maintained to 3 wt%. Thus, upon irradiation at 460 nm, the cure depth could vary from 0.3 cm at 1 wt% to 6.8 cm upon reduction of the dye concentration until 0.016%. Conversely, upon irradiation at 560 nm, the best conversion was obtained at 0.031 wt%, with a polymerization depth of 6.1 cm (See Figure 24). In the case of ceramic suspensions, presence of fillers severely impedes light penetration within the sample. Consequently, a drastic reduction of the cure depth could be evidenced. Thus, cure depth ranging from 0.45 mm at 1 wt% to 0.95 mm at 0.016 wt% could be determined at 460 nm. Conversely, upon irradiation at 560 nm, a cure depth of 1 mm was obtained at the concentration of 0.063 wt%. While reducing the dye concentration to 0.016 and 0.008 wt%, a reduction of the cure depth to 0.8 and 0.6 mm was observed, resulting from less radicals produced within the resin at low concentration.

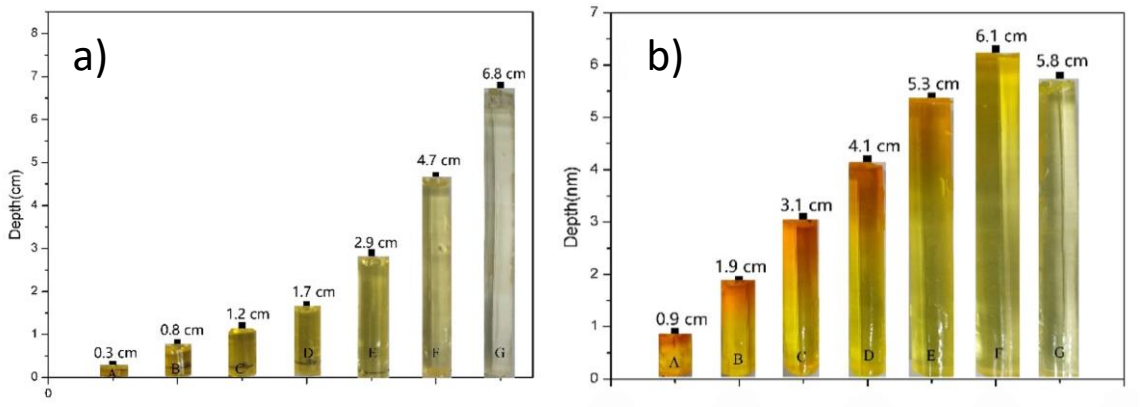

Figure 24. Depth of photocured samples determined as a function of the dye concentration upon irradiation with LEDs at 460 nm and 520 nm. a): 21/TEA under 460 nm LED; b): 26/TEA under 520 nm LED. TPGDA: 100 wt%; TEA: 3 wt%; dye: A:1.000 wt %; B:0.500 wt %; C:0.250 wt %; D:0.125 wt %; E:0.063 wt %; F:0.031 wt %; G:0.016 wt %. Reprinted with permission from Fu et al. [270]

1.8. Flavonol derivatives

In photopolymerization technology, dyes acting as photosensitizers are facing numerous concerns. Indeed, most of the time, dyes are not consumed during the polymerization process so that their potential toxicity, their migratability out of the polymers can constitute major impediment for future uses of the resulting polymers. To address this issue, use of natural products as photoinitiators are more and more widely studied. Flavonols can be found in numerous fruits and vegetables and these structures are well-known to exhibit a low cytotoxicity and a good biocompatibility so that flavonols were candidates of choice for photoinitiation.[271–279] However, flavonols also suffer from an excited state intramolecular

electron transfer (ESIPT) that can adversely affect the photoinitiating properties.[79–81,280–282] Indeed, ESIPT process can be competitive with photoinitiation. To overcome this problem, the hydroxyl group of flavonols can be substituted with various groups, inhibiting the proton transfer, reducing the fluorescence quantum yield and elongating the excited state lifetime. Overall, better photoinitiating properties can be anticipated. In 2021, triphenylamine substituted flavonols were designed to redshift its absorption compared to its parent flavonol. Parallel to this, the hydroxyl group was functionalized with a benzoate or a sulfonate group so that ESIPT could be advantageously avoided (See Figure 25).[283]

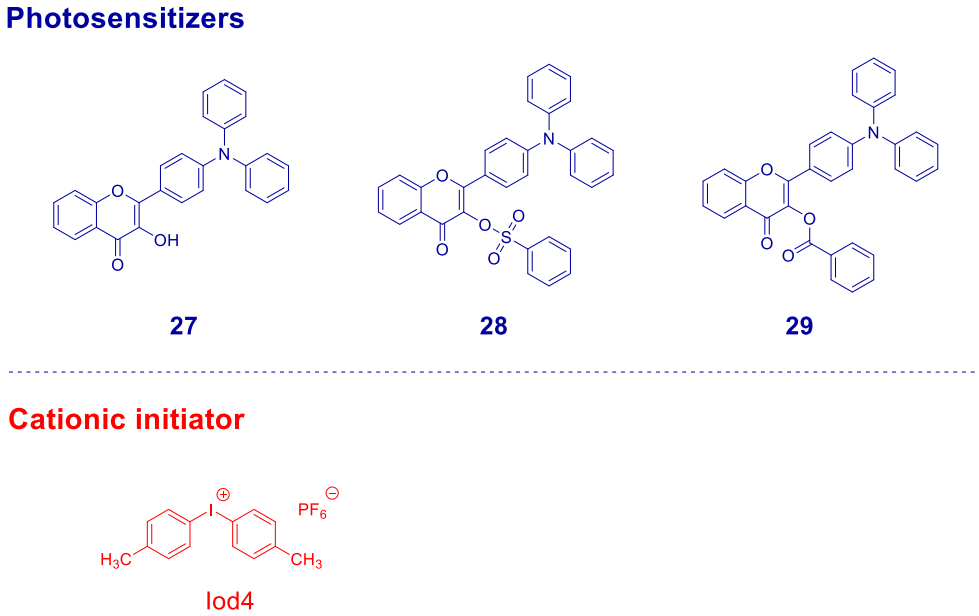

Figure 25. Chemical structures of flavonols 27-29 and Iod4.

From the absorption viewpoint, no modification of the absorption spectra was found between 27, 28 and 29, the three dyes exhibiting absorption maxima located at 396, 386 and 384 nm respectively. Indeed, the benzenesulfonate or the benzoate groups are introduced in lateral positions and do not participate to the electronic delocalization. All dyes exhibited high molar extinction coefficients, ranging between 23 000 $M^{-1}.cm^{-1}$ for 29 to 23800 $M^{-1}.cm^{-1}$ for 28. Interestingly, by replacing the benzoate group in 29 by a sulfonate group in 28, a drastic modification of the solubility properties was evidenced, 29 being soluble in organic solvents and 28 in water. Considering the broadness of the intramolecular charge transfer band ranging between 350 and 470 nm, photopolymerization tests could be carried out at 405 and 460 nm. Photoacid generation was examined using Rhodamine B as the pH indicator.[284] Comparison of the photolysis rates of 29 and 28 in acetonitrile revealed the photolysis process to be faster for 28. Therefore, a higher production of H^+ can be obtained with 28. To support the efficient production of proton, the mechanism depicted in the Scheme 5 was proposed by the authors. Notably, a homolytic cleavage of the sulfonate group can occur upon irradiation, generating a radical pair [dye-$O^{\bullet+}$ $^{\bullet}SO_2Ph$]. The sulfonyl $PhSO_2^{\bullet}$ radical can then react with water, producing benzenesulfonic acid.

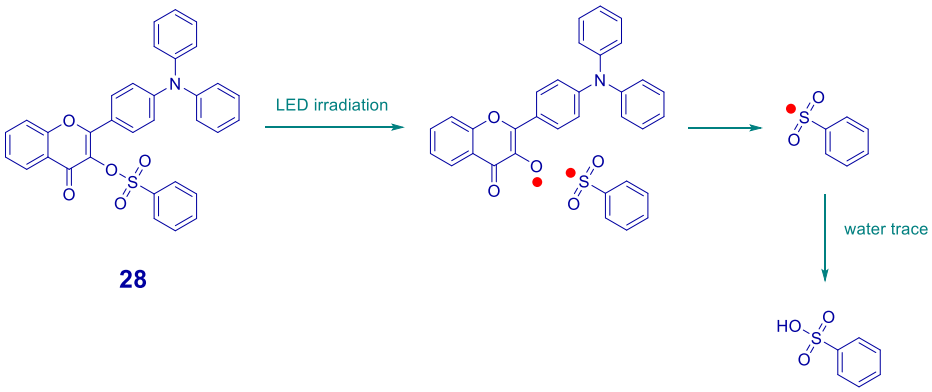

Scheme 5. Chemical mechanism supporting photoacid generation by 28.

Interestingly, all flavonols could act as single component photoinitiator during the FRP of TPGDA upon irradiation at 460 nm. Indeed, as shown during photoacid generation, photoexcitation of the dyes can produce radicals. Dye concentration as low as 0.125 wt% could be used, evidencing the reactivity of the generated radicals. Comparison between 27, 28, 29 and camphorquinone revealed the final monomer conversion of 28 to outperform that of camphorquinone (80% vs. 41% conversion). Conversely, a lower monomer conversion was obtained with 29 (20% conversion after 180 s of irradiation at 460 nm) (See Figure 26). This efficiency trend is consistent with that determined during photoacid generation. Indeed, the first step of photoacid generation consists in a homolytic cleavage of the sulfonate or the carboxylate bond. Flavonols were also tested in more conventional conditions, as photosensitizers for two-component systems with an iodonium salt (Iod4) or triethanolamine (TEA). Using the two-component dye/TEA (0.125%/3% w/w) system, monomer conversion higher than 80% could be obtained within 20 s, greatly higher than that obtained when using flavonols as mono-component systems.

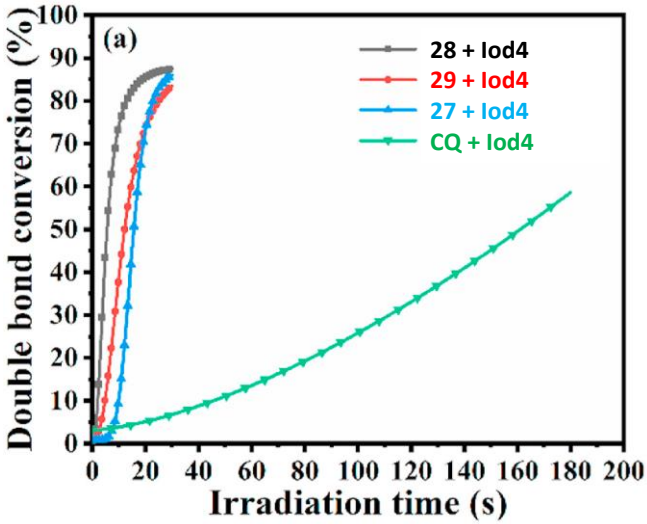

Figure 26. Photopolymerization profiles of TPGDA in the presence of 27-29/Iod4 (0.125%/1.0% w/w) and CQ/Iod4 (0.125%/1.0% w/w) upon irradiation with a 405 nm LED. Reprinted with permission from You et al. [283]

Finally, biocompatibility of the resulting polymers was demonstrated by examining the cells viability of HeLa cells. For these experiments, a BisGMA/TEGDMA blend was used, this mixture of monomers being classically used in dentistry. When using these polymers as a culture medium for HeLa cells for seven days, a cell viability higher than 80% was found for polymers prepared with 29, 28 and camphorquinone. Therefore, the aforementioned photoinitiating systems have great potential for the design of biomaterials. By combining photolysis experiments, cyclic voltammetry and EPR experiments, mechanisms could be deduced for flavonols used in combination with triethanolamine. Notably, aminoalkyl radicals can be formed by photoinduced electron transfer from flavonol (See Figure 27, mechanism B). Parallel to this, homolytic cleavage of the sulfonate group can produced benzenesulfonyl radicals, further evolving as phenyl radical by release of sulfur dioxide (See Figure 27, mechanism A). Finally, in the case of the oxidative process, photoinduced electron transfer from the excited dye towards the iodonium salt can produce initiating aryl radicals (See Figure 27, mechanism C).

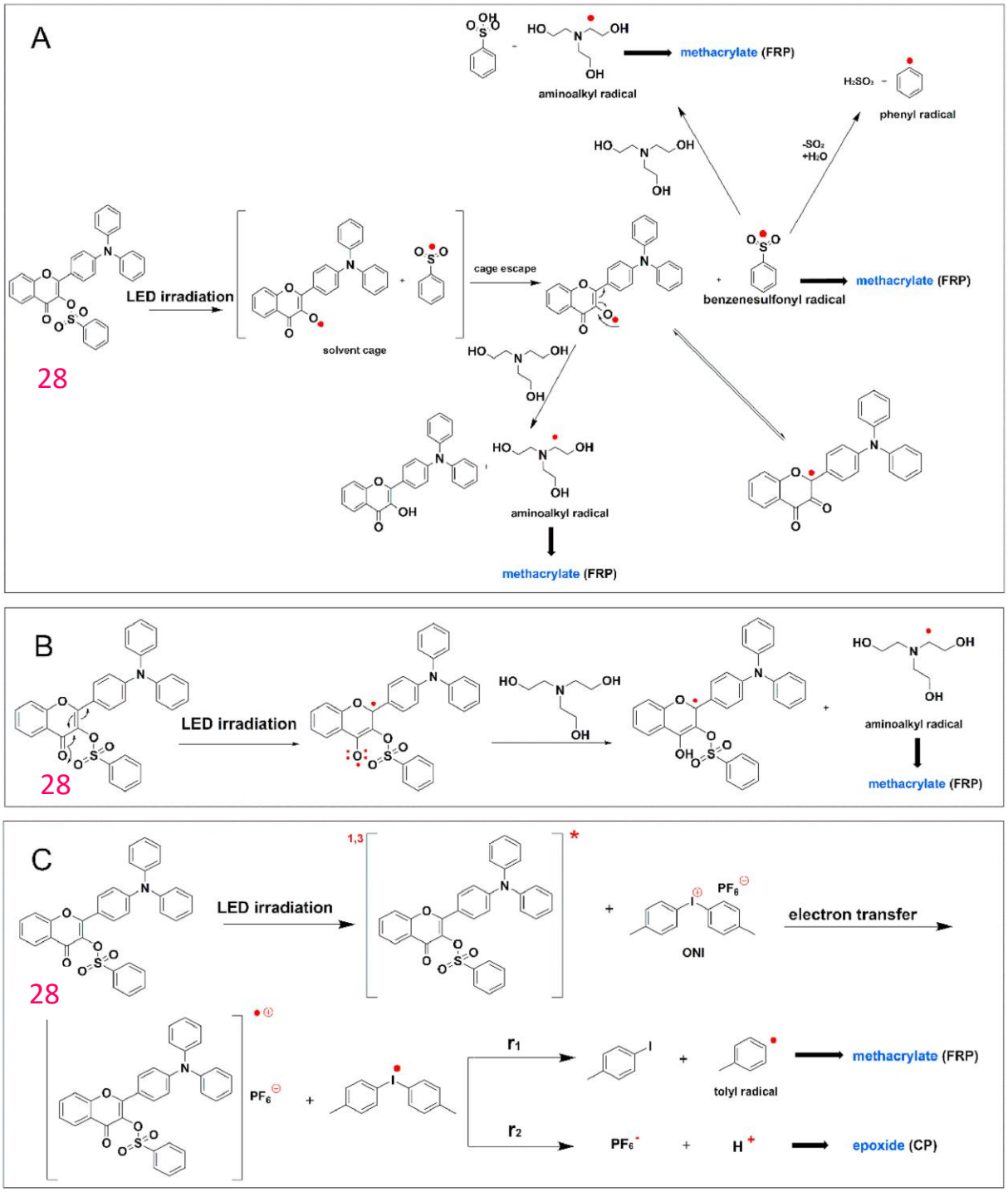

Figure 27. The different photochemical mechanism involved in the FRP of TPGDA using flavonols as the photosensitizers. Reprinted with permission from You et al. [283]

1.9. Chalcone derivatives

Chalcones are promising candidates for photoinitiation and the recent interest for this family of structures is supporting by their bioinspired scaffolds that could provide biocompatibility properties to the resulting polymers.[159,161] In 2020 and 2021, around 100 chalcones have been examined as photoinitiators od polymerization.[153–163] Concerning triphenylamine-based chalcones, six dyes 30-35 have been examined in several studies done by the group of Lalevée and coworkers (See Figure 28).[156,160,285] One year later, Wang and

coworkers revisited the photoinitiating ability of chalcone 34, previously tested by Lalevée and coworkers as visible light photoinitiator of polymerization.[286]

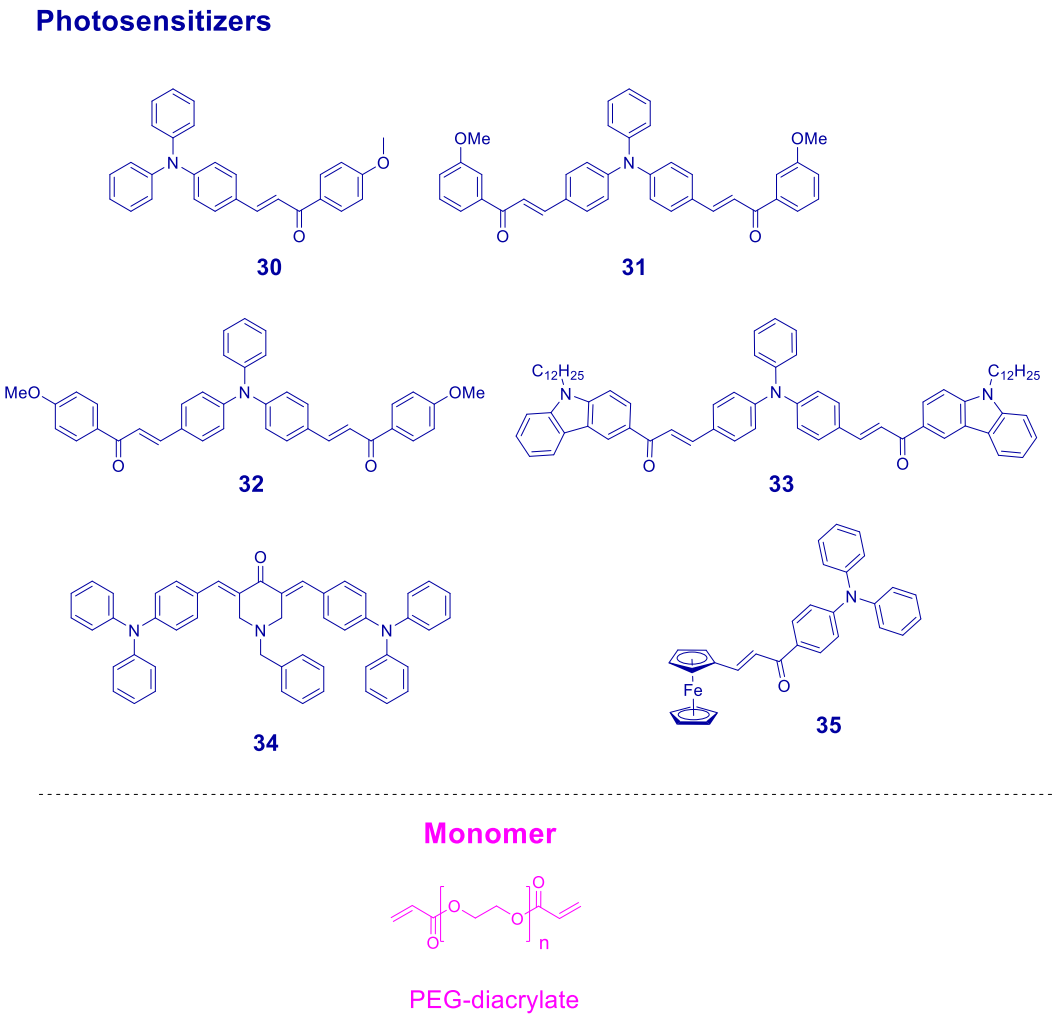

Figure 28. Chemical structures of triphenylamine-based chalcones 30-35.

Among all triphenylamine-based chalcones, only dye 35 showed an absorption maximum centered in the UV range (λ_{max} = 340 nm). For all the other dyes, absorption maxima ranging between 405 nm for chalcone 30 to 434 nm for 34 were determined in acetonitrile (See Table 8). Among all dyes, 34 exhibited the highest molar extinction coefficient (ε = 30800 $M^{-1}.cm^{-1}$), due to the presence of two triphenylamine units in this chalcone.

Table 8. Light absorption properties of chalcones 30-35 in acetonitrile: maximum absorption wavelengths λ_{max}; extinction coefficients at λ_{max} (ε_{max}) and extinction coefficients at the emission wavelength of the LED@405 nm ($\varepsilon_{@405nm}$).

	λ_{max} (nm)	ε_{max} ($M^{-1} cm^{-1}$)	$\varepsilon_{@405nm}$ ($M^{-1} cm^{-1}$)
chalcone 30	405	18740	18740
chalcone 31	430	7990	6760
chalcone 32	428	8540	7200
chalcone 33	430	10500	9020
chalcone 34	434	30800	23000
chalcone 35	340	29840	15340

Chalcones 30-33 were tested in four different photoinitiating systems, namely, chalcone/Iod/EDB (1.5%/1.5%/1.5%, w/w/w) chalcone/Iod (1.5%/1.5%, w/w), chalcone/EDB (1.5%/1.5%, w/w) and chalcones alone (1.5% w/w). Considering that these dyes were tested for 4D printing experiments, the FRP of a hydrophilic monomer was notably examined for dyes 30-33, namely PEG-diacrylate. Two different conditions were also examined i.e. the polymerization of thin (0.1 mm) and thick (2 mm) samples. Among the four polymerization conditions tested, no polymerization was detected with the chalcones, and only a polymerization in thin films was detected with the two-component chalcone/EDB (1.5%/1.5%, w/w) systems. Conversely, efficient monomer conversions were detected with the three-component chalcone/Iod/amine (1.5%/1.5%/1.5%, w/w/w) system as well as the two-component chalcone/Iod (1.5%/1.5%, w/w) systems in thin films. Surprisingly, no improvement of the final monomer conversion was detected between the two and the three-component system, evidencing the high reactivity of the two-component systems. Comparisons with the blank experiments done with the reference Iod/amine (1.5%/1.5% w/w) system revealed the two and three-component systems to outperform the reference system in thin films. Conversely, in thick films, only chalcone 30 could furnish a monomer conversion on par with that of the reference system (See Table 9).

Table 9. Acrylate conversions determined upon irradiation at 405 nm with a LED using chalcone/Iod/amine (1.5%/1.5%/1.5%, w/w/w) and chalcone/Iod (1.5%/1.5%, w/w) systems.

chalcones	chalcone/Iod/EDB		chalcone/ Iod		
	Thin films	Thick molds	Thin films	Thick molds	
30	71%	92%	82%	94%	PEG-diacrylate
31	58%	53%	77%	52%	PEG-diacrylate
32	85%	17%	93%	21%	PEG-diacrylate
33	85%	77%	93%	92%	PEG-diacrylate
35	96%[a]	-			PEG-diacrylate
Blank	50%	93%	-	-	PEG-diacrylate

[a] chalcone/Iod/amine (0.1%/1.5%/1.5%, w/w/w)

Considering the high reactivity of the two-component chalcone 30/Iod (1.5%/1.5%, w/w) system at 405 nm, 3D/4D printing experiments were carried out with this system. Notably, upon immersion of polymer in water for 24h, a swelling ratio of 60% was determined, enabling the volume of the 3D patterns to increase by about two times compared to their initial volume. Interestingly, all patterns could return to their initial shapes and sizes upon heating at 50°C, enabling to design 3D patterns with form memory. This point was notably examined with the combination of swelling and thermally induced dehydration of polymers (See Figure 29). Thus, upon swelling the 3D-printed cross in water for 1 min, a curvature of the cross was observed, what can be suppressed by dehydrating the polymer at 100°C for 100 s. Interestingly, while maintaining the heating at 100°C during 10 min., an inverted curvature of the cross was obtained, resulting from a complete dehydration of the polymer. Finally, while letting the polymer cooling down to room temperature, the cross could return to its initial shape, enabling to design shape-memory objects. Ability to design 3D objects with chalcones were confirmed with chalcone 30.[160] Interestingly, if ferrocene derivatives are often reported as being poor candidates for FRP experiments,[152] in the present case, a PEG-diacrylate conversion as high as 96% could be obtained, outperforming the conversions obtained with chalcones 30-33. Noticeably, this high monomer conversion could only be obtained while reducing the dye concentration to 0.1 wt%, this dye exhibiting a high molar extinction coefficient at 405 nm (See Table 8).

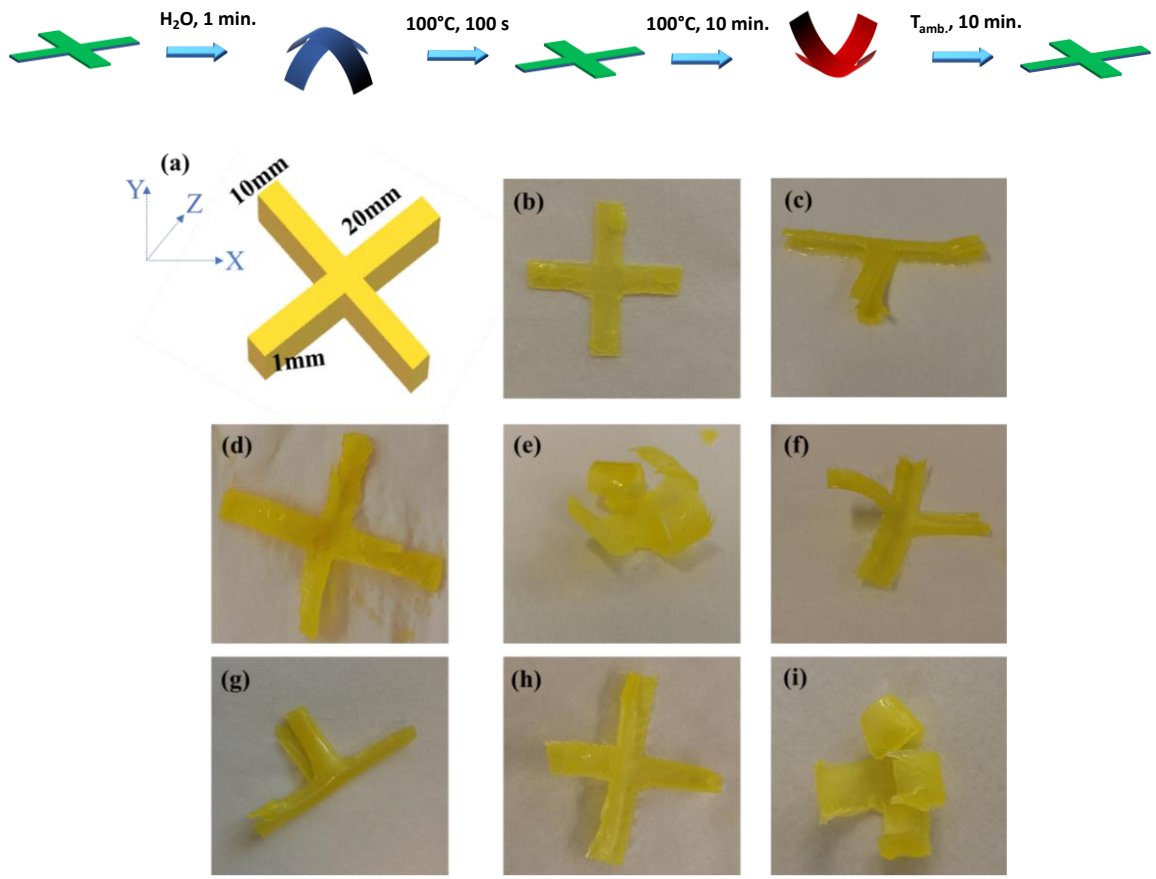

Figure 29. Swelling and dehydration induced actuation of PEG-polymers obtained using the two-component 30/Iod system at 405 nm. (a) the designed geometrical form of the cross; (b) cross of PEG-polymer after photopolymerization; (c) shape of the cross after water swelling for 1 min; (d) shape of the cross after 100 seconds of dehydration (heating at 100°C); (e) shape of the cross after 10 mins of dehydration (heating at 100°C); (f) cross after stay at room temperature for 10 mins; (g) shape of the cross after water swelling again for 1 min; (h) shape of the cross after 100 seconds of dehydration (heating at 100°C); (i) shape of the cross after 10 mins of dehydration (heating at 100°C). Reprinted with permission from Chen et al.[285]

Finally, chalcone 34 was investigated for the polymerization of another acrylic monomer i.e. di(trimethylolpropane) tetraacrylates (TA).[156] Thank to its strong absorption at 405 nm, the dye concentration could be reduced to 0.1 wt%. Using a three-component 34/Iod/EDB (0.1%/2%/2%, w/w/w) for the polymerization of thin TA films, a final monomer conversion of 56% could be determined, higher than the reference system Iod/EDB system (39% conversion after 400 s of irradiation).

1.10. Hexaarylbiimidazole derivatives

Hexaarylbiimidazoles (HABI) also named lophine dimers are historical photoinitiators of polymerization and the first report mentioning their uses was published in 1960.[287] As specificities, hexaarylbiimidazoles possess a carbon-nitrogen bond that can be readily cleaved

photochemically and thermally so that hexaarylbiimidazoles can act as thermal and/or photochemical initiators of polymerization. Hexaarylbiimidazoles are also characterized by a low sensitivity to oxygen, which has stimulated the industrial interest for this family of structures.[288–291] To end, the high yield of lophyl radicals i.e. 2,4,5-triarylimidazolyl radicals make these structures appealing candidates to initiate the FRP of acrylates when combined to hydrogen donor (See Scheme 6). Upon photoexcitation, two lophyl radicals can be formed which can then abstract hydrogens from coinitiators such as amines, enabling to produce initiating radicals. Among HABI, the most common structure is undoubtedly 2-chlorohexaarylbiimidazole. However, absorption of this dye is strongly UV centered[292–294] so that derivatives of this structure exhibiting a red-shifted absorption located in the visible range were designed and synthesized.[295–299]

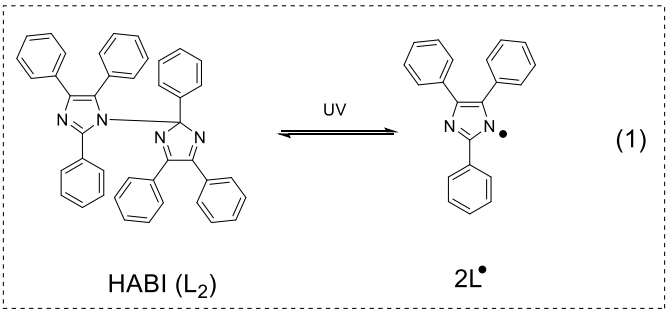

HABI (L_2) ⟶ $2L^{\bullet}$ (1)

$L^{\bullet}$ + DH ⟶ LH + $D^{\bullet}$ (2)

$D^{\bullet}$ + Monomer ⟶ Polymer (3)

Scheme 6. Mechanism involved in the production of radicals upon photocleavage of HABI.

In 2020, a series of triphenylamine-based hexaarylbiimidazoles was examined as photoinitiators for the FRP of acrylates (See Figure 30).[300] Interestingly, modification of the number of methoxy groups on triphenylamine enabled to finely tune both the solubility of dyes in resins but also to modify the position of the absorption maxima. In this study, a series of four dyes was examined (See Figure 30).

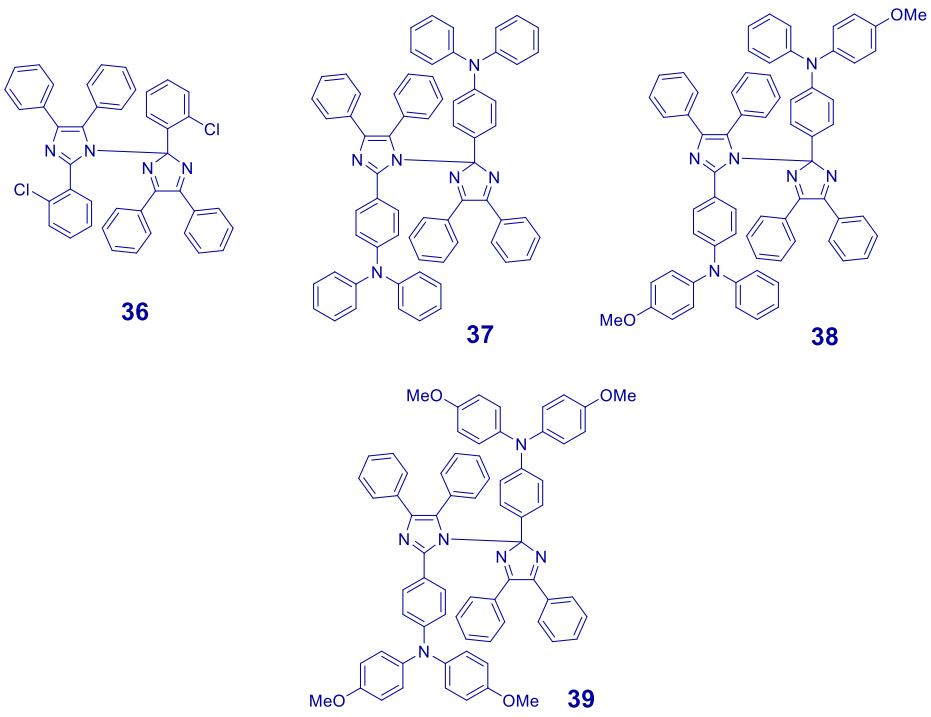

Figure 30. Chemical structures of hexaarylbiimidazole derivatives 36-39.

Upon introduction of methoxy groups onto HABI, a redshift of the absorption spectra was found so that an onset of the absorption spectra at 520, 480 and 470 nm could be determined for 39-37 respectively, consistent with a reduction of the electron donating groups on triphenylamines (See Figure 31). Comparison of the solubility of the different HABI in TMPTA revealed 36 to exhibit a poor solubility contrarily to 37-39. Analysis of the thermal properties by thermogravimetric analysis (TGA) revealed all dyes 37-39 to exhibit similar decomposition temperature than 36. The highest decomposition temperature was found for 34 bearing the greatest number of methoxy groups.

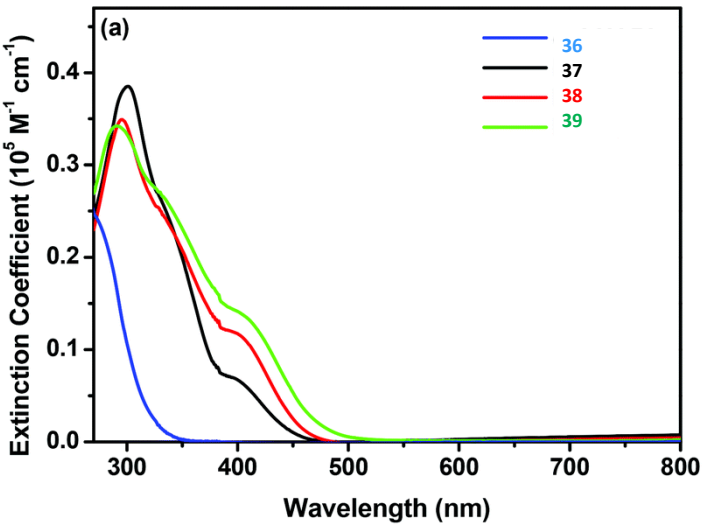

Figure 31. UV-visible absorption spectra of hexaarylbiimidazole derivatives 36-39 in THF. Reprinted with permission from Li et al. [300].

When tested in two-component dye/NPG systems for the FRP of TMPA, despites their absorptions extending until 500 nm, best conversions were obtained upon irradiation in the UV range than in the visible range and these results were assigned to the lower intensity of the white LED (1.75 lm) compared to that of the UV lamp (10 W/m²). Interestingly, increase of the number of methoxy groups resulted in a significant decrease of the polymerization efficiency. Thus, upon irradiation for 11 min. with the white LED, the monomer conversion decreased from 58 to 49% for 37 and 38. Conversely, no polymerization was detected with 39. This counter-performance was assigned to a quenching process of 39 with NPG, but also to the fact that the methoxy group could act as internal hydrogen donors. However, examination of the photoinitiating ability of 38 with and without NPG revealed the presence of NPG to be crucial, no polymerization of TMPTA being detected without NPG. Besides, comparison of the photoinitiating ability of 36 with that of 38 revealed upon visible light irradiation 38 to furnish the same monomer conversions than 36 after 11 min. of irradiation.

1.11. Oxime ester derivatives

Simplification of the photocurable resins is at present the focus of intense research efforts. Indeed, if Type II photoinitiators can furnish highly efficient photoinitiating systems, the necessity to introduce one or two co-initiators in complement to the photosensitizer can constitute a major impediment for future use in industry.[154,301–303] Ideally, a great simplification of the photocurable resin can be obtained while using a mono-component system. In this field, oxime esters that are a specific family of Type I photoinitiators are capable to generate initiating radicals upon homolytic cleavage of a N-O bond.[304–313] Indeed, upon cleavage, an iminyl and a carbonate radical can be formed. Subsequently, the carbonate radical can undergo a decarboxylation reaction, producing carbon-centered radicals. As interesting feature, the carbon dioxide released during the decarboxylation reaction can also contribute to reduce the oxygen inhibition during FRP, CO_2 impeding dioxygen to penetrate inside the resin.[290,314] Concerning triphenylamine-based oxime esters, four structures 35-38 were reported for the first time in 2021.[315] Here again, the substitution of triphenylamine by methoxy groups was examined (See Figure 32).

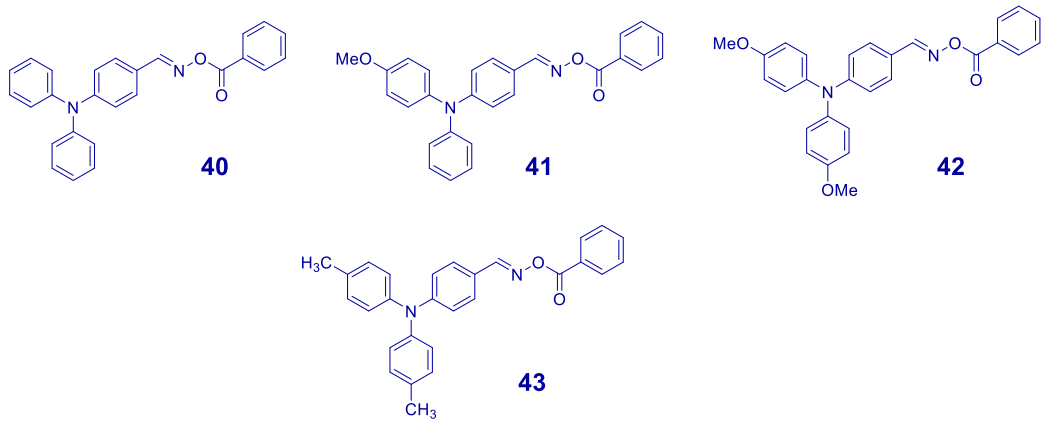

Figure 32. Chemical structures of triphenylamine-based oxime esters 40-43.

From the absorption viewpoint, influence of the substitution pattern of triphenylamine did not significantly modify the position of the absorption maxima. Thus, absorptions ranging between 360 nm for 40 and 42 to 362 nm for 43 and 364 nm for 41 could be determined in dichloromethane (See Figure 33).

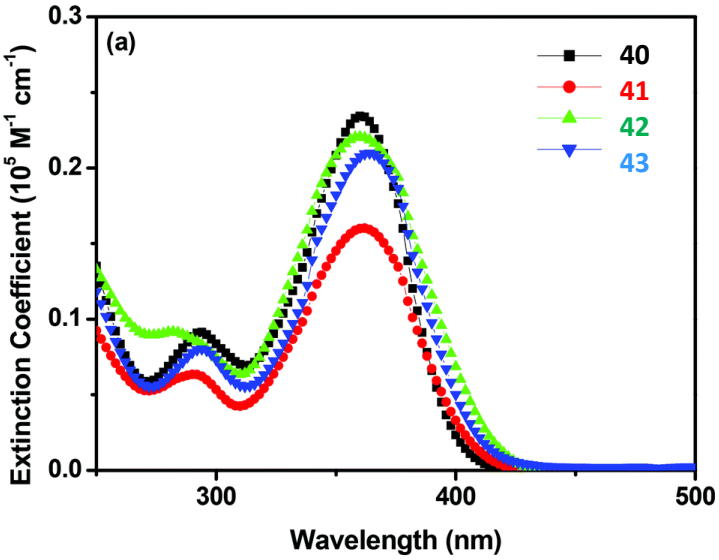

Figure 33. UV-visible absorption spectra of 40-43 in dichloromethane. Reprinted with permission from Lee et al. [315]

Examination of the photoinitiating ability revealed major differences between the four dyes. Thus, while using 2 wt% oxime esters in TMPTA, a severe variation of the final monomer conversions was observed, ranging from 92 to 78, 74 and 72% for 40, 42, 51 and 43 respectively after 6 minutes of irradiation at 405 nm. Besides, until 80 s, similar polymerization kinetics could be evidenced (See Figure 34). The higher monomer conversion obtained with 40 was assigned to first the contribution of the carbon-centered radicals to the polymerization process followed by the contribution of the iminyl radicals to the polymerization process in a later stage.[316] In the case of 41-43, and due to the presence of electron-donating groups onto triphenylamine, a lower contribution of the iminyl radicals to the polymerization process was thus proposed, resulting from shorter radical lifetimes. Considering the low molar extinction coefficient of 41-43 at 405 nm, the sensitization by isopropylthioxanthone (ITX) exhibiting a higher molar extinction coefficient than 40-43 was examined. As anticipated, an efficient sensitization of oxime esters could be obtained, improving the monomer conversion. Thus, upon sensitization of 41, a 4-fold enhancement of the TMPTA conversion could be obtained while using the two-component ITX/41 (1%/0.1% w/w) system compared to 41 (0.1 wt%). Laser flash photolysis experiments revealed the sensitization to occur via the triplet state of ITX.

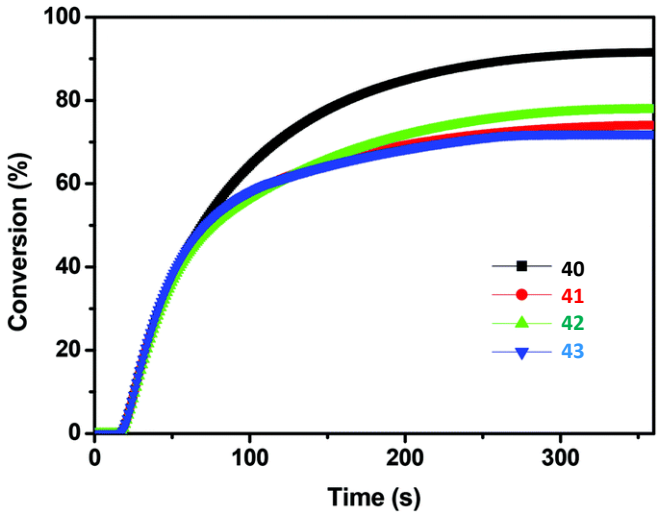

Figure 34. TMPTA conversion obtained with 40-43 upon irradiation at 405 nm and by using 2 wt% dye. Reprinted with permission from Lee et al. [315]

Oxime esters are type I photoinitiators, but these structures can also be used for the sensitization of iodonium salt. This strategy where oxime esters are used as Type II photoinitiators was notably applied to a phenothiazine-based oxime ester i.e. 44 (See Figure 35).[306] When applied to the FRP of TPGDA, introduction of the iodonium salt as the co-initiator enabled to improve the TPGDA conversion from 71% for 44 (1 wt%) alone up to 96% with the two-component 44/Iod (0.2%/2% w/w) upon irradiation at 405 nm with a laser diode.

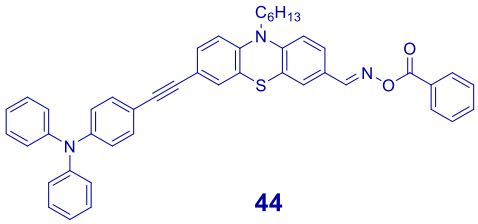

44

Figure 35. Chemical structure of 44.

A summary of the different monomer conversions obtained with the different triphenylamine-based photoinitiating system is provided in the Table 10.

Table 10. Monomer conversions obtained with the different triphenylamine-based photoinitiating systems.

Dye	Photoinitiating systems	Monomers	Light source	Monomer conversion	Ref.
1	1/Iod/amine (0.1%/2%/2% w/w/w)	Ebecryl 40	405 nm	67% (400 s)	204
2	2/Iod/amine (0.1%/2%/2% w/w/w)	Ebecryl 40	405 nm	60% (400 s)	204
3	3/Iod/amine (0.1%/2%/2% w/w/w)	Ebecryl 40	405 nm	90% (400 s)	204
4	4/Iod/amine (0.1%/2%/2% w/w/w)	Ebecryl 40	405 nm	92% (400 s)	204
5	5/Iod/amine (0.1%/2%/2% w/w/w)	Ebecryl 40	405 nm	95% (400 s)	204
6	6/Iod/amine (0.1%/2%/2% w/w/w)	Ebecryl 40	405 nm	58% (400 s)	204
7	7/Iod (0.5%/1% w/w)	EPOX	405 nm	66% (800 s)	207

8	8/Iod (0.5%/1% w/w)	EPOX	405 nm	57% (800 s)	207
7	7/Iod (0.5%/1% w/w)	TMPTA	405 nm	25% (100 s)	207
7	7/NPG (0.5%/1% w/w)	TMPTA	405 nm	62% (100 s)	207
7	7/EDB (0.5%/1% w/w)	TMPTA	405 nm	55% (100 s)	207
7	7/Iod/EDB (0.5%/1% w/w)	TMPTA	405 nm	59% (100 s)	207
8	8/Iod (0.5%/1% w/w)	TMPTA	405 nm	48% (100 s)	207
8	8/NPG (0.5%/1% w/w)	TMPTA	405 nm	61% (100 s)	207
8	8/EDB (0.5%/1% w/w)	TMPTA	405 nm	52% (100 s)	207
8	8/Iod/EDB (0.5%/1% w/w)	TMPTA	405 nm	57% (100 s)	207
9	9/Iod (0.3%/1%, w/w)	TMPTA	405 nm	64% (200 s)	110
10	10/Iod (0.3%/1%, w/w)	TMPTA	405 nm	69% (200 s)	110
9	9/EDB (0.3%/1%, w/w)	TMPTA	405 nm	57% (200 s)	110
10	10/EDB (0.3%/1%, w/w)	TMPTA	405 nm	71% (200 s)	110
9	9/Iod/EDB (0.3%/1%/1% w/w/w)	TMPTA	405 nm	66% (200 s)	110
10	10/Iod/EDB (0.3%/1%/1% w/w/w)	TMPTA	405 nm	75% (200 s)	110
9	9/Iod (0.3%/1%, w/w)	EPOX	405 nm	38% (200 s)	110
10	10/Iod (0.3%/1%, w/w)	EPOX	405 nm	45% (200 s)	110
11	11/Iod/EDB (0.3%/1%/1% w/w/w)	TMPTA	405 nm	68% (200 s)	109
12	12/Iod/EDB (0.3%/1%/1% w/w/w)	TMPTA	405 nm	72% (200 s)	109
13	13/Iod/EDB (0.3%/1%/1% w/w/w)	TMPTA	405 nm	77% (200 s)	109
11	11/Iod (0.3%/1% w/w)	TMPTA	405 nm	65% (200 s)	109
12	12/Iod (0.3%/1% w/w)	TMPTA	405 nm	68% (200 s)	109
13	13/Iod (0.3%/1% w/w)	TMPTA	405 nm	72% (200 s)	109
11	11/EDB (0.3%/1% w/w)	TMPTA	405 nm	60% (200 s)	109
12	12/EDB (0.3%/1% w/w)	TMPTA	405 nm	62% (200 s)	109
13	13/EDB (0.3%/1% w/w)	TMPTA	405 nm	69% (200 s)	109
11	11/Iod (0.3%/1% w/w)	EPOX	405 nm	43% (200 s)	109
12	12/Iod (0.3%/1% w/w)	EPOX	405 nm	41% (200 s)	109
13	13/Iod (0.3%/1% w/w)	EPOX	405 nm	47% (200 s)	109
9	9/TEOA (1%/1% w/w)	TMPTA	405 nm	98% (1200 s)	217
14	14/TEOA (1%/1% w/w)	TMPTA	405 nm	83% (1200 s)	217
15	15/TEOA (1%/1% w/w)	TMPTA	405 nm	n.p.	217
16	16/TEOA (1%/1% w/w)	TMPTA	405 nm	65% (1200 s)	217
17	17/TEOA (1%/1% w/w)	TMPTA	405 nm	65% (1200 s)	217
18	18/Iod (0.1%/1% w/w)	TPGDA	405 nm	98% (60 s)	218
19	19/Iod (0.5%/1% w/w)	EPOX	405 nm	41% (800 s)	220
20	20/Iod (0.5%/1% w/w)	EPOX	405 nm	53% (800 s)	220
19	19/Iod (0.5%/1% w/w)	TMPTA	405 nm	41% (800 s)	220
20	20/Iod (0.5%/1% w/w)	TMPTA	405 nm	47% (800 s)	220
20	20/Iod/EDB (0.01%/1%/1% w/w/w)	TMPTA	405 nm	80% (800 s)	220
20	20/Iod/EDB (0.01%/1%/1%)	BisGMA/TEGDMA	405 nm	65% (800 s)	220
21	21/Iod2 (0.5%/2% w/w)	EPOX	455 nm	60% (800 s)	136
21	21/Iod2 (0.5%/2% w/w)	EPOX	halogen lamp	49% (800 s)	136
22	22/Iod2 (0.5%/2% w/w)	EPOX	455 nm	41% (800 s)	136
22	22/Iod2 (0.5%/2% w/w)	EPOX	halogen lamp	31% (800 s)	136
22	22/Iod2/NVK (0.5%/2%/3% w/w/w)	EPOX	405 nm	55% (800 s)	136

22	22/Iod2/NVK (0.5%/2%/3% w/w/w)	EPOX	halogen lamp	41% (800 s)	136
23	23/Iod (0.2%/2% w/w)	EPOX-Si	Xe-Hg lamp	52% (200 s)	71
24	24/Iod (0.2%/3% w/w)	DGEBA	405 nm	56% (300 s)	242
24	24/Iod (0.2%/3% w/w)	DGEBA	455 nm	46% (300 s)	242
24	24/Iod/NVK (0.2%/3%/2% w/w/w)	DGEBA	455 nm	61% (300 s)	242
24	24/Iod (0.2%/3% w/w)	TPGDA	405 nm	87% (300 s)	242
25	25/Iod (0.2%/3% w/w)	TPGDA	405 nm	83% (300 s)	242
24	24/Iod (0.2%/3% w/w)	TPGDA	455 nm	77% (300 s)	242
25	25/Iod (0.2%/3% w/w)	TPGDA	455 nm	73% (300 s)	242
24	24/Iod/TPP (0.2%/3%/2% w/w/w)	TPGDA	405 nm	70% (20 s)	242
24	24/Iod (0.2%/3% w/w)	TPGDA	405 nm	21% (20 s)	242
26	26/TEOA (0.1%/6% w/w)	TPGDA	460 nm	70% (20 s)	270
26	26/TEOA (0.1%/0.75% w/w)	TPGDA	460 nm	40% (20 s)	270
27	27/TEOA (0.125%/3% w/w)	TPGDA	405 nm	85% (160 s)	283
28	28/TEOA (0.125%/3% w/w)	TPGDA	405 nm	85% (20 s)	283
29	29/TEOA (0.125%/3% w/w)	TPGDA	405 nm	75% (120 s)	283
27	27/TEOA (0.125%/3% w/w)	TPGDA	460 nm	70% (180 s)	283
28	28/TEOA (0.125%/3% w/w)	TPGDA	460 nm	80% (60 s)	283
29	29/TEOA (0.125%/3% w/w)	TPGDA	460 nm	75% (180 s)	283
27	27/TEOA (0.125%/3% w/w)	TPGDA	405 nm	80% (150 s)	283
28	28/TEOA (0.125%/3% w/w)	TPGDA	405 nm	75% (150 s)	283
29	29/TEOA (0.125%/3% w/w)	TPGDA	405 nm	55% (150 s)	283
27	27/TEOA (0.125%/3% w/w)	TPGDA	460 nm	48% (150 s)	283
28	28/TEOA (0.125%/3% w/w)	TPGDA	460 nm	65% (150 s)	283
29	29/TEOA (0.125%/3% w/w)	TPGDA	460 nm	45% (150 s)	283
30	30/Iod/EDB (1.5%/1.5%/1.5%, w/w/w)	PEG-diacrylate	405 nm	71% (200 s)	286
31	31/Iod/EDB (1.5%/1.5%/1.5%, w/w/w)	PEG-diacrylate	405 nm	58% (200 s)	286
32	32/Iod/EDB (1.5%/1.5%/1.5%, w/w/w)	PEG-diacrylate	405 nm	85% (200 s)	286
33	33/Iod/EDB (1.5%/1.5%/1.5%, w/w/w)	PEG-diacrylate	405 nm	85% (200 s)	286
30	30/Iod (1.5%/1.5%, w/w)	PEG-diacrylate	405 nm	82% (200 s)	286
31	31/Iod (1.5%/1.5%, w/w)	PEG-diacrylate	405 nm	77% (200 s)	286
32	32/Iod (1.5%/1.5%, w/w)	PEG-diacrylate	405 nm	93% (200 s)	286
33	33/Iod (1.5%/1.5%, w/w)	PEG-diacrylate	405 nm	93% (200 s)	286
34	34/Iod/EDB (0.1%/2%/2%, w/w/w)	PEG-diacrylate	405 nm	56% (400 s)	146
35	35/Iod/EDB (0.1%/2%/2%, w/w/w)	PEG-diacrylate	405 nm	96% (400 s)	160
36	36/NPG (2%/0.1%, w/w)	TMPTA	white LED	37% (8 min)	300
37	37/NPG (2%/0.1%, w/w)	TMPTA	white LED	80% (8 min)	300
38	38/NPG (2%/0.1%, w/w)	TMPTA	white LED	45% (8 min)	300
39	39/NPG (2%/0.1%, w/w)	TMPTA	white LED	n.p.	300
40	40 (2 wt%)	TMPTA	405 nm	90% (260 s)	315
41	41 (2 wt%)	TMPTA	405 nm	70% (260 s)	315
42	42 (2 wt%)	TMPTA	405 nm	75% (260 s)	315
43	43 (2 wt%)	TMPTA	405 nm	72% (260 s)	315
44	44 (1 wt%)	TPGDA	405 nm	71% (60 s)	306
44	44/Iod (0.2%/2%, w/w)	TPGDA	405 nm	96% (60 s)	306

[a] np: no polymerization.

Conclusion

To conclude, triphenylamine is a versatile scaffold that was at the basis of numerous visible light photoinitiators of polymerization. Ability to design Type I and type II photoinitiators was strongly related to the facile chemical modifications of this scaffold. Over the years, more than 10 different families of dyes have been examined as photoinitiators of polymerization. A clear evolution of the photoinitiator structures can be evidenced. Indeed, if triphenylamine-based photoinitiators were mostly Type II photoinitiators, recently, with aim simplifying the composition of the photocurable resins, Type I photoinitiators are now widely studied. Notably, oxime esters were developed as promising candidates for photoinitiation. However, other families of Type I photoinitiators based on benzoin derivatives, phosphine oxides, benzyl ketals, hydroxyacetophenones or α-aminoalkylacetophenones can be developed in the Future. Future works will also consist in developing water-soluble dyes. In this field, triphenylamines bearing sulfonic groups, carboxylates or ammonium groups could allow to develop interesting dyes. Indeed, with aim at developing more environmentally friendly polymerization conditions and face to the scarcity of water-soluble visible light photoinitiators of polymerization currently available on the market, this family of dyes deserves to be more widely studied in the future. Finally, another interesting research topic could consist in developing bioactive molecules capable to act as bactericides, fungicides or virucides, the search for cleaning products capable to kill COVID-19 being currently an active research field.

Acknowledgments

Aix Marseille University and the Centre National de la Recherche Scientifique (CNRS) are acknowledged for financial supports.

Conflicts of Interest

The authors declare no conflict of interest.

References

[1] Lalevée J, Mokbel H, Fouassier J-P. Recent Developments of Versatile Photoinitiating Systems for Cationic Ring Opening Polymerization Operating at Any Wavelengths and under Low Light Intensity Sources. Molecules 2015;20:7201–21. https://doi.org/10.3390/molecules20047201.

[2] Tehfe MA, Louradour F, Lalevée J, Fouassier J-P. Photopolymerization Reactions: On the Way to a Green and Sustainable Chemistry. Applied Sciences 2013;3:490–514. https://doi.org/10.3390/app3020490.

[3] Xiao P, Zhang J, Dumur F, Tehfe MA, Morlet-Savary F, Graff B, et al. Visible light sensitive photoinitiating systems: Recent progress in cationic and radical photopolymerization reactions under soft conditions. Progress in Polymer Science 2015;41:32–66. https://doi.org/10.1016/j.progpolymsci.2014.09.001.

[4] Sun K, Xiao P, Dumur F, Lalevée J. Organic dye-based photoinitiating systems for visible-light-induced photopolymerization. Journal of Polymer Science 2021;59:1338–89. https://doi.org/10.1002/pol.20210225.
[5] Lalevée J, Telitel S, Xiao P, Lepeltier M, Dumur F, Morlet-Savary F, et al. Metal and metal-free photocatalysts: mechanistic approach and application as photoinitiators of photopolymerization. Beilstein J Org Chem 2014;10:863–76. https://doi.org/10.3762/bjoc.10.83.
[6] Xiao P, Dumur F, Graff B, Fouassier JP, Gigmes D, Lalevée J. Cationic and Thiol–Ene Photopolymerization upon Red Lights Using Anthraquinone Derivatives as Photoinitiators. Macromolecules 2013;46:6744–50. https://doi.org/10.1021/ma401513b.
[7] Tehfe M-A, Gigmes D, Dumur F, Bertin D, Morlet-Savary F, Graff B, et al. Cationic photosensitive formulations based on silyl radical chemistry for green and red diode laser exposure. Polym Chem 2012;3:1899–902. https://doi.org/10.1039/C1PY00460C.
[8] Garra P, Dietlin C, Morlet-Savary F, Dumur F, Gigmes D, Fouassier J-P, et al. Redox two-component initiated free radical and cationic polymerizations: Concepts, reactions and applications. Progress in Polymer Science 2019;94:33–56. https://doi.org/10.1016/j.progpolymsci.2019.04.003.
[9] Jasinski F, Zetterlund PB, Braun AM, Chemtob A. Photopolymerization in dispersed systems. Progress in Polymer Science 2018;84:47–88. https://doi.org/10.1016/j.progpolymsci.2018.06.006.
[10] Noè C, Hakkarainen M, Sangermano M. Cationic UV-Curing of Epoxidized Biobased Resins. Polymers 2021;13:89. https://doi.org/10.3390/polym13010089.
[11] Yuan Y, Li C, Zhang R, Liu R, Liu J. Low volume shrinkage photopolymerization system using hydrogen-bond-based monomers. Progress in Organic Coatings 2019;137:105308. https://doi.org/10.1016/j.porgcoat.2019.105308.
[12] Khudyakov IV, Legg JC, Purvis MB, Overton BJ. Kinetics of Photopolymerization of Acrylates with Functionality of 1−6. Ind Eng Chem Res 1999;38:3353–9. https://doi.org/10.1021/ie990306i.
[13] Dickens SH, Stansbury JW, Choi KM, Floyd CJE. Photopolymerization Kinetics of Methacrylate Dental Resins. Macromolecules 2003;36:6043–53. https://doi.org/10.1021/ma021675k.
[14] Maffezzoli A, Pietra AD, Rengo S, Nicolais L, Valletta G. Photopolymerization of dental composite matrices. Biomaterials 1994;15:1221–8. https://doi.org/10.1016/0142-9612(94)90273-9.
[15] Dikova T, Maximov J, Todorov V, Georgiev G, Panov V. Optimization of Photopolymerization Process of Dental Composites. Processes 2021;9:779. https://doi.org/10.3390/pr9050779.
[16] Zhao H, Sha J, Wang X, Jiang Y, Chen T, Wu T, et al. Spatiotemporal control of polymer brush formation through photoinduced radical polymerization regulated by DMD light modulation. Lab Chip 2019;19:2651–62. https://doi.org/10.1039/C9LC00419J.
[17] Xi W, Peng H, Aguirre-Soto A, Kloxin CJ, Stansbury JW, Bowman CN. Spatial and Temporal Control of Thiol-Michael Addition via Photocaged Superbase in Photopatterning and Two-Stage Polymer Networks Formation. Macromolecules 2014;47:6159–65. https://doi.org/10.1021/ma501366f.
[18] Shao J, Huang Y, Fan Q. Visible light initiating systems for photopolymerization: status, development and challenges. Polym Chem 2014;5:4195–210. https://doi.org/10.1039/C4PY00072B.

[19] Bonardi AH, Dumur F, Grant TM, Noirbent G, Gigmes D, Lessard BH, et al. High Performance Near-Infrared (NIR) Photoinitiating Systems Operating under Low Light Intensity and in the Presence of Oxygen. Macromolecules 2018;51:1314–24. https://doi.org/10.1021/acs.macromol.8b00051.
[20] Garra P, Dietlin C, Morlet-Savary F, Dumur F, Gigmes D, Fouassier J-P, et al. Photopolymerization processes of thick films and in shadow areas: a review for the access to composites. Polym Chem 2017;8:7088–101. https://doi.org/10.1039/C7PY01778B.
[21] Al Mousawi A, Poriel C, Dumur F, Toufaily J, Hamieh T, Fouassier JP, et al. Zinc Tetraphenylporphyrin as High Performance Visible Light Photoinitiator of Cationic Photosensitive Resins for LED Projector 3D Printing Applications. Macromolecules 2017;50:746–53. https://doi.org/10.1021/acs.macromol.6b02596.
[22] Noirbent G, Xu Y, Bonardi A-H, Gigmes D, Lalevée J, Dumur F. Metalated porphyrins as versatile visible light and NIR photoinitiators of polymerization. European Polymer Journal 2020;139:110019. https://doi.org/10.1016/j.eurpolymj.2020.110019.
[23] Garra P, Brunel D, Noirbent G, Graff B, Morlet-Savary F, Dietlin C, et al. Ferrocene-based (photo)redox polymerization under long wavelengths. Polym Chem 2019;10:1431–41. https://doi.org/10.1039/C9PY00059C.
[24] Tehfe M-A, Zein-Fakih A, Lalevée J, Dumur F, Gigmes D, Graff B, et al. New pyridinium salts as versatile compounds for dye sensitized photopolymerization. European Polymer Journal 2013;49:567–74. https://doi.org/10.1016/j.eurpolymj.2012.10.010.
[25] Xiao P, Frigoli M, Dumur F, Graff B, Gigmes D, Fouassier JP, et al. Julolidine or Fluorenone Based Push–Pull Dyes for Polymerization upon Soft Polychromatic Visible Light or Green Light. Macromolecules 2014;47:106–12. https://doi.org/10.1021/ma402196p.
[26] Mokbel H, Dumur F, Graff B, Mayer CR, Gigmes D, Toufaily J, et al. Michler's Ketone as an Interesting Scaffold for the Design of High-Performance Dyes in Photoinitiating Systems Upon Visible Light. Macromolecular Chemistry and Physics 2014;215:783–90. https://doi.org/10.1002/macp.201300779.
[27] Tehfe M-A, Dumur F, Graff B, Morlet-Savary F, Fouassier J-P, Gigmes D, et al. New Push–Pull Dyes Derived from Michler's Ketone For Polymerization Reactions Upon Visible Lights. Macromolecules 2013;46:3761–70. https://doi.org/10.1021/ma400766z.
[28] Mokbel H, Dumur F, Mayer CR, Morlet-Savary F, Graff B, Gigmes D, et al. End capped polyenic structures as visible light sensitive photoinitiators for polymerization of vinylethers. Dyes and Pigments 2014;105:121–9. https://doi.org/10.1016/j.dyepig.2014.02.002.
[29] Telitel S, Dumur F, Kavalli T, Graff B, Morlet-Savary F, Gigmes D, et al. The 1,3-bis(dicyanomethylidene)indane skeleton as a (photo) initiator in thermal ring opening polymerization at RT and radical or cationic photopolymerization. RSC Adv 2014;4:15930–6. https://doi.org/10.1039/C3RA42819B.
[30] Xiao P, Dumur F, Graff B, Morlet-Savary F, Vidal L, Gigmes D, et al. Structural Effects in the Indanedione Skeleton for the Design of Low Intensity 300–500 nm Light Sensitive Initiators. Macromolecules 2014;47:26–34. https://doi.org/10.1021/ma402149g.
[31] Sun K, Liu S, Pigot C, Brunel D, Graff B, Nechab M, et al. Novel Push–Pull Dyes Derived from 1H-cyclopenta[b]naphthalene-1,3(2H)-dione as Versatile Photoinitiators

for Photopolymerization and Their Related Applications: 3D Printing and Fabrication of Photocomposites. Catalysts 2020;10:1196. https://doi.org/10.3390/catal10101196.
[32] Sun K, Liu S, Chen H, Morlet-Savary F, Graff B, Pigot C, et al. N-ethyl carbazole-1-allylidene-based push-pull dyes as efficient light harvesting photoinitiators for sunlight induced polymerization. European Polymer Journal 2021;147:110331. https://doi.org/10.1016/j.eurpolymj.2021.110331.
[33] Tehfe M-A, Dumur F, Graff B, Morlet-Savary F, Gigmes D, Fouassier J-P, et al. Push–pull (thio)barbituric acid derivatives in dye photosensitized radical and cationic polymerization reactions under 457/473 nm laser beams or blue LEDs. Polym Chem 2013;4:3866–75. https://doi.org/10.1039/C3PY00372H.
[34] Sun K, Chen H, Zhang Y, Morlet-Savary F, Graff B, Xiao P, et al. High-performance sunlight induced polymerization using novel push-pull dyes with high light absorption properties. European Polymer Journal 2021;151:110410. https://doi.org/10.1016/j.eurpolymj.2021.110410.
[35] Mokbel H, Dumur F, Telitel S, Vidal L, Xiao P, Versace D-L, et al. Photoinitiating systems of polymerization and in situ incorporation of metal nanoparticles into polymer matrices upon exposure to visible light: push–pull malonate and malononitrile based dyes. Polym Chem 2013;4:5679–87. https://doi.org/10.1039/C3PY00846K.
[36] Sun K, Pigot C, Zhang Y, Borjigin T, Morlet-Savary F, Graff B, et al. Sunlight Induced Polymerization Photoinitiated by Novel Push–Pull Dyes: Indane-1,3-Dione, 1H-Cyclopenta[b]Naphthalene-1,3(2H)-Dione and 4-Dimethoxyphenyl-1-Allylidene Derivatives. Macromolecular Chemistry and Physics 2022;n/a:2100439. https://doi.org/10.1002/macp.202100439.
[37] Zivic N, Bouzrati-Zerrelli M, Villotte S, Morlet-Savary F, Dietlin C, Dumur F, et al. A novel naphthalimide scaffold based iodonium salt as a one-component photoacid/photoinitiator for cationic and radical polymerization under LED exposure. Polym Chem 2016;7:5873–9. https://doi.org/10.1039/C6PY01306F.
[38] Mokbel H, Toufaily J, Hamieh T, Dumur F, Campolo D, Gigmes D, et al. Specific cationic photoinitiators for near UV and visible LEDs: Iodonium versus ferrocenium structures. Journal of Applied Polymer Science 2015;132. https://doi.org/10.1002/app.42759.
[39] Villotte S, Gigmes D, Dumur F, Lalevée J. Design of Iodonium Salts for UV or Near-UV LEDs for Photoacid Generator and Polymerization Purposes. Molecules 2020;25:149. https://doi.org/10.3390/molecules25010149.
[40] Tasdelen MA, Kumbaraci V, Jockusch S, Turro NJ, Talinli N, Yagci Y. Photoacid Generation by Stepwise Two-Photon Absorption: Photoinitiated Cationic Polymerization of Cyclohexene Oxide by Using Benzodioxinone in the Presence of Iodonium Salt. Macromolecules 2008;41:295–7. https://doi.org/10.1021/ma7023649.
[41] Crivello JV, Lam JHW. Diaryliodonium Salts. A New Class of Photoinitiators for Cationic Polymerization. Macromolecules 1977;10:1307–15. https://doi.org/10.1021/ma60060a028.
[42] He Y, Zhou W, Wu F, Li M, Wang E. Photoreaction and photopolymerization studies on squaraine dyes/iodonium salts combination. Journal of Photochemistry and Photobiology A: Chemistry 2004;162:463–71. https://doi.org/10.1016/S1010-6030(03)00390-3.

[43] Jun LI, Miaozhen LI, Huaihai S, Yongyuan Y, Erjian W. Photopolymerization Initiated by Dimethylaminochalcone/Diphenyliodonium Salt Combination System Sensitive to Visible Light. Chinese J Polym Sci 1993;11:163–70.
[44] Zhang J, Campolo D, Dumur F, Xiao P, Gigmes D, Fouassier JP, et al. The carbazole-bound ferrocenium salt as a specific cationic photoinitiator upon near-UV and visible LEDs (365–405 nm). Polym Bull 2016;73:493–507. https://doi.org/10.1007/s00289-015-1506-1.
[45] Al Mousawi A, Dumur F, Garra P, Toufaily J, Hamieh T, Graff B, et al. Carbazole Scaffold Based Photoinitiator/Photoredox Catalysts: Toward New High Performance Photoinitiating Systems and Application in LED Projector 3D Printing Resins. Macromolecules 2017;50:2747–58. https://doi.org/10.1021/acs.macromol.7b00210.
[46] Al Mousawi A, Lara DM, Noirbent G, Dumur F, Toufaily J, Hamieh T, et al. Carbazole Derivatives with Thermally Activated Delayed Fluorescence Property as Photoinitiators/Photoredox Catalysts for LED 3D Printing Technology. Macromolecules 2017;50:4913–26. https://doi.org/10.1021/acs.macromol.7b01114.
[47] Al Mousawi A, Garra P, Dumur F, Bui T-T, Goubard F, Toufaily J, et al. Novel Carbazole Skeleton-Based Photoinitiators for LED Polymerization and LED Projector 3D Printing. Molecules 2017;22:2143. https://doi.org/10.3390/molecules22122143.
[48] Mousawi AA, Arar A, Ibrahim-Ouali M, Duval S, Dumur F, Garra P, et al. Carbazole-based compounds as photoinitiators for free radical and cationic polymerization upon near visible light illumination. Photochem Photobiol Sci 2018;17:578–85. https://doi.org/10.1039/C7PP00400A.
[49] Abdallah M, Magaldi D, Hijazi A, Graff B, Dumur F, Fouassier J-P, et al. Development of new high-performance visible light photoinitiators based on carbazole scaffold and their applications in 3d printing and photocomposite synthesis. Journal of Polymer Science Part A: Polymer Chemistry 2019;57:2081–92. https://doi.org/10.1002/pola.29471.
[50] Dumur F. Recent advances on carbazole-based photoinitiators of polymerization. European Polymer Journal 2020;125:109503. https://doi.org/10.1016/j.eurpolymj.2020.109503.
[51] Liu S, Graff B, Xiao P, Dumur F, Lalevée J. Nitro-Carbazole Based Oxime Esters as Dual Photo/Thermal Initiators for 3D Printing and Composite Preparation. Macromolecular Rapid Communications 2021;42:2100207. https://doi.org/10.1002/marc.202100207.
[52] Abdallah M, Bui T-T, Goubard F, Theodosopoulou D, Dumur F, Hijazi A, et al. Phenothiazine derivatives as photoredox catalysts for cationic and radical photosensitive resins for 3D printing technology and photocomposite synthesis. Polym Chem 2019;10:6145–56. https://doi.org/10.1039/C9PY01265F.
[53] Dumur F. Recent advances on visible light Phenothiazine-based photoinitiators of polymerization. European Polymer Journal 2022;165:110999. https://doi.org/10.1016/j.eurpolymj.2022.110999.
[54] Mokbel H, Dumur F, Lalevée J. On demand NIR activated photopolyaddition reactions. Polym Chem 2020;11:4250–9. https://doi.org/10.1039/D0PY00639D.
[55] Mokbel H, Graff B, Dumur F, Lalevée J. NIR Sensitizer Operating under Long Wavelength (1064 nm) for Free Radical Photopolymerization Processes. Macromolecular Rapid Communications 2020;41:2000289. https://doi.org/10.1002/marc.202000289.

[56] Launay V, Dumur F, Gigmes D, Lalevée J. Near-infrared light for polymer re-shaping and re-processing applications. Journal of Polymer Science 2021;59:2193–200. https://doi.org/10.1002/pol.20210450.
[57] Caron A, Noirbent G, Gigmes D, Dumur F, Lalevée J. Near-Infrared PhotoInitiating Systems: Photothermal versus Triplet–Triplet Annihilation-Based Upconversion Polymerization. Macromolecular Rapid Communications 2021;42:2100047. https://doi.org/10.1002/marc.202100047.
[58] Bonardi A-H, Bonardi F, Morlet-Savary F, Dietlin C, Noirbent G, Grant TM, et al. Photoinduced Thermal Polymerization Reactions. Macromolecules 2018;51:8808–20. https://doi.org/10.1021/acs.macromol.8b01741.
[59] Tehfe M-A, Dumur F, Telitel S, Gigmes D, Contal E, Bertin D, et al. Zinc-based metal complexes as new photocatalysts in polymerization initiating systems. European Polymer Journal 2013;49:1040–9. https://doi.org/10.1016/j.eurpolymj.2013.01.023.
[60] Zhang J, Zivic N, Dumur F, Guo C, Li Y, Xiao P, et al. Panchromatic photoinitiators for radical, cationic and thiol-ene polymerization reactions: A search in the diketopyrrolopyrrole or indigo dye series. Materials Today Communications 2015;4:101–8. https://doi.org/10.1016/j.mtcomm.2015.06.007.
[61] Xiao P, Hong W, Li Y, Dumur F, Graff B, Fouassier JP, et al. Diketopyrrolopyrrole dyes: Structure/reactivity/efficiency relationship in photoinitiating systems upon visible lights. Polymer 2014;55:746–51. https://doi.org/10.1016/j.polymer.2014.01.003.
[62] Xiao P, Hong W, Li Y, Dumur F, Graff B, Fouassier JP, et al. Green light sensitive diketopyrrolopyrrole derivatives used in versatile photoinitiating systems for photopolymerizations. Polym Chem 2014;5:2293–300. https://doi.org/10.1039/C3PY01599H.
[63] Lalevée J, Peter M, Dumur F, Gigmes D, Blanchard N, Tehfe M-A, et al. Subtle Ligand Effects in Oxidative Photocatalysis with Iridium Complexes: Application to Photopolymerization. Chemistry – A European Journal 2011;17:15027–31. https://doi.org/10.1002/chem.201101445.
[64] Lalevée J, Tehfe M-A, Dumur F, Gigmes D, Blanchard N, Morlet-Savary F, et al. Iridium Photocatalysts in Free Radical Photopolymerization under Visible Lights. ACS Macro Lett 2012;1:286–90. https://doi.org/10.1021/mz2001753.
[65] Lalevée J, Dumur F, Mayer CR, Gigmes D, Nasr G, Tehfe M-A, et al. Photopolymerization of N-Vinylcarbazole Using Visible-Light Harvesting Iridium Complexes as Photoinitiators. Macromolecules 2012;45:4134–41. https://doi.org/10.1021/ma3005229.
[66] Tehfe M-A, Lepeltier M, Dumur F, Gigmes D, Fouassier J-P, Lalevée J. Structural Effects in the Iridium Complex Series: Photoredox Catalysis and Photoinitiation of Polymerization Reactions under Visible Lights. Macromolecular Chemistry and Physics 2017;218:1700192. https://doi.org/10.1002/macp.201700192.
[67] Telitel S, Dumur F, Telitel S, Soppera O, Lepeltier M, Guillaneuf Y, et al. Photoredox catalysis using a new iridium complex as an efficient toolbox for radical, cationic and controlled polymerizations under soft blue to green lights. Polym Chem 2014;6:613–24. https://doi.org/10.1039/C4PY01358A.
[68] Telitel S, Dumur F, Lepeltier M, Gigmes D, Fouassier J-P, Lalevée J. Photoredox process induced polymerization reactions: Iridium complexes for panchromatic photoinitiating systems. Comptes Rendus Chimie 2016;19:71–8. https://doi.org/10.1016/j.crci.2015.06.016.

[69] Dumur F, Bertin D, Gigmes D. Iridium (III) complexes as promising emitters for solid–state Light–Emitting Electrochemical Cells (LECs). International Journal of Nanotechnology 2012;9:377–95. https://doi.org/10.1504/IJNT.2012.045343.
[70] Tehfe M-A, Dumur F, Contal E, Graff B, Morlet-Savary F, Gigmes D, et al. New insights into radical and cationic polymerizations upon visible light exposure: role of novel photoinitiator systems based on the pyrene chromophore. Polym Chem 2013;4:1625–34. https://doi.org/10.1039/C2PY20950K.
[71] Telitel S, Dumur F, Faury T, Graff B, Tehfe M-A, Gigmes D, et al. New core-pyrene π structure organophotocatalysts usable as highly efficient photoinitiators. Beilstein J Org Chem 2013;9:877–90. https://doi.org/10.3762/bjoc.9.101.
[72] Uchida N, Nakano H, Igarashi T, Sakurai T. Nonsalt 1-(arylmethyloxy)pyrene photoinitiators capable of initiating cationic polymerization. Journal of Applied Polymer Science 2014;131. https://doi.org/10.1002/app.40510.
[73] Mishra A, Daswal S. 1-(Bromoacetyl)pyrene, a novel photoinitiator for the copolymerization of styrene and methylmethacrylate. Radiation Physics and Chemistry 2006;75:1093–100. https://doi.org/10.1016/j.radphyschem.2006.01.013.
[74] Tehfe M-A, Dumur F, Graff B, Morlet-Savary F, Gigmes D, Fouassier J-P, et al. Design of new Type I and Type II photoinitiators possessing highly coupled pyrene–ketone moieties. Polym Chem 2013;4:2313–24. https://doi.org/10.1039/C3PY21079K.
[75] Dumur F. Recent advances on pyrene-based photoinitiators of polymerization. European Polymer Journal 2020;126:109564. https://doi.org/10.1016/j.eurpolymj.2020.109564.
[76] Tehfe M-A, Dumur F, Vilà N, Graff B, Mayer CR, Fouassier JP, et al. A Multicolor Photoinitiator for Cationic Polymerization and Interpenetrated Polymer Network Synthesis: 2,7-Di-tert-butyldimethyldihydropyrene. Macromolecular Rapid Communications 2013;34:1104–9. https://doi.org/10.1002/marc.201300302.
[77] Corakci B, Hacioglu SO, Toppare L, Bulut U. Long wavelength photosensitizers in photoinitiated cationic polymerization: The effect of quinoxaline derivatives on photopolymerization. Polymer 2013;54:3182–7. https://doi.org/10.1016/j.polymer.2013.04.008.
[78] Xiao P, Dumur F, Thirion D, Fagour S, Vacher A, Sallenave X, et al. Multicolor Photoinitiators for Radical and Cationic Polymerization: Monofunctional vs Polyfunctional Thiophene Derivatives. Macromolecules 2013;46:6786–93. https://doi.org/10.1021/ma401389t.
[79] Tehfe M-A, Dumur F, Xiao P, Graff B, Morlet-Savary F, Fouassier J-P, et al. New chromone based photoinitiators for polymerization reactions under visible light. Polym Chem 2013;4:4234–44. https://doi.org/10.1039/C3PY00536D.
[80] You J, Fu H, Zhao D, Hu T, Nie J, Wang T. Flavonol dyes with different substituents in photopolymerization. Journal of Photochemistry and Photobiology A: Chemistry 2020;386:112097. https://doi.org/10.1016/j.jphotochem.2019.112097.
[81] Al Mousawi A, Garra P, Schmitt M, Toufaily J, Hamieh T, Graff B, et al. 3-Hydroxyflavone and N-Phenylglycine in High Performance Photoinitiating Systems for 3D Printing and Photocomposites Synthesis. Macromolecules 2018;51:4633–41. https://doi.org/10.1021/acs.macromol.8b00979.
[82] Giacoletto N, Ibrahim-Ouali M, Dumur F. Recent advances on squaraine-based photoinitiators of polymerization. European Polymer Journal 2021;150:110427. https://doi.org/10.1016/j.eurpolymj.2021.110427.

[83] Xiao P, Dumur F, Bui TT, Goubard F, Graff B, Morlet-Savary F, et al. Panchromatic Photopolymerizable Cationic Films Using Indoline and Squaraine Dye Based Photoinitiating Systems. ACS Macro Lett 2013;2:736–40. https://doi.org/10.1021/mz400316y.
[84] Launay V, Caron A, Noirbent G, Gigmes D, Dumur F, Lalevée J. NIR Organic Dyes as Innovative Tools for Reprocessing/Recycling of Plastics: Benefits of the Photothermal Activation in the Near-Infrared Range. Advanced Functional Materials 2021;31:2006324. https://doi.org/10.1002/adfm.202006324.
[85] Bonardi A, Bonardi F, Noirbent G, Dumur F, Dietlin C, Gigmes D, et al. Different NIR dye scaffolds for polymerization reactions under NIR light. Polym Chem 2019;10:6505–14. https://doi.org/10.1039/C9PY01447K.
[86] Abdallah M, Hijazi A, Graff B, Fouassier J-P, Rodeghiero G, Gualandi A, et al. Coumarin derivatives as versatile photoinitiators for 3D printing, polymerization in water and photocomposite synthesis. Polym Chem 2019;10:872–84. https://doi.org/10.1039/C8PY01708E.
[87] Abdallah M, Dumur F, Hijazi A, Rodeghiero G, Gualandi A, Cozzi PG, et al. Keto-coumarin scaffold for photoinitiators for 3D printing and photocomposites. Journal of Polymer Science 2020;58:1115–29. https://doi.org/10.1002/pol.20190290.
[88] Abdallah M, Hijazi A, Dumur F, Lalevée J. Coumarins as Powerful Photosensitizers for the Cationic Polymerization of Epoxy-Silicones under Near-UV and Visible Light and Applications for 3D Printing Technology. Molecules 2020;25:2063. https://doi.org/10.3390/molecules25092063.
[89] Abdallah M, Hijazi A, Cozzi PG, Gualandi A, Dumur F, Lalevée J. Boron Compounds as Additives for the Cationic Polymerization Using Coumarin Derivatives in Epoxy Silicones. Macromolecular Chemistry and Physics 2021;222:2000404. https://doi.org/10.1002/macp.202000404.
[90] Chen Q, Yang Q, Gao P, Chi B, Nie J, He Y. Photopolymerization of Coumarin-Containing Reversible Photoresponsive Materials Based on Wavelength Selectivity. Ind Eng Chem Res 2019;58:2970–5. https://doi.org/10.1021/acs.iecr.8b05164.
[91] Li Z, Zou X, Zhu G, Liu X, Liu R. Coumarin-Based Oxime Esters: Photobleachable and Versatile Unimolecular Initiators for Acrylate and Thiol-Based Click Photopolymerization under Visible Light-Emitting Diode Light Irradiation. ACS Appl Mater Interfaces 2018;10:16113–23. https://doi.org/10.1021/acsami.8b01767.
[92] Rahal M, Mokbel H, Graff B, Toufaily J, Hamieh T, Dumur F, et al. Mono vs. Difunctional Coumarin as Photoinitiators in Photocomposite Synthesis and 3D Printing. Catalysts 2020;10:1202. https://doi.org/10.3390/catal10101202.
[93] Rajeshirke M, Sreenath MC, Chitrambalam S, Joe IH, Sekar N. Enhancement of NLO Properties in OBO Fluorophores Derived from Carbazole–Coumarin Chalcones Containing Carboxylic Acid at the N-Alykl Terminal End. J Phys Chem C 2018;122:14313–25. https://doi.org/10.1021/acs.jpcc.8b02937.
[94] Rahal M, Graff B, Toufaily J, Hamieh T, Dumur F, Lalevée J. Design of keto-coumarin based photoinitiator for Free Radical Photopolymerization: Towards 3D printing and photocomposites applications. European Polymer Journal 2021;154:110559. https://doi.org/10.1016/j.eurpolymj.2021.110559.
[95] Rahal M, Graff B, Toufaily J, Hamieh T, Noirbent G, Gigmes D, et al. 3-Carboxylic Acid and Formyl-Derived Coumarins as Photoinitiators in Photo-Oxidation or Photo-Reduction Processes for Photopolymerization upon Visible Light: Photocomposite

Synthesis and 3D Printing Applications. Molecules 2021;26. https://doi.org/10.3390/molecules26061753.
[96] Hammoud F, Giacoletto N, Noirbent G, Graff B, Hijazi A, Nechab M, et al. Substituent effects on the photoinitiation ability of coumarin-based oxime-ester photoinitiators for free radical photopolymerization. Mater Chem Front 2021;5:8361–70. https://doi.org/10.1039/D1QM01310F.
[97] Dumur F. Recent advances on coumarin-based photoinitiators of polymerization. European Polymer Journal 2022;163:110962. https://doi.org/10.1016/j.eurpolymj.2021.110962.
[98] Mousawi AA, Dumur F, Garra P, Toufaily J, Hamieh T, Goubard F, et al. Azahelicenes as visible light photoinitiators for cationic and radical polymerization: Preparation of photoluminescent polymers and use in high performance LED projector 3D printing resins. Journal of Polymer Science Part A: Polymer Chemistry 2017;55:1189–99. https://doi.org/10.1002/pola.28476.
[99] Al Mousawi A, Schmitt M, Dumur F, Ouyang J, Favereau L, Dorcet V, et al. Visible Light Chiral Photoinitiator for Radical Polymerization and Synthesis of Polymeric Films with Strong Chiroptical Activity. Macromolecules 2018;51:5628–37. https://doi.org/10.1021/acs.macromol.8b01085.
[100] Ghali M, Benltifa M, Brahmi C, Elbassi L, Dumur F, Simonnet-Jégat C, et al. LED and solar photodecomposition of erythrosine B and rose Bengal using H3PMo12O40/polymer photocatalyst. European Polymer Journal 2021;159:110743. https://doi.org/10.1016/j.eurpolymj.2021.110743.
[101] Brahmi C, Benltifa M, Ghali M, Dumur F, Simonnet-Jégat C, Valérie M, et al. Performance improvement of the photocatalytic process for the degradation of pharmaceutical compounds using new POM/polymer photocatalysts. Journal of Environmental Chemical Engineering 2021;9:106015. https://doi.org/10.1016/j.jece.2021.106015.
[102] Brahmi C, Benltifa M, Vaulot C, Michelin L, Dumur F, Millange F, et al. New hybrid MOF/polymer composites for the photodegradation of organic dyes. European Polymer Journal 2021;154:110560. https://doi.org/10.1016/j.eurpolymj.2021.110560.
[103] Zhang J, Dumur F, Horcajada P, Livage C, Xiao P, Fouassier JP, et al. Iron-Based Metal-Organic Frameworks (MOF) as Photocatalysts for Radical and Cationic Polymerizations under Near UV and Visible LEDs (385–405 nm). Macromolecular Chemistry and Physics 2016;217:2534–40. https://doi.org/10.1002/macp.201600352.
[104] Brahmi C, Benltifa M, Vaulot C, Michelin L, Dumur F, Gkaniatsou E, et al. New Hybrid Fe-based MOFs/Polymer Composites for the Photodegradation of Organic Dyes. ChemistrySelect 2021;6:8120–32. https://doi.org/10.1002/slct.202102194.
[105] Zhang J, Lalevée J, Zhao J, Graff B, Stenzel MH, Xiao P. Dihydroxyanthraquinone derivatives: natural dyes as blue-light-sensitive versatile photoinitiators of photopolymerization. Polym Chem 2016;7:7316–24. https://doi.org/10.1039/C6PY01550F.
[106] Liu S, Chen H, Zhang Y, Sun K, Xu Y, Morlet-Savary F, et al. Monocomponent Photoinitiators based on Benzophenone-Carbazole Structure for LED Photoinitiating Systems and Application on 3D Printing. Polymers 2020;12:1394. https://doi.org/10.3390/polym12061394.
[107] Xiao P, Dumur F, Graff B, Gigmes D, Fouassier JP, Lalevée J. Variations on the Benzophenone Skeleton: Novel High Performance Blue Light Sensitive Photoinitiating Systems. Macromolecules 2013;46:7661–7. https://doi.org/10.1021/ma401766v.

[108] Zhang J, Frigoli M, Dumur F, Xiao P, Ronchi L, Graff B, et al. Design of Novel Photoinitiators for Radical and Cationic Photopolymerizations under Near UV and Visible LEDs (385, 395, and 405 nm). Macromolecules 2014;47:2811–9. https://doi.org/10.1021/ma500612x.
[109] Liu S, Brunel D, Noirbent G, Mau A, Chen H, Morlet-Savary F, et al. New multifunctional benzophenone-based photoinitiators with high migration stability and their applications in 3D printing. Mater Chem Front 2021;5:1982–94. https://doi.org/10.1039/D0QM00885K.
[110] Liu S, Brunel D, Sun K, Zhang Y, Chen H, Xiao P, et al. Novel Photoinitiators Based on Benzophenone-Triphenylamine Hybrid Structure for LED Photopolymerization. Macromolecular Rapid Communications 2020;41:2000460. https://doi.org/10.1002/marc.202000460.
[111] Liu S, Brunel D, Sun K, Xu Y, Morlet-Savary F, Graff B, et al. A monocomponent bifunctional benzophenone–carbazole type II photoinitiator for LED photoinitiating systems. Polym Chem 2020;11:3551–6. https://doi.org/10.1039/D0PY00644K.
[112] Qin X, Ding G, Gong Y, Jing C, Peng G, Liu S, et al. Stilbene-benzophenone dyads for free radical initiating polymerization of methyl methacrylate under visible light irradiation. Dyes and Pigments 2016;132:27–40. https://doi.org/10.1016/j.dyepig.2016.04.035.
[113] Jing C, Ding G, Qin X, Peng G, Huang H, Wang J, et al. New near UV photoinitiators containing benzophenone part for photoinitiating polymerization of methyl methacrylate. Progress in Organic Coatings 2017;110:150–61. https://doi.org/10.1016/j.porgcoat.2017.04.038.
[114] Huang T-L, Chen Y-C. Ketone Number and Substitution Effect of Benzophenone Derivatives on the Free Radical Photopolymerization of Visible-Light Type-II Photoinitiators. Polymers 2021;13. https://doi.org/10.3390/polym13111801.
[115] Kamoun EA, Winkel A, Eisenburger M, Menzel H. Carboxylated camphorquinone as visible-light photoinitiator for biomedical application: Synthesis, characterization, and application. Arabian Journal of Chemistry 2016;9:745–54. https://doi.org/10.1016/j.arabjc.2014.03.008.
[116] Santini A, Gallegos IT, Felix CM. Photoinitiators in Dentistry: A Review. Prim Dent J 2013;2:30–3. https://doi.org/10.1308/205016814809859563.
[117] Abdallah M, Le H, Hijazi A, Schmitt M, Graff B, Dumur F, et al. Acridone derivatives as high performance visible light photoinitiators for cationic and radical photosensitive resins for 3D printing technology and for low migration photopolymer property. Polymer 2018;159:47–58. https://doi.org/10.1016/j.polymer.2018.11.021.
[118] Zhang J, Dumur F, Bouzrati M, Xiao P, Dietlin C, Morlet-Savary F, et al. Novel panchromatic photopolymerizable matrices: N,N′-dibutylquinacridone as an efficient and versatile photoinitiator. Journal of Polymer Science Part A: Polymer Chemistry 2015;53:1719–27. https://doi.org/10.1002/pola.27615.
[119] Karaca N, Ocal N, Arsu N, Jockusch S. Thioxanthone-benzothiophenes as photoinitiator for free radical polymerization. Journal of Photochemistry and Photobiology A: Chemistry 2016;331:22–8. https://doi.org/10.1016/j.jphotochem.2016.01.017.
[120] Balta DK, Cetiner N, Temel G, Turgut Z, Arsu N. An annelated thioxanthone as a new Type II initiator. Journal of Photochemistry and Photobiology A: Chemistry 2008;199:316–21. https://doi.org/10.1016/j.jphotochem.2008.06.008.

[121] Balta DK, Temel G, Goksu G, Ocal N, Arsu N. Thioxanthone–Diphenyl Anthracene: Visible Light Photoinitiator. Macromolecules 2012;45:119–25. https://doi.org/10.1021/ma202168m.
[122] Dadashi-Silab S, Aydogan C, Yagci Y. Shining a light on an adaptable photoinitiator: advances in photopolymerizations initiated by thioxanthones. Polym Chem 2015;6:6595–615. https://doi.org/10.1039/C5PY01004G.
[123] Eren TN, Yasar N, Aviyente V, Morlet-Savary F, Graff B, Fouassier JP, et al. Photophysical and Photochemical Studies of Novel Thioxanthone-Functionalized Methacrylates through LED Excitation. Macromolecular Chemistry and Physics 2016;217:1501–12. https://doi.org/10.1002/macp.201600051.
[124] Qiu J, Wei J. Thioxanthone photoinitiator containing polymerizable N-aromatic maleimide for photopolymerization. J Polym Res 2014;21:559. https://doi.org/10.1007/s10965-014-0559-4.
[125] Tar H, Sevinc Esen D, Aydin M, Ley C, Arsu N, Allonas X. Panchromatic Type II Photoinitiator for Free Radical Polymerization Based on Thioxanthone Derivative. Macromolecules 2013;46:3266–72. https://doi.org/10.1021/ma302641d.
[126] Wu Q, Wang X, Xiong Y, Yang J, Tang H. Thioxanthone based one-component polymerizable visible light photoinitiator for free radical polymerization. RSC Adv 2016;6:66098–107. https://doi.org/10.1039/C6RA15349F.
[127] Wu Q, Tang K, Xiong Y, Wang X, Yang J, Tang H. High-Performance and Low Migration One-Component Thioxanthone Visible Light Photoinitiators. Macromolecular Chemistry and Physics 2017;218:1600484. https://doi.org/10.1002/macp.201600484.
[128] Wu X, Jin M, Malval J-P, Wan D, Pu H. Visible light-emitting diode-sensitive thioxanthone derivatives used in versatile photoinitiating systems for photopolymerizations. Journal of Polymer Science Part A: Polymer Chemistry 2017;55:4037–45. https://doi.org/10.1002/pola.28871.
[129] Bonardi A-H, Zahouily S, Dietlin C, Graff B, Morlet-Savary F, Ibrahim-Ouali M, et al. New 1,8-Naphthalimide Derivatives as Photoinitiators for Free-Radical Polymerization Upon Visible Light. Catalysts 2019;9:637. https://doi.org/10.3390/catal9080637.
[130] Zhang J, Zivic N, Dumur F, Xiao P, Graff B, Fouassier JP, et al. Naphthalimide-Tertiary Amine Derivatives as Blue-Light-Sensitive Photoinitiators. ChemPhotoChem 2018;2:481–9. https://doi.org/10.1002/cptc.201800006.
[131] Xiao P, Dumur F, Zhang J, Graff B, Gigmes D, Fouassier JP, et al. Naphthalimide Derivatives: Substituent Effects on the Photoinitiating Ability in Polymerizations under Near UV, Purple, White and Blue LEDs (385, 395, 405, 455, or 470 nm). Macromolecular Chemistry and Physics 2015;216:1782–90. https://doi.org/10.1002/macp.201500150.
[132] Xiao P, Dumur F, Zhang J, Graff B, Gigmes D, Fouassier JP, et al. Naphthalimide-phthalimide derivative based photoinitiating systems for polymerization reactions under blue lights. Journal of Polymer Science Part A: Polymer Chemistry 2015;53:665–74. https://doi.org/10.1002/pola.27490.
[133] Zhang J, Zivic N, Dumur F, Xiao P, Graff B, Gigmes D, et al. A benzophenone-naphthalimide derivative as versatile photoinitiator of polymerization under near UV and visible lights. Journal of Polymer Science Part A: Polymer Chemistry 2015;53:445–51. https://doi.org/10.1002/pola.27451.

[134] Zhang J, Zivic N, Dumur F, Xiao P, Graff B, Fouassier JP, et al. N-[2-(Dimethylamino)ethyl]-1,8-naphthalimide derivatives as photoinitiators under LEDs. Polym Chem 2018;9:994–1003. https://doi.org/10.1039/C8PY00055G.
[135] Zhang J, Dumur F, Xiao P, Graff B, Bardelang D, Gigmes D, et al. Structure Design of Naphthalimide Derivatives: Toward Versatile Photoinitiators for Near-UV/Visible LEDs, 3D Printing, and Water-Soluble Photoinitiating Systems. Macromolecules 2015;48:2054–63. https://doi.org/10.1021/acs.macromol.5b00201.
[136] Zhang J, Zivic N, Dumur F, Xiao P, Graff B, Fouassier JP, et al. UV-violet-blue LED induced polymerizations: Specific photoinitiating systems at 365, 385, 395 and 405 nm. Polymer 2014;55:6641–8. https://doi.org/10.1016/j.polymer.2014.11.002.
[137] Xiao P, Dumur F, Graff B, Gigmes D, Fouassier JP, Lalevée J. Blue Light Sensitive Dyes for Various Photopolymerization Reactions: Naphthalimide and Naphthalic Anhydride Derivatives. Macromolecules 2014;47:601–8. https://doi.org/10.1021/ma402376x.
[138] Xiao P, Dumur F, Frigoli M, Tehfe M-A, Graff B, Fouassier JP, et al. Naphthalimide based methacrylated photoinitiators in radical and cationic photopolymerization under visible light. Polym Chem 2013;4:5440–8. https://doi.org/10.1039/C3PY00766A.
[139] Noirbent G, Dumur F. Recent advances on naphthalic anhydrides and 1,8-naphthalimide-based photoinitiators of polymerization. European Polymer Journal 2020;132:109702. https://doi.org/10.1016/j.eurpolymj.2020.109702.
[140] Rahal M, Mokbel H, Graff B, Pertici V, Gigmes D, Toufaily J, et al. Naphthalimide-Based Dyes as Photoinitiators under Visible Light Irradiation and their Applications: Photocomposite Synthesis, 3D printing and Polymerization in Water. ChemPhotoChem 2021;5:476–90. https://doi.org/10.1002/cptc.202000306.
[141] Rahal M, Graff B, Toufaily J, Hamieh T, Ibrahim-Ouali M, Dumur F, et al. Naphthyl-Naphthalimides as High-Performance Visible Light Photoinitiators for 3D Printing and Photocomposites Synthesis. Catalysts 2021;11. https://doi.org/10.3390/catal11111269.
[142] Zivic N, Zhang J, Bardelang D, Dumur F, Xiao P, Jet T, et al. Novel naphthalimide–amine based photoinitiators operating under violet and blue LEDs and usable for various polymerization reactions and synthesis of hydrogels. Polym Chem 2015;7:418–29. https://doi.org/10.1039/C5PY01617G.
[143] Xiao P, Dumur F, Graff B, Morlet-Savary F, Gigmes D, Fouassier JP, et al. Design of High Performance Photoinitiators at 385–405 nm: Search around the Naphthalene Scaffold. Macromolecules 2014;47:973–8. https://doi.org/10.1021/ma402622v.
[144] Xiao P, Dumur F, Frigoli M, Graff B, Morlet-Savary F, Wantz G, et al. Perylene derivatives as photoinitiators in blue light sensitive cationic or radical curable films and panchromatic thiol-ene polymerizable films. European Polymer Journal 2014;53:215–22. https://doi.org/10.1016/j.eurpolymj.2014.01.024.
[145] Xiao P, Dumur F, Graff B, Gigmes D, Fouassier JP, Lalevée J. Red-Light-Induced Cationic Photopolymerization: Perylene Derivatives as Efficient Photoinitiators. Macromolecular Rapid Communications 2013;34:1452–8. https://doi.org/10.1002/marc.201300383.
[146] Dumur F. Recent advances on perylene-based photoinitiators of polymerization. European Polymer Journal 2021;159:110734. https://doi.org/10.1016/j.eurpolymj.2021.110734.
[147] Tehfe M-A, Dumur F, Graff B, Gigmes D, Fouassier J-P, Lalevée J. Green-Light-Induced Cationic Ring Opening Polymerization Reactions: Perylene-3,4:9,10-bis(Dicarboximide)

as Efficient Photosensitizers. Macromolecular Chemistry and Physics 2013;214:1052–60. https://doi.org/10.1002/macp.201200728.
[148] Telitel S, Dumur F, Campolo D, Poly J, Gigmes D, Fouassier JP, et al. Iron complexes as potential photocatalysts for controlled radical photopolymerizations: A tool for modifications and patterning of surfaces. Journal of Polymer Science Part A: Polymer Chemistry 2016;54:702–13. https://doi.org/10.1002/pola.27896.
[149] Zhang J, Campolo D, Dumur F, Xiao P, Fouassier JP, Gigmes D, et al. Iron complexes as photoinitiators for radical and cationic polymerization through photoredox catalysis processes. Journal of Polymer Science Part A: Polymer Chemistry 2015;53:42–9. https://doi.org/10.1002/pola.27435.
[150] Zhang J, Campolo D, Dumur F, Xiao P, Fouassier JP, Gigmes D, et al. Visible-light-sensitive photoredox catalysis by iron complexes: Applications in cationic and radical polymerization reactions. Journal of Polymer Science Part A: Polymer Chemistry 2016;54:2247–53. https://doi.org/10.1002/pola.28098.
[151] Zhang J, Campolo D, Dumur F, Xiao P, Fouassier JP, Gigmes D, et al. Iron Complexes in Visible-Light-Sensitive Photoredox Catalysis: Effect of Ligands on Their Photoinitiation Efficiencies. ChemCatChem 2016;8:2227–33. https://doi.org/10.1002/cctc.201600320.
[152] Dumur F. Recent advances on ferrocene-based photoinitiating systems. European Polymer Journal 2021;147:110328. https://doi.org/10.1016/j.eurpolymj.2021.110328.
[153] Chen H, Noirbent G, Sun K, Brunel D, Gigmes D, Morlet-Savary F, et al. Photoinitiators derived from natural product scaffolds: monochalcones in three-component photoinitiating systems and their applications in 3D printing. Polym Chem 2020;11:4647–59. https://doi.org/10.1039/D0PY00568A.
[154] Tang L, Nie J, Zhu X. A high performance phenyl-free LED photoinitiator for cationic or hybrid photopolymerization and its application in LED cationic 3D printing. Polym Chem 2020;11:2855–63. https://doi.org/10.1039/D0PY00142B.
[155] Xu Y, Noirbent G, Brunel D, Ding Z, Gigmes D, Graff B, et al. Allyloxy ketones as efficient photoinitiators with high migration stability in free radical polymerization and 3D printing. Dyes and Pigments 2021;185:108900. https://doi.org/10.1016/j.dyepig.2020.108900.
[156] Xu Y, Ding Z, Zhu H, Graff B, Knopf S, Xiao P, et al. Design of ketone derivatives as highly efficient photoinitiators for free radical and cationic photopolymerizations and application in 3D printing of composites. Journal of Polymer Science 2020;58:3432–45. https://doi.org/10.1002/pol.20200658.
[157] Chen H, Noirbent G, Liu S, Brunel D, Graff B, Gigmes D, et al. Bis-chalcone derivatives derived from natural products as near-UV/visible light sensitive photoinitiators for 3D/4D printing. Mater Chem Front 2021;5:901–16. https://doi.org/10.1039/D0QM00755B.
[158] Liu S, Zhang Y, Sun K, Graff B, Xiao P, Dumur F, et al. Design of photoinitiating systems based on the chalcone-anthracene scaffold for LED cationic photopolymerization and application in 3D printing. European Polymer Journal 2021;147:110300. https://doi.org/10.1016/j.eurpolymj.2021.110300.
[159] Giacoletto N, Dumur F. Recent Advances in bis-Chalcone-Based Photoinitiators of Polymerization: From Mechanistic Investigations to Applications. Molecules 2021;26:3192. https://doi.org/10.3390/molecules26113192.
[160] Chen H, Noirbent G, Zhang Y, Sun K, Liu S, Brunel D, et al. Photopolymerization and 3D/4D applications using newly developed dyes: Search around the natural chalcone

scaffold in photoinitiating systems. Dyes and Pigments 2021;188:109213. https://doi.org/10.1016/j.dyepig.2021.109213.
[161] Ibrahim-Ouali M, Dumur F. Recent Advances on Chalcone-based Photoinitiators of Polymerization. European Polymer Journal 2021:110688. https://doi.org/10.1016/j.eurpolymj.2021.110688.
[162] Chen H, Noirbent G, Liu S, Zhang Y, Sun K, Morlet-Savary F, et al. In situ generation of Ag nanoparticles during photopolymerization by using newly developed dyes-based three-component photoinitiating systems and the related 3D printing applications and their shape change behavior. Journal of Polymer Science 2021;59:843–59. https://doi.org/10.1002/pol.20210154.
[163] Chen H, Vahdati M, Xiao P, Dumur F, Lalevée J. Water-Soluble Visible Light Sensitive Photoinitiating System Based on Charge Transfer Complexes for the 3D Printing of Hydrogels. Polymers 2021;13. https://doi.org/10.3390/polym13183195.
[164] Tehfe M-A, Dumur F, Xiao P, Delgove M, Graff B, Fouassier J-P, et al. Chalcone derivatives as highly versatile photoinitiators for radical, cationic, thiol–ene and IPN polymerization reactions upon exposure to visible light. Polym Chem 2014;5:382–90. https://doi.org/10.1039/C3PY00922J.
[165] Sun K, Xu Y, Dumur F, Morlet-Savary F, Chen H, Dietlin C, et al. In silico rational design by molecular modeling of new ketones as photoinitiators in three-component photoinitiating systems: application in 3D printing. Polym Chem 2020;11:2230–42. https://doi.org/10.1039/C9PY01874C.
[166] Xiao P, Dumur F, Zhang J, Fouassier JP, Gigmes D, Lalevée J. Copper Complexes in Radical Photoinitiating Systems: Applications to Free Radical and Cationic Polymerization upon Visible LEDs. Macromolecules 2014;47:3837–44. https://doi.org/10.1021/ma5006793.
[167] Xiao P, Dumur F, Zhang J, Gigmes D, Fouassier JP, Lalevée J. Copper complexes: the effect of ligands on their photoinitiation efficiencies in radical polymerization reactions under visible light. Polym Chem 2014;5:6350–7. https://doi.org/10.1039/C4PY00925H.
[168] Xiao P, Zhang J, Campolo D, Dumur F, Gigmes D, Fouassier JP, et al. Copper and iron complexes as visible-light-sensitive photoinitiators of polymerization. Journal of Polymer Science Part A: Polymer Chemistry 2015;53:2673–84. https://doi.org/10.1002/pola.27762.
[169] Garra P, Carré M, Dumur F, Morlet-Savary F, Dietlin C, Gigmes D, et al. Copper-Based (Photo)redox Initiating Systems as Highly Efficient Systems for Interpenetrating Polymer Network Preparation. Macromolecules 2018;51:679–88. https://doi.org/10.1021/acs.macromol.7b02491.
[170] Garra P, Dumur F, Morlet-Savary F, Dietlin C, Gigmes D, Fouassier JP, et al. Mechanosynthesis of a Copper complex for redox initiating systems with a unique near infrared light activation. Journal of Polymer Science Part A: Polymer Chemistry 2017;55:3646–55. https://doi.org/10.1002/pola.28750.
[171] Garra P, Dumur F, Mousawi AA, Graff B, Gigmes D, Morlet-Savary F, et al. Mechanosynthesized copper(I) complex based initiating systems for redox polymerization: towards upgraded oxidizing and reducing agents. Polym Chem 2017;8:5884–96. https://doi.org/10.1039/C7PY01244F.
[172] Mokbel H, Anderson D, Plenderleith R, Dietlin C, Morlet-Savary F, Dumur F, et al. Copper photoredox catalyst "G1": a new high performance photoinitiator for near-UV and visible LEDs. Polym Chem 2017;8:5580–92. https://doi.org/10.1039/C7PY01016H.

[173] Mokbel H, Anderson D, Plenderleith R, Dietlin C, Morlet-Savary F, Dumur F, et al. Simultaneous initiation of radical and cationic polymerization reactions using the "G1" copper complex as photoredox catalyst: Applications of free radical/cationic hybrid photopolymerization in the composites and 3D printing fields. Progress in Organic Coatings 2019;132:50–61. https://doi.org/10.1016/j.porgcoat.2019.02.044.
[174] Mousawi AA, Kermagoret A, Versace D-L, Toufaily J, Hamieh T, Graff B, et al. Copper photoredox catalysts for polymerization upon near UV or visible light: structure/reactivity/efficiency relationships and use in LED projector 3D printing resins. Polym Chem 2017;8:568–80. https://doi.org/10.1039/C6PY01958G.
[175] Mau A, Noirbent G, Dietlin C, Graff B, Gigmes D, Dumur F, et al. Panchromatic Copper Complexes for Visible Light Photopolymerization. Photochem 2021;1. https://doi.org/10.3390/photochem1020010.
[176] Mau A, Dietlin C, Dumur F, Lalevée J. Concomitant initiation of radical and cationic polymerisations using new copper complexes as photoinitiators: Synthesis and characterisation of acrylate/epoxy interpenetrated polymer networks. European Polymer Journal 2021;152:110457. https://doi.org/10.1016/j.eurpolymj.2021.110457.
[177] Garra P, Dumur F, Gigmes D, Al Mousawi A, Morlet-Savary F, Dietlin C, et al. Copper (Photo)redox Catalyst for Radical Photopolymerization in Shadowed Areas and Access to Thick and Filled Samples. Macromolecules 2017;50:3761–71. https://doi.org/10.1021/acs.macromol.7b00622.
[178] Garra P, Dumur F, Morlet-Savary F, Dietlin C, Fouassier JP, Lalevée J. A New Highly Efficient Amine-Free and Peroxide-Free Redox System for Free Radical Polymerization under Air with Possible Light Activation. Macromolecules 2016;49:6296–309. https://doi.org/10.1021/acs.macromol.6b01615.
[179] Garra P, Kermagoret A, Mousawi AA, Dumur F, Gigmes D, Morlet-Savary F, et al. New copper(I) complex based initiating systems in redox polymerization and comparison with the amine/benzoyl peroxide reference. Polym Chem 2017;8:4088–97. https://doi.org/10.1039/C7PY00726D.
[180] Tehfe M-A, Dumur F, Contal E, Graff B, Gigmes D, Fouassier J-P, et al. Novel Highly Efficient Organophotocatalysts: Truxene–Acridine-1,8-diones as Photoinitiators of Polymerization. Macromolecular Chemistry and Physics 2013;214:2189–201. https://doi.org/10.1002/macp.201300362.
[181] Xiao P, Dumur F, Tehfe M-A, Graff B, Gigmes D, Fouassier JP, et al. Difunctional acridinediones as photoinitiators of polymerization under UV and visible lights: Structural effects. Polymer 2013;54:3458–66. https://doi.org/10.1016/j.polymer.2013.04.055.
[182] Xiao P, Dumur F, Tehfe M-A, Graff B, Gigmes D, Fouassier JP, et al. Acridinediones: Effect of Substituents on Their Photoinitiating Abilities in Radical and Cationic Photopolymerization. Macromolecular Chemistry and Physics 2013;214:2276–82. https://doi.org/10.1002/macp.201300363.
[183] Lalevée J, Dumur F, Tehfe M-A, Zein-Fakih A, Gigmes D, Morlet-Savary F, et al. Dye photosensitized cationic ring-opening polymerization: Search for new dye skeletons. Polymer 2012;53:4947–54. https://doi.org/10.1016/j.polymer.2012.08.067.
[184] Li J, Zhang X, Ali S, Akram MY, Nie J, Zhu X. The effect of polyethylene glycoldiacrylate complexation on type II photoinitiator and promotion for visible light initiation system. Journal of Photochemistry and Photobiology A: Chemistry 2019;384:112037. https://doi.org/10.1016/j.jphotochem.2019.112037.

[185] Li J, Li S, Li Y, Li R, Nie J, Zhu X. In situ monitoring of photopolymerization by photoinitiator with luminescence characteristics. Journal of Photochemistry and Photobiology A: Chemistry 2020;389:112225. https://doi.org/10.1016/j.jphotochem.2019.112225.
[186] Li J, Hao Y, Zhong M, Tang L, Nie J, Zhu X. Synthesis of furan derivative as LED light photoinitiator: One-pot, low usage, photobleaching for light color 3D printing. Dyes and Pigments 2019;165:467–73. https://doi.org/10.1016/j.dyepig.2019.03.011.
[187] Xu Y, Noirbent G, Brunel D, Ding Z, Gigmes D, Graff B, et al. Novel ketone derivative-based photoinitiating systems for free radical polymerization under mild conditions and 3D printing. Polym Chem 2020;11:5767–77. https://doi.org/10.1039/D0PY00990C.
[188] Mahmood A. Triphenylamine based dyes for dye sensitized solar cells: A review. Solar Energy 2016;123:127–44. https://doi.org/10.1016/j.solener.2015.11.015.
[189] Sakong C, Kim HJ, Kim SH, Namgoong JW, Park JH, Ryu J-H, et al. Synthesis and applications of new triphenylamine dyes with donor–donor–(bridge)–acceptor structure for organic dye-sensitized solar cells. New J Chem 2012;36:2025–32. https://doi.org/10.1039/C2NJ40374A.
[190] Holliman PJ, Mohsen M, Connell A, Kershaw CP, Meza-Rojas D, Jones EW, et al. Double Linker Triphenylamine Dyes for Dye-Sensitized Solar Cells. Energies 2020;13. https://doi.org/10.3390/en13184637.
[191] Marinado T, Nonomura K, Nissfolk J, Karlsson MartinK, Hagberg DP, Sun L, et al. How the Nature of Triphenylamine-Polyene Dyes in Dye-Sensitized Solar Cells Affects the Open-Circuit Voltage and Electron Lifetimes. Langmuir 2010;26:2592–8. https://doi.org/10.1021/la902897z.
[192] Padalkar VS, Sakamaki D, Kuwada K, Tohnai N, Akutagawa T, Sakai K, et al. AIE active triphenylamine–benzothiazole based motifs: ESIPT or ICT emission. RSC Adv 2016;6:26941–9. https://doi.org/10.1039/C6RA02417C.
[193] Blanchard P, Malacrida C, Cabanetos C, Roncali J, Ludwigs S. Triphenylamine and some of its derivatives as versatile building blocks for organic electronic applications. Polymer International 2019;68:589–606. https://doi.org/10.1002/pi.5695.
[194] Hou Q, Chen Y, Zhen H, Ma Z, Hong W, Shi G, et al. A triphenylamine-based four-armed molecule for solution-processed organic solar cells with high photo-voltage. J Mater Chem A 2013;1:4937–40. https://doi.org/10.1039/C3TA10401J.
[195] Rybakiewicz R, Zagorska M, Pron A. Triphenylamine-based electroactive compounds: synthesis, properties and application to organic electronics. Chemical Papers 2017;71:243–68. https://doi.org/10.1007/s11696-016-0097-0.
[196] Agarwala P, Kabra D. A review on triphenylamine (TPA) based organic hole transport materials (HTMs) for dye sensitized solar cells (DSSCs) and perovskite solar cells (PSCs): evolution and molecular engineering. J Mater Chem A 2017;5:1348–73. https://doi.org/10.1039/C6TA08449D.
[197] Yen H-J, Liou G-S. Recent advances in triphenylamine-based electrochromic derivatives and polymers. Polym Chem 2018;9:3001–18. https://doi.org/10.1039/C8PY00367J.
[198] Manifar T, Rohani S. Synthesis and Analysis of Triphenylamine: A Review. The Canadian Journal of Chemical Engineering 2004;82:323–34. https://doi.org/10.1002/cjce.5450820213.
[199] Data P, Pander P, Zassowski P, Mimaite V, Karon K, Lapkowski M, et al. Electrochemically Induced Synthesis of Triphenylamine-based Polyhydrazones. Electrochimica Acta 2017;230:10–21. https://doi.org/10.1016/j.electacta.2017.01.132.

[200] Schaub TA, Mekelburg T, Dral PO, Miehlich M, Hampel F, Meyer K, et al. A Spherically Shielded Triphenylamine and Its Persistent Radical Cation. Chemistry – A European Journal 2020;26:3264–9. https://doi.org/10.1002/chem.202000355.
[201] Gómez MAR, Kurva M, Gámez-Montaño R. Synthesis of Triphenylamine-Imidazo[1,2-a]pyridine via Groebke–Blackburn–Bienaymé Reaction. Chemistry Proceedings 2021;3. https://doi.org/10.3390/ecsoc-24-08422.
[202] Chen S, Liu X, Huang J, Ge X, Wang Q, Yao M, et al. Triphenylamine/carbazole-modified ruthenium(ii) Schiff base compounds: synthesis, biological activity and organelle targeting. Dalton Trans 2020;49:8774–84. https://doi.org/10.1039/D0DT01547D.
[203] Brunel F, Lautard C, di Giorgio C, Garzino F, Raimundo J-M, Bolla J-M, et al. Antibacterial activities of mono-, di- and tri-substituted triphenylamine-based phosphonium ionic liquids. Bioorganic & Medicinal Chemistry Letters 2018;28:926–9. https://doi.org/10.1016/j.bmcl.2018.01.057.
[204] Sun K, Pigot C, Chen H, Nechab M, Gigmes D, Morlet-Savary F, et al. Free Radical Photopolymerization and 3D Printing Using Newly Developed Dyes: Indane-1,3-Dione and 1H-Cyclopentanaphthalene-1,3-Dione Derivatives as Photoinitiators in Three-Component Systems. Catalysts 2020;10:463. https://doi.org/10.3390/catal10040463.
[205] Pigot C, Noirbent G, Bui T-T, Péralta S, Gigmes D, Nechab M, et al. Push-Pull Chromophores Based on the Naphthalene Scaffold: Potential Candidates for Optoelectronic Applications. Materials 2019;12. https://doi.org/10.3390/ma12081342.
[206] Lee Y, Jo A, Park SB. Rational Improvement of Molar Absorptivity Guided by Oscillator Strength: A Case Study with Furoindolizine-Based Core Skeleton. Angewandte Chemie International Edition 2015;54:15689–93. https://doi.org/10.1002/anie.201506429.
[207] Abdallah M, Dumur F, Graff B, Hijazi A, Lalevée J. High performance dyes based on triphenylamine, cinnamaldehyde and indane-1,3-dione derivatives for blue light induced polymerization for 3D printing and photocomposites. Dyes and Pigments 2020;182:108580. https://doi.org/10.1016/j.dyepig.2020.108580.
[208] Noirbent G, Dumur F. Photoinitiators of polymerization with reduced environmental impact: Nature as an unlimited and renewable source of dyes. European Polymer Journal 2021;142:110109. https://doi.org/10.1016/j.eurpolymj.2020.110109.
[209] Karaca Balta D, Karahan Ö, Avci D, Arsu N. Synthesis, photophysical and photochemical studies of benzophenone based novel monomeric and polymeric photoinitiators. Progress in Organic Coatings 2015;78:200–7. https://doi.org/10.1016/j.porgcoat.2014.09.003.
[210] Temel G, Karaca N, Arsu N. Synthesis of main chain polymeric benzophenone photoinitiator via thiol-ene click chemistry and Its use in free radical polymerization. Journal of Polymer Science Part A: Polymer Chemistry 2010;48:5306–12. https://doi.org/10.1002/pola.24330.
[211] Carbone ND, Ene M, Lancaster JR, Koberstein JT. Kinetics and Mechanisms of Radical-Based Branching/Cross-Linking Reactions in Preformed Polymers Induced by Benzophenone and Bis-Benzophenone Photoinitiators. Macromolecules 2013;46:5434–44. https://doi.org/10.1021/ma4007347.
[212] Temel G, Enginol B, Aydin M, Balta DK, Arsu N. Photopolymerization and photophysical properties of amine linked benzophenone photoinitiator for free radical polymerization. Journal of Photochemistry and Photobiology A: Chemistry 2011;219:26–31. https://doi.org/10.1016/j.jphotochem.2011.01.012.

[213] Schmitt M. Method to analyse energy and intensity dependent photo-curing of acrylic esters in bulk. RSC Adv 2015;5:67284–98. https://doi.org/10.1039/C5RA11427F.
[214] Lalevée J, Tehfe M-A, Dumur F, Gigmes D, Graff B, Morlet-Savary F, et al. Light-Harvesting Organic Photoinitiators of Polymerization. Macromolecular Rapid Communications 2013;34:239–45. https://doi.org/10.1002/marc.201200578.
[215] Telitel S, Dumur F, Gigmes D, Graff B, Fouassier JP, Lalevée J. New functionalized aromatic ketones as photoinitiating systems for near visible and visible light induced polymerizations. Polymer 2013;54:2857–64. https://doi.org/10.1016/j.polymer.2013.03.062.
[216] Arslan M, Kiskan B, Yagci Y. Post-Modification of Polybutadienes by Photoinduced Hydrogen Abstraction from Benzoxazines and Their Thermally Activated Curing. Macromolecules 2016;49:5026–32. https://doi.org/10.1021/acs.macromol.6b01329.
[217] Huang T-L, Li Y-H, Chen Y-C. Benzophenone derivatives as novel organosoluble visible light Type II photoinitiators for UV and LED photoinitiating systems. Journal of Polymer Science 2020;58:2914–25. https://doi.org/10.1002/pol.20200437.
[218] Jia X, Zhao D, You J, Hao T, Li X, Nie J, et al. Acetylene bridged D-(π-A)2 type dyes containing benzophenone moieties: Photophysical properties, and the potential application as photoinitiators. Dyes and Pigments 2021;184:108583. https://doi.org/10.1016/j.dyepig.2020.108583.
[219] Kondo R, Yasuda T, Yang YS, Kim JY, Adachi C. Highly luminescent π-conjugated dithienometalloles: photophysical properties and their application in organic light-emitting diodes. J Mater Chem 2012;22:16810–6. https://doi.org/10.1039/C2JM33526C.
[220] Al Mousawi A, Garra P, Sallenave X, Dumur F, Toufaily J, Hamieh T, et al. π-Conjugated Dithienophosphole Derivatives as High Performance Photoinitiators for 3D Printing Resins. Macromolecules 2018;51:1811–21. https://doi.org/10.1021/acs.macromol.8b00044.
[221] Chen L, Yu Q, Wang Y, Li H. BisGMA/TEGDMA dental composite containing high aspect-ratio hydroxyapatite nanofibers. Dental Materials 2011;27:1187–95. https://doi.org/10.1016/j.dental.2011.08.403.
[222] Alizadehgharib S, Östberg A-K, Dahlstrand Rudin A, Dahlgren U, Christenson K. The effects of the dental methacrylates TEGDMA, Bis-GMA, and UDMA on neutrophils in vitro. Clinical and Experimental Dental Research 2020;6:439–47. https://doi.org/10.1002/cre2.296.
[223] Götz DCG, Gehrold AC, Dorazio SJ, Daddario P, Samankumara L, Bringmann G, et al. Indaphyrins and Indachlorins: Optical and Chiroptical Properties of a Family of Helimeric Porphyrinoids. European Journal of Organic Chemistry 2015;2015:3913–22. https://doi.org/10.1002/ejoc.201500511.
[224] Luo S, Zhu W, Liu F, He J. Preparation of a Bis-GMA-Free Dental Resin System with Synthesized Fluorinated Dimethacrylate Monomers. International Journal of Molecular Sciences 2016;17. https://doi.org/10.3390/ijms17122014.
[225] Rüttermann S, Dluzhevskaya I, Großsteinbeck C, Raab WH-M, Janda R. Impact of replacing Bis-GMA and TEGDMA by other commercially available monomers on the properties of resin-based composites. Dental Materials 2010;26:353–9. https://doi.org/10.1016/j.dental.2009.12.006.
[226] Sigman MS, Harper KC, Bess EN, Milo A. The Development of Multidimensional Analysis Tools for Asymmetric Catalysis and Beyond. Acc Chem Res 2016;49:1292–301. https://doi.org/10.1021/acs.accounts.6b00194.

[227] Bouzrati-Zerelli M, Maier M, Fik CP, Dietlin C, Morlet-Savary F, Fouassier JP, et al. A low migration phosphine to overcome the oxygen inhibition in new high performance photoinitiating systems for photocurable dental type resins. Polymer International 2017;66:504–11. https://doi.org/10.1002/pi.5262.
[228] Metri N, Sallenave X, Beouch L, Plesse C, Goubard F, Chevrot C. New star-shaped molecules derived from thieno[3,2-b]thiophene unit and triphenylamine. Tetrahedron Letters 2010;51:6673–6. https://doi.org/10.1016/j.tetlet.2010.10.082.
[229] Xiao P, Lalevée J, Zhao J, Stenzel MH. N-Vinylcarbazole as Versatile Photoinaddimer of Photopolymerization under Household UV LED Bulb (392 nm). Macromolecular Rapid Communications 2015;36:1675–80. https://doi.org/10.1002/marc.201500214.
[230] Tehfe M-A, Dumur F, Graff B, Clément J-L, Gigmes D, Morlet-Savary F, et al. New Cleavable Photoinitiator Architecture with Huge Molar Extinction Coefficients for Polymerization in the 340–450 nm Range. Macromolecules 2013;46:736–46. https://doi.org/10.1021/ma3024359.
[231] Wang X-P, Wang Q-X, Lin H-P, Chang N. Anti-tumor bioactivities of curcumin on mice loaded with gastric carcinoma. Food Funct 2017;8:3319–26. https://doi.org/10.1039/C7FO00555E.
[232] Prasad S, Tyagi AK. Curcumin and its analogues: a potential natural compound against HIV infection and AIDS. Food Funct 2015;6:3412–9. https://doi.org/10.1039/C5FO00485C.
[233] Khan MA, El-Khatib R, Rainsford KD, Whitehouse MW. Synthesis and anti-inflammatory properties of some aromatic and heterocyclic aromatic curcuminoids. Bioorganic Chemistry 2012;40:30–8. https://doi.org/10.1016/j.bioorg.2011.11.004.
[234] Zhao J, Lalevée J, Lu H, MacQueen R, Kable SH, Schmidt TW, et al. A new role of curcumin: as a multicolor photoinitiator for polymer fabrication under household UV to red LED bulbs. Polym Chem 2015;6:5053–61. https://doi.org/10.1039/C5PY00661A.
[235] Mishra A, Daswal S. Curcumin, a natural colorant as initiator for photopolymerization of styrene: kinetics and mechanism. Colloid and Polymer Science 2007;285:1109–17. https://doi.org/10.1007/s00396-007-1662-4.
[236] Mishra A, Daswal S. Curcumin, A Novel Natural Photoinitiator for the Copolymerization of Styrene and Methylmethacrylate. Null 2005;42:1667–78. https://doi.org/10.1080/10601320500246974.
[237] Lalevée J, Tehfe M-A, Zein-Fakih A, Ball B, Telitel S, Morlet-Savary F, et al. N-Vinylcarbazole: An Additive for Free Radical Promoted Cationic Polymerization upon Visible Light. ACS Macro Lett 2012;1:802–6. https://doi.org/10.1021/mz3002325.
[238] Dietlin C, Schweizer S, Xiao P, Zhang J, Morlet-Savary F, Graff B, et al. Photopolymerization upon LEDs: new photoinitiating systems and strategies. Polym Chem 2015;6:3895–912. https://doi.org/10.1039/C5PY00258C.
[239] Priyadarsini KI. Photophysics, photochemistry and photobiology of curcumin: Studies from organic solutions, bio-mimetics and living cells. Journal of Photochemistry and Photobiology C: Photochemistry Reviews 2009;10:81–95. https://doi.org/10.1016/j.jphotochemrev.2009.05.001.
[240] Crivello JV, Bulut U. Indian Turmeric and its Use in Cationic Photopolymerizations. Macromolecular Symposia 2006;240:1–11. https://doi.org/10.1002/masy.200650801.
[241] Crivello JV, Bulut U. Curcumin: A naturally occurring long-wavelength photosensitizer for diaryliodonium salts. Journal of Polymer Science Part A: Polymer Chemistry 2005;43:5217–31. https://doi.org/10.1002/pola.21017.

[242] Han W, Fu H, Xue T, Liu T, Wang Y, Wang T. Facilely prepared blue-green light sensitive curcuminoids with excellent bleaching properties as high performance photosensitizers in cationic and free radical photopolymerization. Polym Chem 2018;9:1787–98. https://doi.org/10.1039/C8PY00166A.
[243] Bi Y, Neckers DC. A Visible Light Initiating System for Free Radical Promoted Cationic Polymerization. Macromolecules 1994;27:3683–93. https://doi.org/10.1021/ma00092a001.
[244] Belon C, Allonas X, Croutxé-barghorn C, Lalevée J. Overcoming the oxygen inhibition in the photopolymerization of acrylates: A study of the beneficial effect of triphenylphosphine. Journal of Polymer Science Part A: Polymer Chemistry 2010;48:2462–9. https://doi.org/10.1002/pola.24017.
[245] Gentry SP, Halloran JW. Absorption effects in photopolymerized ceramic suspensions. Journal of the European Ceramic Society 2013;33:1989–94. https://doi.org/10.1016/j.jeurceramsoc.2013.03.004.
[246] Grotzinger C, Burget D, Jacques P, Fouassier JP. Visible light induced photopolymerization: speeding up the rate of polymerization by using co-initiators in dye/amine photoinitiating systems. Polymer 2003;44:3671–7. https://doi.org/10.1016/S0032-3861(03)00286-6.
[247] Tomeckova V, Halloran JW. Critical energy for photopolymerization of ceramic suspensions in acrylate monomers. Journal of the European Ceramic Society 2010;30:3273–82. https://doi.org/10.1016/j.jeurceramsoc.2010.08.003.
[248] Tomeckova V, Norton SJ, Love BJ, Halloran JW. Photopolymerization of acrylate suspensions with visible dyes. Journal of the European Ceramic Society 2013;33:699–707. https://doi.org/10.1016/j.jeurceramsoc.2012.10.015.
[249] Garra P, Morlet-Savary F, Dietlin C, Fouassier JP, Lalevée J. On-Demand Visible Light Activated Amine/Benzoyl Peroxide Redox Initiating Systems: A Unique Tool To Overcome the Shadow Areas in Photopolymerization Processes. Macromolecules 2016;49:9371–81. https://doi.org/10.1021/acs.macromol.6b02167.
[250] Guimarães T, Schneider LF, Braga RR, Pfeifer CS. Mapping camphorquinone consumption, conversion and mechanical properties in methacrylates with systematically varied CQ/amine compositions. Dental Materials 2014;30:1274–9. https://doi.org/10.1016/j.dental.2014.08.379.
[251] Schneider LFJ, Cavalcante LM, Prahl SA, Pfeifer CS, Ferracane JL. Curing efficiency of dental resin composites formulated with camphorquinone or trimethylbenzoyl-diphenyl-phosphine oxide. Dental Materials 2012;28:392–7. https://doi.org/10.1016/j.dental.2011.11.014.
[252] Schneider LFJ, Pfeifer CSC, Consani S, Prahl SA, Ferracane JL. Influence of photoinitiator type on the rate of polymerization, degree of conversion, hardness and yellowing of dental resin composites. Dental Materials 2008;24:1169–77. https://doi.org/10.1016/j.dental.2008.01.007.
[253] Schroeder WF, Vallo CI. Effect of different photoinitiator systems on conversion profiles of a model unfilled light-cured resin. Dental Materials 2007;23:1313–21. https://doi.org/10.1016/j.dental.2006.11.010.
[254] Cook WD. Photopolymerization kinetics of dimethacrylates using the camphorquinone/amine initiator system. Polymer 1992;33:600–9. https://doi.org/10.1016/0032-3861(92)90738-I.

[255] Cumpston BH, Ananthavel SP, Barlow S, Dyer DL, Ehrlich JE, Erskine LL, et al. Two-photon polymerization initiators for three-dimensional optical data storage and microfabrication. Nature 1999;398:51–4. https://doi.org/10.1038/17989.
[256] Wang X, Jin F, Chen Z, Liu S, Wang X, Duan X, et al. A New Family of Dendrimers with Naphthaline Core and Triphenylamine Branching as a Two-Photon Polymerization Initiator. J Phys Chem C 2011;115:776–84. https://doi.org/10.1021/jp1081005.
[257] Xue J, Zhao Y, Wu F, Fang D-C. Effect of Bridging Position on the Two-Photon Polymerization Initiating Efficiencies of Novel Coumarin/Benzylidene Cyclopentanone Dyes. J Phys Chem A 2010;114:5171–9. https://doi.org/10.1021/jp909745q.
[258] Allen NS, Corrales T, Edge M, Catalina F, Blanco-Pina M, Green A. Photochemistry and photopolymerization activities of novel phenylthiobenzophenone and diphenylthiophene photoinitiators. Polymer 1998;39:903–9. https://doi.org/10.1016/S0032-3861(97)00357-1.
[259] Allen NS, Pullen G, Shah M, Edge M, Weddell I, Swart R, et al. Photochemistry and photoinitiator properties of 2-substituted anthraquinones: 2. Photopolymerization and flash photolysis. Polymer 1995;36:4665–74. https://doi.org/10.1016/0032-3861(95)96834-U.
[260] Corrales T, Peinado C, Catalina F, Neumann MG, Allen NS, Rufs AM, et al. Photopolymerization of methyl methacrylate initiated by thioxanthone derivatives: photoinitiation mechanism. Polymer 2000;41:9103–9. https://doi.org/10.1016/S0032-3861(00)00292-5.
[261] Ghosh SK, Mandal BM. Studies on the kinetics of inverse emulsion polymerization of acrylamide using α-ketoglutaric acid as photoinitiator. Polymer 1993;34:4287–90. https://doi.org/10.1016/0032-3861(93)90190-L.
[262] Huang X, Wang X, Zhao Y. Study on a series of water-soluble photoinitiators for fabrication of 3D hydrogels by two-photon polymerization. Dyes and Pigments 2017;141:413–9. https://doi.org/10.1016/j.dyepig.2017.02.040.
[263] Guo H, Jiang H, Luo L, Wu C, Guo H, Wang X, et al. Two-photon polymerization of gratings by interference of a femtosecond laser pulse. Chemical Physics Letters 2003;374:381–4. https://doi.org/10.1016/S0009-2614(03)00704-8.
[264] Pucher N, Rosspeintner A, Satzinger V, Schmidt V, Gescheidt G, Stampfl J, et al. Structure−Activity Relationship in D-π-A-π-D-Based Photoinitiators for the Two-Photon-Induced Photopolymerization Process. Macromolecules 2009;42:6519–28. https://doi.org/10.1021/ma9007785.
[265] Wu J, Zhao Y, Li X, Shi M, Wu F, Fang X. Multibranched benzylidene cyclopentanone dyes with large two-photon absorption cross-sections. New J Chem 2006;30:1098–103. https://doi.org/10.1039/B604695A.
[266] Jiang X, Xu H, Yin J. Polymeric amine bearing side-chain thioxanthone as a novel photoinitiator for photopolymerization. Polymer 2004;45:133–40. https://doi.org/10.1016/j.polymer.2003.10.058.
[267] Sun GJ, Chae KH. Properties of 2,3-butanedione and 1-phenyl-1,2-propanedione as new photosensitizers for visible light cured dental resin composites. Polymer 2000;41:6205–12. https://doi.org/10.1016/S0032-3861(99)00832-0.
[268] Tehfe M-A, Lalevée J, Telitel S, Sun J, Zhao J, Graff B, et al. Iridium complexes incorporating coumarin moiety as catalyst photoinitiators: Towards household green LED bulb and halogen lamp irradiation. Polymer 2012;53:2803–8. https://doi.org/10.1016/j.polymer.2012.05.009.

[269] Wang H, Wei J, Jiang X, Yin J. Novel chemical-bonded polymerizable sulfur-containing photoinitiators comprising the structure of planar N-phenylmaleimide and benzophenone for photopolymerization. Polymer 2006;47:4967–75. https://doi.org/10.1016/j.polymer.2006.04.027.
[270] Fu H, Qiu Y, You J, Hao T, Fan B, Nie J, et al. Photopolymerization of acrylate resin and ceramic suspensions with benzylidene ketones under blue/green LED. Polymer 2019;184:121841. https://doi.org/10.1016/j.polymer.2019.121841.
[271] Rao YJ, Sowjanya T, Thirupathi G, Murthy NYS, Kotapalli SS. Synthesis and biological evaluation of novel flavone/triazole/benzimidazole hybrids and flavone/isoxazole-annulated heterocycles as antiproliferative and antimycobacterial agents. Molecular Diversity 2018;22:803–14. https://doi.org/10.1007/s11030-018-9833-4.
[272] Balasuriya N, Rupasinghe HPV. Antihypertensive properties of flavonoid-rich apple peel extract. Food Chemistry 2012;135:2320–5. https://doi.org/10.1016/j.foodchem.2012.07.023.
[273] Kawai M, Hirano T, Higa S, Arimitsu J, Maruta M, Kuwahara Y, et al. Flavonoids and related compounds as anti-allergic substances. Allergol Int 2007;56:113–23. https://doi.org/10.2332/allergolint.R-06-135.
[274] Orhan DD, Özçelik B, Özgen S, Ergun F. Antibacterial, antifungal, and antiviral activities of some flavonoids. Microbiological Research 2010;165:496–504. https://doi.org/10.1016/j.micres.2009.09.002.
[275] Forbes A M, Lin H, Meadows G G, Meier G Patrick. Synthesis and anticancer activity of new flavonoid analogs and inconsistencies in assays related to proliferation and viability measurements. Int J Oncol 2014;45:831–42. https://doi.org/10.3892/ijo.2014.2452.
[276] Liu B, Luo Z, Si S, Zhou X, Pan C, Wang L. A photostable triphenylamine-based flavonoid dye: Solvatochromism, aggregation-induced emission enhancement, fabrication of organic nanodots, and cell imaging applications. Dyes and Pigments 2017;142:32–8. https://doi.org/10.1016/j.dyepig.2017.03.023.
[277] Dziuba D, Postupalenko VY, Spadafora M, Klymchenko AS, Guérineau V, Mély Y, et al. A Universal Nucleoside with Strong Two-Band Switchable Fluorescence and Sensitivity to the Environment for Investigating DNA Interactions. J Am Chem Soc 2012;134:10209–13. https://doi.org/10.1021/ja3030388.
[278] Yushchenko DA, Fauerbach JA, Thirunavukkuarasu S, Jares-Erijman EA, Jovin TM. Fluorescent Ratiometric MFC Probe Sensitive to Early Stages of α-Synuclein Aggregation. J Am Chem Soc 2010;132:7860–1. https://doi.org/10.1021/ja102838n.
[279] Klymchenko AS, Demchenko AP. Electrochromic Modulation of Excited-State Intramolecular Proton Transfer: The New Principle in Design of Fluorescence Sensors. J Am Chem Soc 2002;124:12372–9. https://doi.org/10.1021/ja027669l.
[280] Sengupta PK, Kasha M. Excited state proton-transfer spectroscopy of 3-hydroxyflavone and quercetin. Chemical Physics Letters 1979;68:382–5. https://doi.org/10.1016/0009-2614(79)87221-8.
[281] McMorrow D, Kasha M. Intramolecular excited-state proton transfer in 3-hydroxyflavone. Hydrogen-bonding solvent perturbations. J Phys Chem 1984;88:2235–43. https://doi.org/10.1021/j150655a012.
[282] Ameer-Beg S, Ormson SM, Brown RG, Matousek P, Towrie M, Nibbering ETJ, et al. Ultrafast Measurements of Excited State Intramolecular Proton Transfer (ESIPT) in Room Temperature Solutions of 3-Hydroxyflavone and Derivatives. J Phys Chem A 2001;105:3709–18. https://doi.org/10.1021/jp0031101.

[283] You J, Cao D, Hu T, Ye Y, Jia X, Li H, et al. Novel Norrish type I flavonoid photoinitiator for safe LED light with high activity and low toxicity by inhibiting the ESIPT process. Dyes and Pigments 2021;184:108865. https://doi.org/10.1016/j.dyepig.2020.108865.
[284] Jin M, Zhou R, Yu M, Pan H, Wan D. D-π-a-type oxime sulfonate photoacid generators for cationic polymerization under UV–visible LED irradiation. Journal of Polymer Science Part A: Polymer Chemistry 2018;56:1146–54. https://doi.org/10.1002/pola.28996.
[285] Chen H, Noirbent G, Zhang Y, Brunel D, Gigmes D, Morlet-Savary F, et al. Novel D–π-A and A–π-D–π-A three-component photoinitiating systems based on carbazole/triphenylamino based chalcones and application in 3D and 4D printing. Polym Chem 2020;11:6512–28. https://doi.org/10.1039/D0PY01197E.
[286] Hu T, Fu H, Xiong J, Wang T. Benzylidene piperidones as photosensitizers for visible light photopolymerization. Journal of Photochemistry and Photobiology A: Chemistry 2021;405:112968. https://doi.org/10.1016/j.jphotochem.2020.112968.
[287] Hayashi T, Maeda K. Preparation of a New Phototropic Substance. Bulletin of the Chemical Society of Japan 1960;33:565–6. https://doi.org/10.1246/bcsj.33.565.
[288] Sathe SS, Ahn D, Scott TF. Re-examining the Photomediated Dissociation and Recombination Kinetics of Hexaarylbiimidazoles. Ind Eng Chem Res 2015;54:4203–12. https://doi.org/10.1021/ie504230c.
[289] White DM, Sonnenberg J. Oxidation of Triarylimidazoles. Structures of the Photochromic and Piezochromic Dimers of Triarylimidazyl Radicals1. J Am Chem Soc 1966;88:3825–9. https://doi.org/10.1021/ja00968a027.
[290] Chen Y-C, Kuo Y-T. Photocuring Kinetic Studies of TMPTMA Monomer by Type II Photoinitiators of Different Weight Ratios of 2-Chlorohexaaryl Biimidazole (o-Cl-HABI) and N-Phenylglycine (NPG). Journal of Photopolymer Science and Technology 2018;31:487–92. https://doi.org/10.2494/photopolymer.31.487.
[291] Chen Y-C, Kuo Y-T, Ho T-H. Photo-polymerization properties of type-II photoinitiator systems based on 2-chlorohexaaryl biimidazole (o-Cl-HABI) and various N-phenylglycine (NPG) derivatives! Photochemical & Photobiological Sciences 2019;18:190–7. https://doi.org/10.1039/c8pp00300a.
[292] Ahn D, Zavada SR, Scott TF. Rapid, Photomediated Healing of Hexaarylbiimidazole-Based Covalently Cross-Linked Gels. Chem Mater 2017;29:7023–31. https://doi.org/10.1021/acs.chemmater.7b02640.
[293] Liu AD, Trifunac AD, Krongauz VV. Photodissociation of hexaarylbiimidazole. 2. Direct and sensitized dissociation. J Phys Chem 1992;96:207–11. https://doi.org/10.1021/j100180a040.
[294] Kimoto A, Niitsu S, Iwahori F, Abe J. Formation of hexaarylbiimidazole heterodimers via the cross recombination of two lophyl radicals. New J Chem 2009;33:1339–42. https://doi.org/10.1039/B823277F.
[295] Allonas X, Fouassier JP, Kaji M, Miyasaka M, Hidaka T. Two and three component photoinitiating systems based on coumarin derivatives. Polymer 2001;42:7627–34. https://doi.org/10.1016/S0032-3861(01)00275-0.
[296] Kikuchi A, Iyoda T, Abe J. Electronic structure of light-induced lophyl radical derived from a novel hexaarylbiimidazole with π-conjugated chromophore. Chem Commun 2002:1484–5. https://doi.org/10.1039/B203814E.

[297] Shi Y, Yin J, Kaji M, Yori H. Photopolymerization of acrylate derivatives initiated by hexaarylbiimidazole with ether groups. Polymer International 2006;55:330–9. https://doi.org/10.1002/pi.1968.
[298] Shi Y, Yin J, Kaji M, Yori H. Synthesis of a novel hexaarylbiimidazole with ether groups and characterization of its photoinitiation properties for acrylate derivatives. Polymer Engineering & Science 2006;46:474–9. https://doi.org/10.1002/pen.20501.
[299] Shi Y, Wang B, Jiang X, Yin J, Kaji M, Yori H. Photoinitiation properties of heterocyclic hexaarylbiimidazoles with high UV-vis absorbance. Journal of Applied Polymer Science 2007;105:2027–35. https://doi.org/10.1002/app.26301.
[300] Li Y-H, Chen Y-C. Triphenylamine-hexaarylbiimidazole derivatives as hydrogen-acceptor photoinitiators for free radical photopolymerization under UV and LED light. Polym Chem 2020;11:1504–13. https://doi.org/10.1039/C9PY01605H.
[301] Ma X, Cao D, Hu X, Nie J, Wang T. Carbazolyl α-diketones as novel photoinitiators in photopolymerization under LEDs. Progress in Organic Coatings 2020;144:105651. https://doi.org/10.1016/j.porgcoat.2020.105651.
[302] Marcille H, Malval J-P, Presset M, Bogliotti N, Blacha-Grzechnik A, Brezová V, et al. Diphenyl functional porphyrins and their metal complexes as visible-light photoinitiators for free-radical, cationic and thiol–ene polymerizations. Polym Chem 2020;11:4237–49. https://doi.org/10.1039/D0PY00468E.
[303] Batibay GS, Gunkara OT, Ocal N, Arsu N. Thioxanthone attached polyhedral oligomeric silsesquioxane (POSS) nano-photoinitiator for preparation of PMMA hybrid networks in air atmosphere. Progress in Organic Coatings 2020;149:105939. https://doi.org/10.1016/j.porgcoat.2020.105939.
[304] Jöckle P, Kamm PW, Lamparth I, Moszner N, Unterreiner A-N, Barner-Kowollik C. More than Expected: Overall Initiation Efficiencies of Mono-, Bis-, and Tetraacylgermane Radical Initiators. Macromolecules 2019;52:281–91. https://doi.org/10.1021/acs.macromol.8b02404.
[305] Yu J, Gao Y, Jiang S, Sun F. Naphthalimide Aryl Sulfide Derivative Norrish Type I Photoinitiators with Excellent Stability to Sunlight under Near-UV LED. Macromolecules 2019;52:1707–17. https://doi.org/10.1021/acs.macromol.8b02309.
[306] Ma X, Gu R, Yu L, Han W, Li J, Li X, et al. Conjugated phenothiazine oxime esters as free radical photoinitiators. Polym Chem 2017;8:6134–42. https://doi.org/10.1039/C7PY00797C.
[307] Ma X, Cao D, Fu H, You J, Gu R, Fan B, et al. Multicomponent photoinitiating systems containing arylamino oxime ester for visible light photopolymerization. Progress in Organic Coatings 2019;135:517–24. https://doi.org/10.1016/j.porgcoat.2019.06.027.
[308] Hu P, Qiu W, Naumov S, Scherzer T, Hu Z, Chen Q, et al. Conjugated Bifunctional Carbazole-Based Oxime Esters: Efficient and Versatile Photoinitiators for 3D Printing under One- and Two-Photon Excitation. ChemPhotoChem 2020;4:224–32. https://doi.org/10.1002/cptc.201900246.
[309] Qiu W, Hu P, Zhu J, Liu R, Li Z, Hu Z, et al. Cleavable Unimolecular Photoinitiators Based on Oxime-Ester Chemistry for Two-Photon Three-Dimensional Printing. ChemPhotoChem 2019;3:1090–4. https://doi.org/10.1002/cptc.201900164.
[310] Qiu W, Zhu J, Dietliker K, Li Z. Polymerizable Oxime Esters: An Efficient Photoinitiator with Low Migration Ability for 3D Printing to Fabricate Luminescent Devices. ChemPhotoChem 2020;4:5296–303. https://doi.org/10.1002/cptc.202000146.

[311] Qiu W, Li M, Yang Y, Li Z, Dietliker K. Cleavable coumarin-based oxime esters with terminal heterocyclic moieties: photobleachable initiators for deep photocuring under visible LED light irradiation. Polym Chem 2020;11:1356–63. https://doi.org/10.1039/C9PY01690B.
[312] Zhou R, Malval J-P, Jin M, Spangenberg A, Pan H, Wan D, et al. A two-photon active chevron-shaped type I photoinitiator designed for 3D stereolithography. Chem Commun 2019;55:6233–6. https://doi.org/10.1039/C9CC02923K.
[313] Chen S, Jin M, Malval J-P, Fu J, Morlet-Savary F, Pan H, et al. Substituted stilbene-based oxime esters used as highly reactive wavelength-dependent photoinitiators for LED photopolymerization. Polym Chem 2019;10:6609–21. https://doi.org/10.1039/C9PY01330J.
[314] Fast DE, Lauer A, Menzel JP, Kelterer A-M, Gescheidt G, Barner-Kowollik C. Wavelength-Dependent Photochemistry of Oxime Ester Photoinitiators. Macromolecules 2017;50:1815–23. https://doi.org/10.1021/acs.macromol.7b00089.
[315] Lee Z-H, Hammoud F, Hijazi A, Graff B, Lalevée J, Chen Y-C. Synthesis and free radical photopolymerization of triphenylamine-based oxime ester photoinitiators. Polym Chem 2021;12:1286–97. https://doi.org/10.1039/D0PY01768J.
[316] Chae KH. Thermal curing reaction of poly(glycidyl methacrylate) using photogenerated amines from oxime-urethane derivatives. Macromolecular Rapid Communications 1998;19:1–4. https://doi.org/10.1002/(SICI)1521-3927(19980101)19:1<1::AID-MARC1>3.0.CO;2-6.